POLITECNICO DI TORINO

Corso di Laurea Magistrale in Ingegneria Meccanica (Mechanical Engineering)

Politecnico
di Torino
1859

ENVIRONMENT
PARK Parco Scientifico
Tecnologico per l'Ambiente

PLASMA NANO-TECH
EnviPark - Trattamenti con nanotecnologie al plasma

Master's Degree Thesis

Effect and characterization of plasma treatments on adhesively bonded joints for automotive applications

Supervisors:
Prof. Giovanni Belingardi
Prof. Davide Salvatore Paolino
Ing. Raffaele Ciardiello

Company supervisor:
Ph.D. Domenico D'Angelo

Candidate:
Andrea Iadarola

Academic Year 2020/2021

July 2021

Index

Index of Figures

Index of Tables

1 Abstract

In the present study, the effect of plasma treatments is analysed for a 12% talc-filled polypropylene (PP) substrate in order to find an efficient procedure that is able to increase the mechanical properties of single lap joints (SLJs) bonded using three different adhesives typically adopted in the automotive industry: Methacrylate (MA) adhesive, polyurethane (PUR) adhesive and polyolefin hot-melt adhesive (HMA).

Polypropylene is a non-polar polyolefin and, for this reason, the bonding with the structural polar adhesives (PUR and MA) is almost impossible without any surface treatment. In this case study, the critical issue was that the adhesives under investigation have different properties and they interact in different ways with the polyolefin PP substrate. Therefore, the effect of plasma treatments on PP substrates was analysed in order to find a procedure that makes possible the use of polar adhesives also for these kinds of polymeric materials. Whereas, in the case of the non-polar polyolefin HMA, the surface treatments should not produce functional polar groups (FPGs) on the surface of the substrates and, for this reason, plasma treatments may result ineffective in increasing the mechanical properties of the bonded joints.

For structural polar adhesives was used a Cold Atmospheric Pressure Plasma Jet (CAPPJ) system to treat the PP substrates. Whereas, in the case of polyolefin HMA, it was used a Low-Pressure vacuum Plasma system, in order to reduce, as much as possible, the presence of oxygen and FPGs on the surface of the adherent.

The effect of these treatments was studied through a chemical and optical surface characterization, analysing the outermost surface of the substrates using Scanning Electron Microscopy (SEM) analysis, Energy Dispersive X-Ray (EDX) analysis and Attenuated Total Reflection (ATR) spectroscopy.

After the chemical and optical characterization, untreated and plasma-treated specimens were used to create SLJs and subsequently tested by lap shear test in order to evaluate the mechanical characteristics of the bonded joint.

The SLJs bonded with structural adhesives were subjected to three different ageing processes and their mechanical properties were compared with the simply treated bonded joints, highlighting the sensitivity of these adhesives to temperature and relative humidity variations.

Experimental results showed that plasma treatments were very useful in order to increase the adhesion with the polar structural adhesive. By contrast, they resulted almost ineffective for the use of thermoplastic polyolefin HMA.

2 Introduction

In recent years, the automotive industry is moving towards the usage of lighter and more sustainable materials such as thermoplastic polymers and composite materials [1]. Lighten the vehicles is a direct consequence of the need to reduce fuel consumption and environmental pollution of fuel running vehicles and increase the life cycle of batteries for hybrid and electrical ones. Indeed, it has been demonstrated that reducing the vehicle weight of 100 kg, CO_2 emissions may reduce by as much as 8g/km depending on the vehicle size and powertrain type [2].

Exploiting these new lightweight materials leads to the necessity of joining techniques that are different from the more traditional mechanical techniques commonly used for metals. Using fasteners like bolts and screws requires much time and labor, and the bolts are subjected to corrosion and may loosen over time. Welding is sometimes possible, but it is expensive and labor-intensive. Moreover, welding may create damage in the material creating brittle zones due to the high-temperature gradient to which the material is subjected. Adhesive joints represent a good solution for joining parts made of different materials which are difficult or even impossible to join together in other ways, not only regarding the automotive industry but also in many other applications. The use of adhesives allows also to obtain hybrid structures which are one of the most innovative solutions leading towards lightweight vehicle design.

Adhesives have different advantages such as the lack of corrosion compared to mechanical joints, reduction of noise and vibration and the possibility to add tackifiers which can increase the surface wetting of the substrates by reducing the adhesive's viscosity. Furthermore, one of the most important advantages is the ability to improve the stress distribution along the lap zone by properly design the geometry of the joint [3, 4]. Moreover, due to their versatility, adhesives allow shortening the manufacturing time sustaining the strict production pace of automotive industries. Therefore, in the last decades, adhesives have been progressively adopted also in structural applications and they represent a good solution in order to simplify the vehicle assembly reducing the weight and guaranteeing high strength and elastic modulus.

The need to increase the adhesion properties of the substrate material together with the need for more clean and environmentally friendly alternatives to chemical pre-treatments led to the development of various interesting techniques (flame treatment, corona treatment, plasma treatment, laser treatment, etc.). Among these, plasma activation (or plasma functionalization) has been reported as one of the most effective techniques due to its long-term durability and its ability to retain the bulk properties of the material [5, 6]. The major differentiation for plasma treatment systems consists in vacuum plasma systems and atmospheric ones.

Vacuum plasma systems allow to remove the ambient air from the controlled process chamber and insert in it only the gasses that have to be ionized. The main advantages of this plasma system are that it allows to have complete control of the process atmosphere and to have the possibility to treat a large number of components in a single treatment session, depending on the dimensions of the process chamber. Whereas atmospheric plasma systems work in the ambient air and the plasma species coming from the source gets in contact with the air during the flight time defined by the distance of the source (working distance). The main advantage of this last is the possibility to have a simplified treatment system that can be applied to a fast pace production line which, usually, leads to a faster and more efficient process.

One of the most common plasma treatment methods is the cold atmospheric pressure plasma jet (CAPPJ) because of its good compatibility for in-line industrial application and the large number of operational parameters which can be adjusted in order to achieve the best adhesion results (process gas composition, the working distance of the jet, electrical power, treatment time, etc.) [7, 8].

Plasma is an ionized gas consisting of excited electrons and atomic or molecular radical species which is obtained when gases are subjected to strong electrical fields. Plasma exposure can modify the polymer's surface in different ways such as producing highly reactive zones by means of reactive radicals deposition (surface activation), cleaning from contaminants and etching [9, 10]. Depending on the gas used it is possible to obtain different mixtures of ions, radicals and functional polar groups (FPGs) which may affect in different ways the surface properties of the treated samples. The activation of the polymer surfaces may significantly improve the adhesion performance and increase its hydrophilicity.

Polypropylene (PP) is one of the most used and versatile thermoplastic polymers in industrial applications (especially in automotive ones) due to its moderate cost and favourable properties such as high strength-to-weight ratio and excellent chemical resistance [1, 11]. On the other hand, due to its inert molecular structure, PP exhibits low surface energy involving in poor adhesion properties and a strong hydrophobic behaviour which makes bonding with adhesives inefficient [5]. Therefore, in order to avoid adhesive failure and to increase the range of use of this polymer, it is essential to increase the surface energy by means of surface pre-treatments. Higher surface energy enhances the ability of the substrate surface to become wet by the adhesive, thus leading to a better spreading of the adhesive on the surface and therefore to a more uniform contact with the substrate [9, 12].

The disadvantage of PP originates also from the lack of oxygen-based functional polar groups and amide moieties on the surface. The presence of stable FPGs on the PP surface would impart better adhesive properties and improved hydrophilicity. Obviously, this is true only if the adhesive is compatible with the new surface properties (e.g., non-polar adhesive needs non-polar surfaces and vice versa).

Plasma treatments can originate polar surfaces by increasing the concentration of FPGs on the polymer surface by imparting a large number of oxygen radical ions, oxygen radicals and UV photons [13, 9]. These oxygen radicals would react with carbon atoms on the PP surface more readily than oxygen molecules, thus forming a larger number of oxygen-based FPGs.

The heat from the plasma source will induce also a thermal oxidation effect facilitating the abstraction of hydrogen atoms from the surface PP units (CH_2=CH–CH_3) to produce polymeric macro radicals or alkali radicals, as in the case of UV-induced oxidation [13, 14]. These kinds of polymeric radicals will react with oxygen radicals and ions to a greater extent than with oxygen molecules, thus contributing to an increase in the amount of oxygen-based FPGs.

Oxidation of PP units and, consequently, the formation of FPGs leads to chain scission, which in turn may lead to the formation of the so called low-molecular-weight-oxidized-material (LMWOM).

The presence of LMWOM on the surface is always accompanied by a significant amount of carboxyl (COO) functional groups [15]. These molecular structures appear on the polymer surface as mounds with a spherical shape and their size is influenced by the relative humidity (RH) in the gas process and the energy of the plasma jet [15, 7, 8]. For this reason, LMWOM modify also the surface topography of the treated polymer [16, 17, 18]. Strobel et al. concluded that LMWOM may have positive effects on adhesion properties of PP surface only if the adhesive is able to incorporate this material, otherwise LMWOM may reduce the adhesion properties acting as a week boundary layer [19, 20]. The chemical groups created on the polymer surfaces which are responsible for increasing the adhesion tend to vanish with time and they are influenced by environmental conditions. Moreover, also the bonding of joined specimens may be subjected to degradation when exposed to extreme conditions [9].

Therefore, the treatment of PP is usually aimed to create FPGs on the substrate surface in order to be bonded to chemically related polar adhesives. Many studies have been presented considering the adhesion with polyurethane and epoxy adhesives.

Mühlhan et al. performed vacuum plasma treatments using pure oxygen as a process gas for polypropylene substrates in order to increase the adhesion with an ethil(2)cyanoacrilate based adhesive. They discovered that the plasma treatment is more effective for short time of plasma exposure; the FPGs which are formed on the PP surface by higher exposure time are bonded weakly.

Green et al. studied the effect of vacuum and atmospheric pressure plasma treatments on PP substrates considering the modification of the O:C ratio on the surface and how this may influence the adhesion properties with a polyurethane adhesive. Atmospheric pressure plasma treatment showed a lower O:C ratio and higher roughness with respect to low-pressure vacuum plasma. They also noticed that a higher O:C ratio leads to higher shear strength of the bonded joint. Both plasma treatments showed high levels of deep-positioned oxygen functional groups in the substrate [21].

Dorai and Kushner presented a plasma chemistry model capable of explaining the change in surface properties of PP by varying the principal plasma treatment operational parameters using humid air in atmospheric conditions [22]. In order to measure the effects of the operational parameters on surface energy variation, the simplest and most common method is the wettability evaluation by means of contact angle measurement [23, 24, 10]. Bhattacharya et al. reported that contact angle is strongly correlated to the bond strength of polymer materials [25, 10].

Gas flow rate may affect the hydrophilicity but the result is strongly influenced by the gas admixture used for the functionalization. Kawakami et al. observed a better wettability for lower flow rates using atmospheric pressure air plasma compared to higher flow rates, whereas using argon (Ar) plasma the results were minimally affected by the flow rates [13].

The effect of **treatment time** variation has been analysed in different studies maintaining constant both gas admixture and working distance (WD). It was observed a sharp decrease in contact angle (increased wettability) in the first few seconds (~15 s depending on the WD and gas admixture used) of plasma exposure, followed by a much slower reduction. Shaw et al. observed almost 40% of the total contact angle reduction in the first 1.5 s using helium (He) gas with a small admixture of oxygen [26, 8, 12, 13, 27].

Increasing the **working distance** between the nozzle of the CAPPJ and the polymer surface usually has negative effects on contact angle; the bigger is the distance, the higher is the contact angle and the lower is the resultant wettability of the surface [26].

Keher et al. observed that both peel strength and surface free energy (SFE) on the surfaces of treated PP samples significantly increase for smaller WDs for both air and nitrogen (N_2) atmospheric pressure plasma gases. The maximum peel force values, which correspond to cohesive failure of the adhesive, are obtained for WDs between 4 mm and 8 mm and it reaches higher values in the case of N_2 plasma [7]. Surface free energy is higher for air plasma as long as the WD is small whereas, increasing WD, N_2 plasma shows higher SFE.

This behaviour can be explained by the fact that N_2 plasma in atmospheric conditions is able to produce a higher concentration of water-soluble LMWOM (due to higher deposition of carboxyl functional groups) which may increase the surface energy of the substrate [15, 7]. Oxygen molecules can dissociate thanks to the impact of vibrationally excited N_2 molecules thus helping to generate more reactive oxygen radicals (through the reaction $N_2+O_2 \rightarrow O+O+N_2$), as it happens with the impact of electrons (e.g., through the reaction $e+O_2 \rightarrow 2O+e$) [13, 28, 29].

Another operational parameter that has a high influence on the adhesion results is the radio frequency (RF) **power** setting. In literature, it was observed that, increasing the plasma RF power in atmospheric conditions, the surface contact angle greatly decreases together with an increase of the surface energy and a high increase in the surface roughness. Obviously, this effect can be amplified by increasing, together with the RF power, also the treatment time [30, 31].

Depending on these parameters, many studies have shown that, in the initial part of the process, the interaction of ions, electrons and radicals with the substrate may cause a rapid removal of contaminants (processing aids, adsorbed species, etc.) on the amorphous region of the surface, this process can be identified as "plasma cleaning" effect [14, 10, 30]. For a longer treatment time, after this cleaning effect, a deeper ablation process of the crystalline fraction of the polymer is possible, strongly increasing the surface roughness. Cleaning and ablation are grouped in the "etching effects". The various steps involved in the etching process that takes place during plasma treatments are represented in Figure 1.

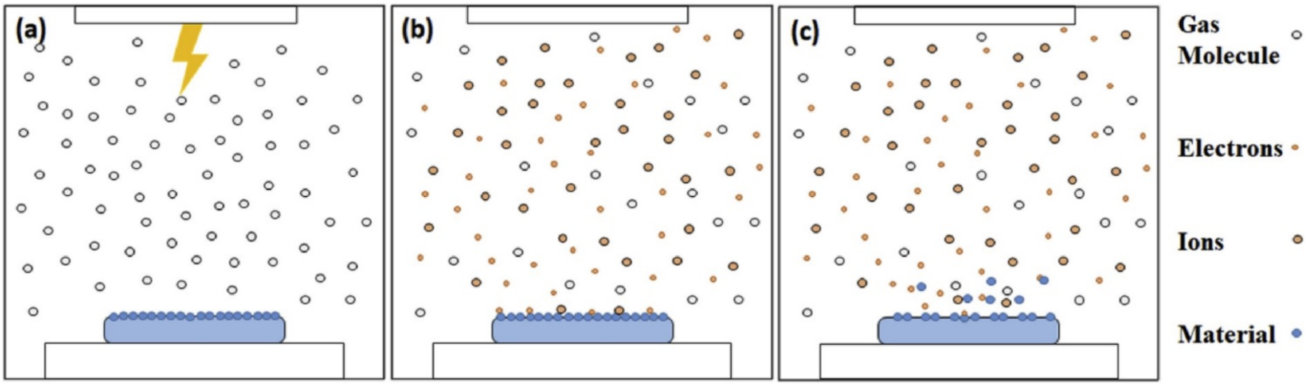

Figure 1: (a) Plasma generation, (b) collision of plasma species on the substrate surface and (c) removal of the material due to etching effect of the plasma [9]

Not only the surface chemical and electrostatic forces contribute to adhesion between the substrate and the adhesive [9]. Adhesion properties are also heavily influenced by the surface topology. Surface roughness is a fundamental aspect to be considered in bonding because the adhesive can penetrate crevices, pores and other polymer surface irregularities making possible a mechanical coupling (mechanical interlocking) between the two surfaces, as illustrated in Figure 2.

Vishnuvarthanan and Rajeswari studied the effect of the variation of some low-pressure plasma operational parameters on peel strength and tensile strength of the treated PP samples. Peel strength increases by increasing RF power and treatment time due to a higher production of FPGs on the surface layer and an increased effect of mechanical interlocking due to the increased roughness. These results obviously depend on the type of adhesive used. Whereas, the tensile strength was greatly reduced because of an increased etching effect of the surface.

Indeed, most of the time, differences in adhesion properties obtained from different plasma gases derive from different surface topologies rather than differences in the surface chemistry. The most common methods to investigate the surface morphology of the sample are Atomic Force Microscopy (AFM) or Scanning Electron Microscopy (SEM) [9, 32, 33, 34, 17].

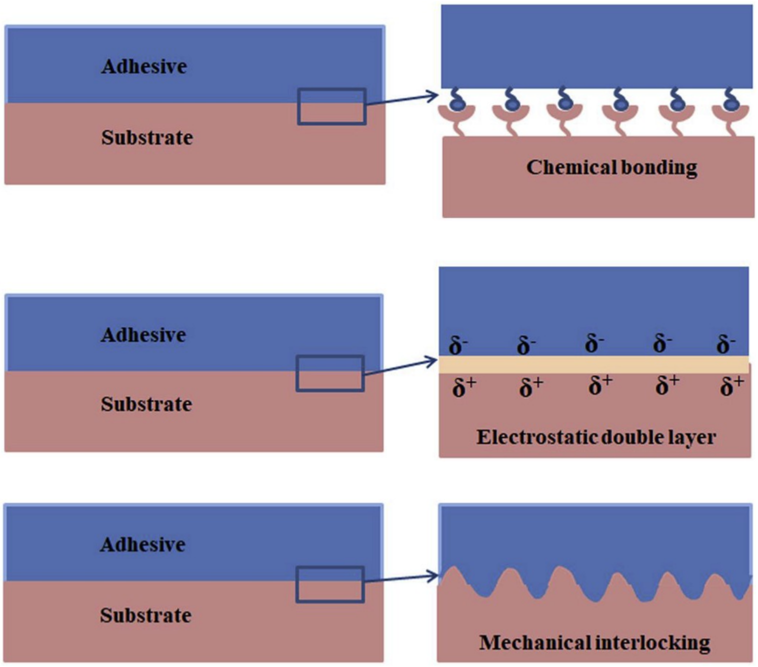

Figure 2: Schematic of different adhesion mechanisms [9]

In literature, CAPPJ has been used for surface treatments of PP using different types of process gas admixtures. Kehrer et al. studied the concentrations of FPGs deposited on the PP surface for both pure air and pure N_2 plasma gasses. Pure air plasma shows a higher concentration of oxygen (O), hydroxyl (C–OH) and carbonyl (C=O) functional groups with respect to pure N_2 plasma which always shows a higher concentration of carboxyl (COO) groups [7].

As soon as water (H_2O) is added to the process gas mixture, the concentration of all FPGs decreases (especially COO groups). The addition of water vapour to the gas admixture results in a decrease in electron density due to electron attachment and a high rate of electron collisions with water molecules. The polymer surface free energy significantly drops in the case of air plasma whereas it remains almost constant using N_2 as process gas, this is due to the presence of a lower amount of LMWOM [15, 7].

Moreover, significant changes for both oxygen-based FPGs and nitrogen induced species in the surface chemistry can be observed by adding oxygen (O_2) in pure N_2 process gas. Increasing O_2 concentration, the surface shows a continuous increase in hydroxyl groups and an increase of carbonyl groups until the 30 vol.% of O_2 in pure N_2. The relative concentration of carboxyl (COO) groups continuously decreases adding O_2 in pure N_2 until 40 vol.% is reached and the concentration of COO groups becomes almost zero. For concentrations of O_2 >10% in the gas admixture, the concentrations of nitrogen induced species (e.g., nitroso, oxime, amides, etc.), which are present on the surface for pure N_2 plasma (0% O_2), start to decrease together with a continuous increase of NO_3 groups; once reached 40 vol.% of O_2, only NO_3 groups are present on the surface [7].

Kawakami et al. studied the difference in functional groups deposition between air and Ar plasmas in atmospheric pressure. Air plasma always shows a higher concentration of oxygen-based FPGs on the surface in a short treatment time (1 min) together with a stronger etching effect of the substrate with respect to Ar plasma. For this reason, air plasma treated samples are characterized by higher surface energy and lower contact angle. On the other hand, Ar plasma treated samples shows surface chemistry much more similar to the untreated PP samples with a much lower concentration of oxygen-based FPGs and higher concentration of non-polar bonds such as C–C / C=C / C–H with respect to air plasma treatment [13]. For this reason, Ar plasma treatment results to be more suitable for bonding PP with polyolefin-based adhesives such as some hot-melt adhesives. Anyway, Ar plasma reduces the concentration of C–C and C–H bonds on the surface of PP polymer increasing the concentration of C–O, C=O, O–C=O bonds and creating a few C–N bonds. Also in this case, adding water vapour to pure Ar feeding gas, PP surface shows a more pronounced oxygen incorporation [35].

Neither air nor Ar gas admixture provide a large number of N_2 species on the surface. Moreover, considering the same gas flow rate and WD, air plasma shows higher temperature on the treated surface together with higher etching of the substrate, compared with Ar plasma treatment [13].

In the automotive industry thermosetting adhesives, such as Methacrylate, Epoxy and Polyurethane adhesives, have been preferred for structural applications because of their greater strength and elastic modulus with respect to thermoplastic ones, such as HMA.

Polyurethane adhesives (PUR) are one of the most important types of structural adhesives. They are formed from the reaction of organic (poly)diisocyanates with (oligomeric) diol compounds, which leads to urethane linkages in the backbone (-NH-C(=O)-O-). The high reactivity of the isocyantes allows for fast cure, but slow cure can also be achieved by adjusting the catalyst level. Most polyurethane adhesives are either polyester or polyether based. They are present in the isocyanate prepolymers and in the active hydrogen containing hardener component (polyol) [36].

They present unique characteristics due to the possibility to vary most of their physical properties by modifying their formulation. Their properties can be tailored over a wide range for a large number of applications. They can be both rigid and hard, or flexible and soft. The main advantages are the wide temperature range applicability, long term bond assembly durability, high modulus, high tensile strength, high elongation at break, good sealing properties and room temperature curing as well as accelerated curing options [37, 38].

Polyurethane adhesives can be found as two-component or one component urethane adhesive. In the case of two-component, the first contains the diisocyanates and/or the isocyanate prepolymers, whereas the second consists of polyols (and amine/hydroxyl chain extenders). Sometimes, a catalyst may be added to speed up the cure (usually a tin salt or a tertiary amine).

The polar urethane group makes possible adhesion to different kinds of surfaces, especially polar ones. In the case of non-polar adherents, such as polypropylene, surface treatments have to be used in order to increase the adhesion between the substrates and the PUR adhesive.

Methacrylate adhesives (MA) are structural adhesives that are usually made of resin and a hardener. Sometimes rubber tougheners and additional strengthening agents, similar to those used in epoxy adhesives, are added to improve the toughness and flexibility of the relative brittle methacrylate-based adhesives. These rubbers are sometimes terminated with reactive groups to allow for crosslinking with the methacrylate matrix [36].

The main advantage of MA adhesives is that it cures quickly at room temperature and it reaches its full bond strength soon after application. Unlike other structural adhesives, such as two-part epoxies, MAs do not require heat to cure, it creates an exothermic polymerization reaction. The induction time can be adjusted over a wide range, allowing the assembly of large and complex structures, not uncommon in boat manufacturing and other assembly areas.

Moreover, they have good chemical, environmental and temperature resistance and also good resistance to shear, peel, and impact stress. Toughness, flexibility and ease of use make this type of adhesive very common in a large variety of industrial applications [39].

Methacrylate adhesives often suffer of air-inhibition, which can result in insufficient cure when the adhesive is exposed to air. This can lead to poor corrosion resistance. Furthermore, their heat resistance, maximal service temperature and bond performance are usually lower than those of high-performance structural epoxy adhesives [36].

Epoxy adhesives are more brittle and do not allow for expansion and contraction; this may lead to cracks and ultimately bond failure. Polyurethane adhesives need more surface preparation and often require priming or treatments of the surface, adding additional steps to the bonding procedure. Methacrylate adhesives are less brittle than epoxy adhesives and they have higher bond strength, better resilience and also better fatigue resistance than urethanes.

These kinds of structural adhesives are characterized by a strongly polar chemical composition that makes it very difficult the bonding with non-polar substrates, such as polypropylene. For this reason, surface treatments are necessary in order to create FPGs on the surface, enhancing the adhesion and making the substrate surface suitable for the use of these adhesives.

In the last two decades, the use of new thermoplastic adhesives has progressively increased also for structural applications due to their ability to reduce manufacturing cost and improve manufacturing efficiency where the pace of production is very strict [40].

Hot-melt adhesives (HMAs) are thermoplastic materials, so they can repeatedly melt by heating and solidify by cooling at room temperature. They are applied on the substrates in the molten state and, by rapid solidification, the adhesive bond formation takes place in few minutes. HMAs basically consist of a thermoplastic polymer backbone with tackifiers and a number of functional additives such as antioxidants, waxes, plasticizers and oils [41]. Therefore, many HMAs exist and, in order to obtain the desired performances, they have to be selected carefully based on the specific application. Moreover, HMAs have some limitations due to temperature sensitivity: at high temperatures they soften losing strength and become susceptible to creep; whereas at much lower temperature they become brittle [36, 41].

Polyolefin based hot-melt adhesives are one of the most efficient adhesives in order to joint difficult-to-bond polymers like non-polar polyolefins (such as polyethylene and polypropylene) and so they are usually not recommended for polar substrates due to their non-polar nature [36]. They are widely used in packaging and product assembly industry, especially in automotive applications for both exterior and interior parts (bumper subsystems, door panels, overhead system, seat subsystem, instrument panels, etc.). Polyolefin-based HMAs have excellent chemical resistance to polar solvents and solutions including acids, esters and alcohols and poor chemical resistance against non-polar solvents like alkanes, ethers and oils [41, 36]. The properties of these adhesives are generally influenced by the molecular weight of the polyolefin. As the molecular weight increases, the adhesive strength becomes less sensitive to the temperature and the hot tack and melt viscosity properties also increase. Conversely, as the molecular weight decreases, the stiffness and the low temperature performances increase [42, 43]. When compared with other HMAs, polyolefin-based adhesives offer excellent resistance to high and low temperatures, a large combination of desirable properties, very good cohesive strength and excellent resistance to ageing and peeling.

In the present work, three different adhesives were chosen in order to bond PP substrates, commonly used in the automotive industry, made of pure PP with 12% talc addition. The adhesives considered for this study are two structural adhesives (methacrylate and polyurethane adhesives) and one thermoplastic adhesive (polyolefin HMA).

The aim of this work is to assess the possibility to join these PP substrates with structural and thermoplastic adhesives, highlighting the differences that characterize them and their adhesive properties when they are used to bond polypropylene. As previously stated, those adhesives are not able to join components made from PP, or to exploit the maximum adhesion with them, without any surface treatment, so it is necessary to perform a treatment of the PP substrate in order to make it possible. In this study, the effect of atmospheric pressure and low-pressure plasma treatments is studied and critically analysed from a chemical and a mechanical point of view. More precisely, we wanted to define the mechanical properties of the plasma-treated and untreated bonded joints.

The final objective is to define a surface treatment and a joining technique suitable for industrial applications, that is at the same time efficient, flexible and easy to replicate in a fast pace production line. Moreover, to find a procedure which is able to make possible the use of the same adhesive for different applications allows to simplify the production process and reduce the costs.

In order to evaluate the mechanical properties of bonded joints, we exploited the single lap joint configuration by lap shear test, evaluating the maximum load and shear strength of the bonded joints. The analysis of the fracture surfaces led us to understand whether the treatments were effective in order to obtain a cohesive failure of the adhesive or, better, the failure of the substrate itself. A graphical review of the different failure modes is reported in Figure 3.

Moreover, in the case of structural adhesives, the joint's mechanical properties were also studied by evaluating the effect of the treatment after an accelerated ageing process.

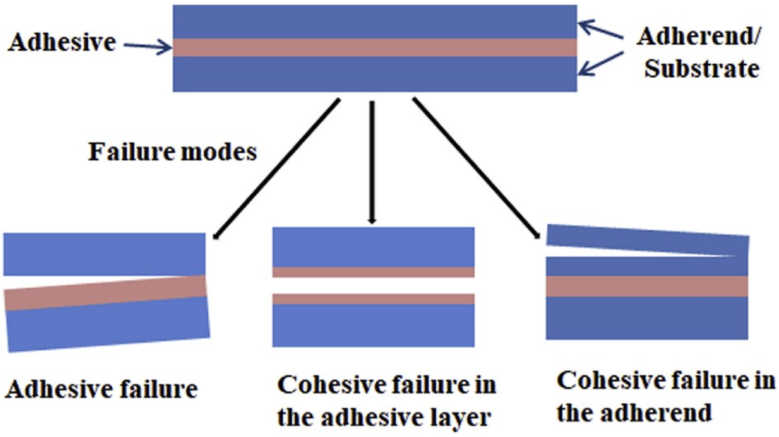

Figure 3: Different failure modes in a bonded joint [9]

Treated specimens were joined together just after the plasma exposure and, after the mechanical characterization, they were compared to the untreated ones.

The surfaces of untreated and treated substrates were chemically and optically characterized before bonding by means of Scanning Electron Microscopy (SEM) analysis, Energy Dispersive X-Ray (EDX) analysis and Attenuated Total Reflection (ATR) spectroscopy in order to understand the surface chemical composition of the substrates; thus, allowing to identify easily the best treatment to be used for bonding PP substrates with the considered adhesives.

In conclusion, the analysis of the mechanical results and the fracture surfaces, allowed us to evaluate the effectiveness of plasma treatments for the use of the different structural adhesives and to evaluate the effect of plasma for the polyolefin HMA bonded with PP substrates.

3 Materials and methods

The purpose of this study is to investigate the effects of plasma treatments (using both atmospheric pressure and low-pressure plasma systems) on the mechanical behaviour and adhesion characteristics of SLJs prepared with polypropylene samples. This activity is aimed to find an efficient and flexible treatment that would possibly be easy to replicate in a fast pace production line for polymeric materials commonly used in the automotive industry. In particular, the correlation between the shear strength of bonded joints and surface modification provided by the plasma to the samples was assessed through a lap-shear test analysis along with the evaluation of the chemical composition and morphology of the surface of the substrates.

From this point onwards, the untreated polypropylene substrates will be called "**P sample**".

3.1 Materials

The substrates used in this study are provided by LyondellBasell © with the commercial name Hostacom CR 1171 G1A. These specimens are used to create single lap bonded joints, as described in paragraph 3.4. They are rectangular specimens of dimensions 100 mm × 20 mm × 3 mm made of a 12% talc-filled PP copolymer, with a medium melt flow rate, high impact resistance and excellent UV resistance. In Table 1 are reported the technical information for these specimens. For this study, two different production lots have been used: one for bonding the polyurethane and methacrylate adhesives, the other for bonding the polyolefin hot-melt adhesive.

Three adhesives have been used in this study and they present different characteristics. The main properties and commercial names are reported here below.

The polyurethane adhesive used in this study is a two-component urethane compound (Isocyanate-Polyol) provided by DOW Automotive Systems with the commercial name of BETAFORCE 2850L. Technical information is reported in Table 3.

As shown in Figure 6, the adhesive is provided in two syringes containing the two components of the adhesive to be mixed using a dual-component adhesive variable-ratio pneumatic dispenser, shown in Figure 7. For this adhesive, the mixing ratio is 1:1.

The methacrylate adhesive used in this study is a two-part methacrylate adhesive designed for structural bonding provided by ITW Plexus with the commercial name of Plexus® MA920, represented in Figure 8. The mixing ratio (A:B) in this case is 10:1, where part A is the adhesive and part B is the activator. It may be applied manually or with automated equipment, similar to the one used for the polyurethane adhesive. Technical information is reported in Table 4.

The thermoplastic polyolefin-based HMA provided by Sika Automotive GmbH with the commercial name of SikaMelt®-9171 OT. Technical information is reported in Table 2.

As shown in Figure 4, the adhesive is provided in blocks and it needs a pressurized melting gun working at 4 bar (Figure 5) and around 190°C to be spread on the surface.

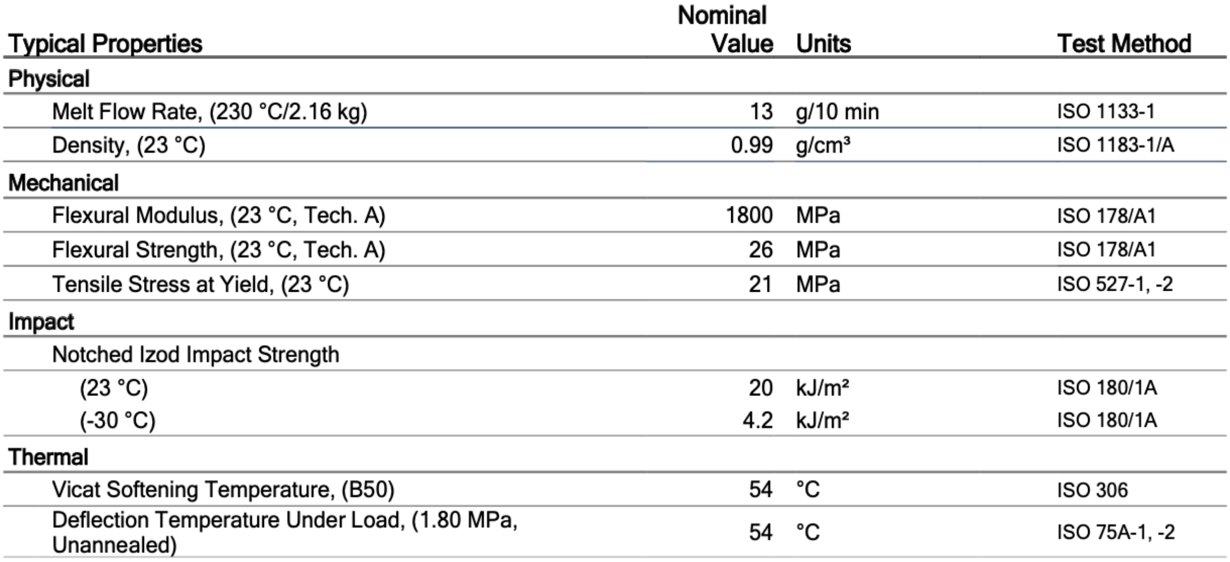

Typical Properties	Nominal Value	Units	Test Method
Physical			
Melt Flow Rate, (230 °C/2.16 kg)	13	g/10 min	ISO 1133-1
Density, (23 °C)	0.99	g/cm³	ISO 1183-1/A
Mechanical			
Flexural Modulus, (23 °C, Tech. A)	1800	MPa	ISO 178/A1
Flexural Strength, (23 °C, Tech. A)	26	MPa	ISO 178/A1
Tensile Stress at Yield, (23 °C)	21	MPa	ISO 527-1, -2
Impact			
Notched Izod Impact Strength			
(23 °C)	20	kJ/m²	ISO 180/1A
(-30 °C)	4.2	kJ/m²	ISO 180/1A
Thermal			
Vicat Softening Temperature, (B50)	54	°C	ISO 306
Deflection Temperature Under Load, (1.80 MPa, Unannealed)	54	°C	ISO 75A-1, -2

Table 1: Mechanical and thermal properties of the PP substrate used for the study [44]

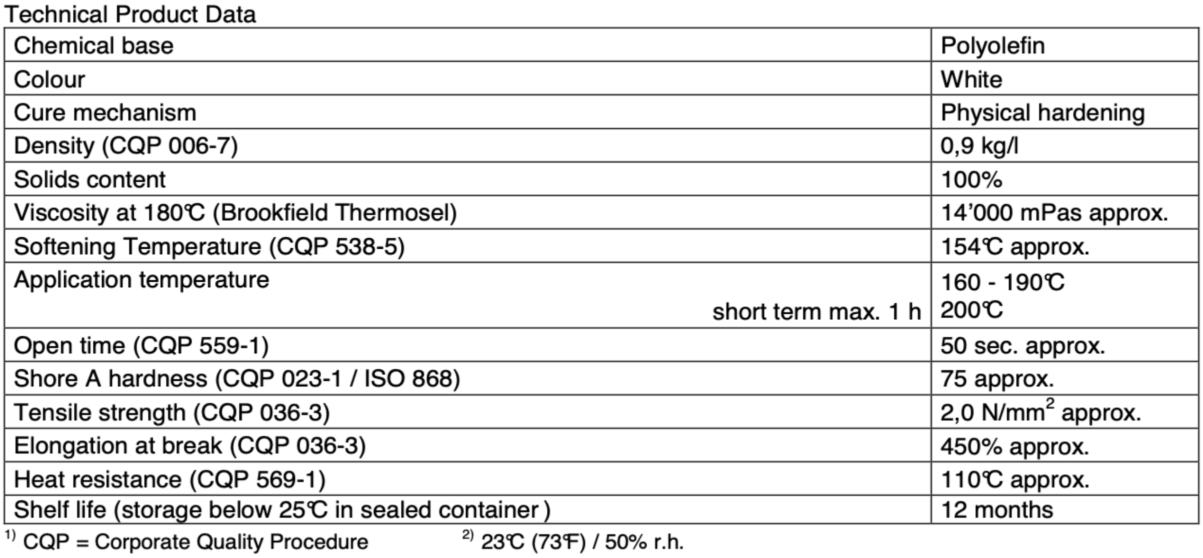

Technical Product Data

Chemical base	Polyolefin
Colour	White
Cure mechanism	Physical hardening
Density (CQP 006-7)	0,9 kg/l
Solids content	100%
Viscosity at 180℃ (Brookfield Thermosel)	14’000 mPas approx.
Softening Temperature (CQP 538-5)	154℃ approx.
Application temperature short term max. 1 h	160 - 190℃ 200℃
Open time (CQP 559-1)	50 sec. approx.
Shore A hardness (CQP 023-1 / ISO 868)	75 approx.
Tensile strength (CQP 036-3)	2,0 N/mm^2 approx.
Elongation at break (CQP 036-3)	450% approx.
Heat resistance (CQP 569-1)	110℃ approx.
Shelf life (storage below 25℃ in sealed container)	12 months

[1] CQP = Corporate Quality Procedure [2] 23℃ (73℉) / 50% r.h.

Table 2: Technical data of the polyolefin hot-melt adhesive

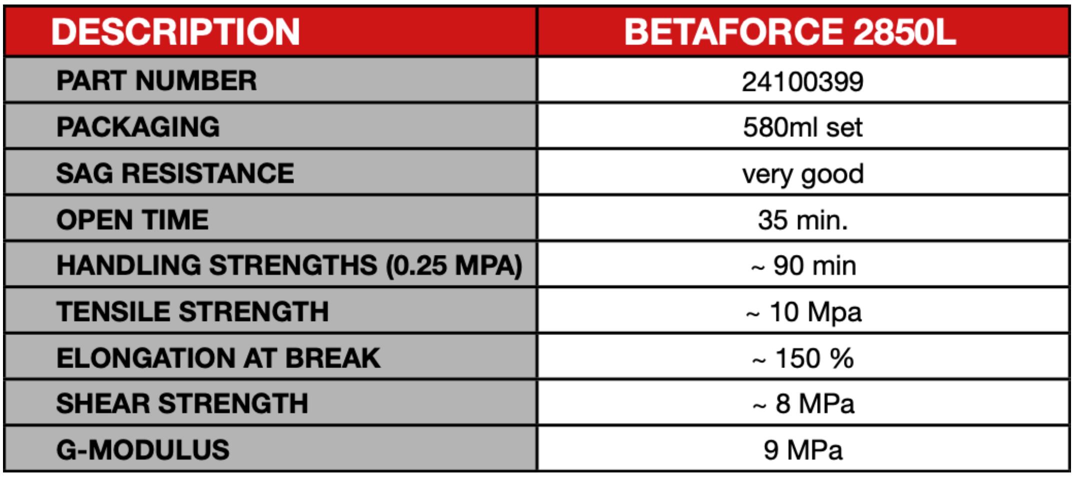

DESCRIPTION	BETAFORCE 2850L
PART NUMBER	24100399
PACKAGING	580ml set
SAG RESISTANCE	very good
OPEN TIME	35 min.
HANDLING STRENGTHS (0.25 MPA)	~ 90 min
TENSILE STRENGTH	~ 10 Mpa
ELONGATION AT BREAK	~ 150 %
SHEAR STRENGTH	~ 8 MPa
G-MODULUS	9 MPa

Table 3: Technical data of the two-component polyurethane adhesive (Betaforce 2850L)

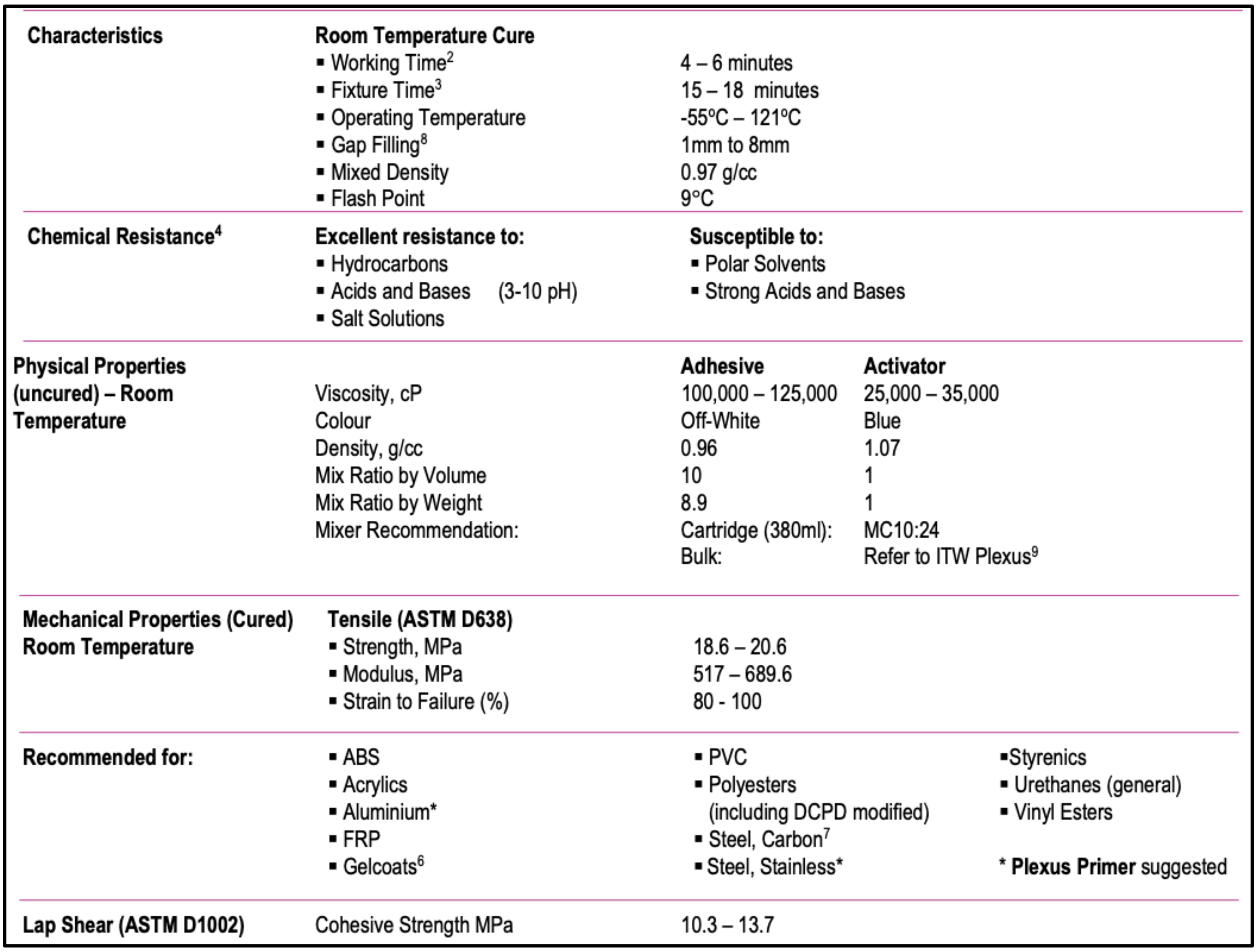

Characteristics	**Room Temperature Cure**		
	▪ Working Time[2]	4 – 6 minutes	
	▪ Fixture Time[3]	15 – 18 minutes	
	▪ Operating Temperature	-55°C – 121°C	
	▪ Gap Filling[8]	1mm to 8mm	
	▪ Mixed Density	0.97 g/cc	
	▪ Flash Point	9°C	
Chemical Resistance[4]	**Excellent resistance to:**	**Susceptible to:**	
	▪ Hydrocarbons	▪ Polar Solvents	
	▪ Acids and Bases (3-10 pH)	▪ Strong Acids and Bases	
	▪ Salt Solutions		
Physical Properties (uncured) – Room Temperature		**Adhesive**	**Activator**
	Viscosity, cP	100,000 – 125,000	25,000 – 35,000
	Colour	Off-White	Blue
	Density, g/cc	0.96	1.07
	Mix Ratio by Volume	10	1
	Mix Ratio by Weight	8.9	1
	Mixer Recommendation:	Cartridge (380ml):	MC10:24
		Bulk:	Refer to ITW Plexus[9]
Mechanical Properties (Cured) Room Temperature	**Tensile (ASTM D638)**		
	▪ Strength, MPa	18.6 – 20.6	
	▪ Modulus, MPa	517 – 689.6	
	▪ Strain to Failure (%)	80 - 100	
Recommended for:	▪ ABS	▪ PVC	▪Styrenics
	▪ Acrylics	▪ Polyesters (including DCPD modified)	▪ Urethanes (general)
	▪ Aluminium*	▪ Steel, Carbon[7]	▪ Vinyl Esters
	▪ FRP	▪ Steel, Stainless*	* **Plexus Primer** suggested
	▪ Gelcoats[6]		
Lap Shear (ASTM D1002)	Cohesive Strength MPa	10.3 – 13.7	

Table 4: Technical data of the methacrylate adhesive (Plexus MA920)

Figure 4: Polyolefin HMA used for this study

Figure 5: Melting gun for hot-melt adhesive

Figure 6: Two-component polyurethane adhesive used in this study

Figure 7: Dual-component adhesive variable-ratio pneumatic dispenser

Figure 8: Two-part methacrylate adhesive used in this study

For plasma treatments, two different machines were used. Low-pressure vacuum plasma treatments were carried out using a Diener electronic GmbH (Nagold, Germany) system model PICO, shown in Figure 9.

This system gives the possibility to insert two different gasses into the vacuum chamber, allowing to have the control of the ionization inside the process chamber avoiding the influence of contaminants coming from the surrounding air.

Whereas, for atmospheric pressure plasma treatments it was used a plasma jet system from Plasmatreat GmbH (Steinhagen, Germany), shown in Figure 10.

In this case, the plasma gas coming out of the jet gets in contact with the surrounding air along the distance between the source and the specimen to be treated. Therefore, even if we use the same gas mixture, we may obtain different results in the functionalization of the polymer surface.

Figure 9: Low-pressure vacuum plasma system

Figure 10: Cold Atmospheric Pressure Plasma Jet (CAPPJ) system

In order to perform the lap shear tensile test as reported in paragraph 3.5, it was used an Instron 8801 test machine (Figure 11) with 100 kN hydraulic wedge grips. Technical data and information are reported in Table 5.

Figure 11: Tensile test machine used for the tensile lap shear tests

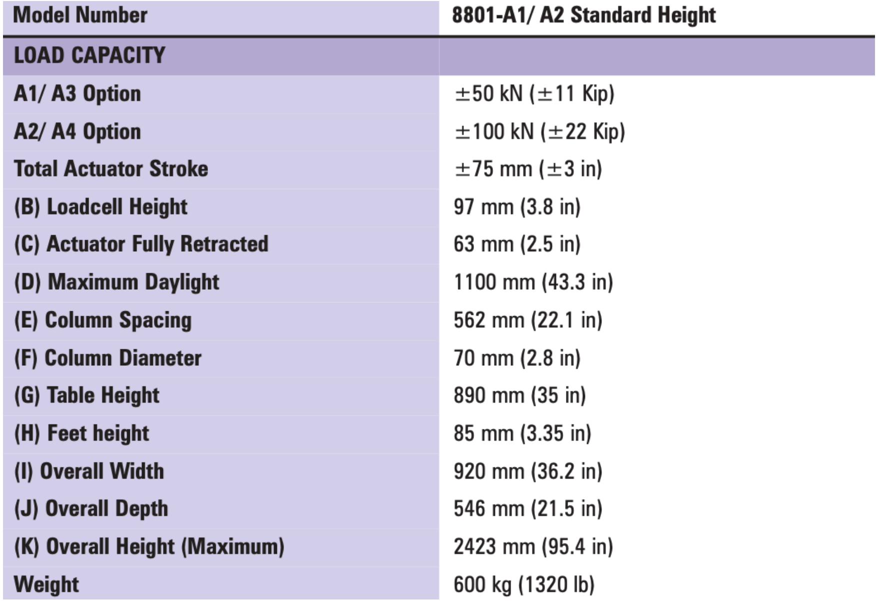

Model Number	**8801-A1/ A2 Standard Height**
LOAD CAPACITY	
A1/ A3 Option	±50 kN (±11 Kip)
A2/ A4 Option	±100 kN (±22 Kip)
Total Actuator Stroke	±75 mm (±3 in)
(B) Loadcell Height	97 mm (3.8 in)
(C) Actuator Fully Retracted	63 mm (2.5 in)
(D) Maximum Daylight	1100 mm (43.3 in)
(E) Column Spacing	562 mm (22.1 in)
(F) Column Diameter	70 mm (2.8 in)
(G) Table Height	890 mm (35 in)
(H) Feet height	85 mm (3.35 in)
(I) Overall Width	920 mm (36.2 in)
(J) Overall Depth	546 mm (21.5 in)
(K) Overall Height (Maximum)	2423 mm (95.4 in)
Weight	600 kg (1320 lb)

Table 5: Technical data of the INSTRON test machine

Scanning Electron Microscopy (SEM) and Energy Dispersive X-Ray (EDX) analysis were performed using ESEM Quanta 200 machine (FEI Company) with EDX microprobe (EDAX). Working at low pressure without metallizing the sample. The working conditions are reported in Table 6, whereas the system layout is shown in Figure 12.

Pressure	90 Pa
Working distance	10 mm
Voltage	20 kV

Table 6: Working conditions for SEM machine

Figure 12: SEM + EDX machine layout – FEI ESEM Quanta 200

The machine used for Attenuated Total Reflection (ATR) spectroscopy is provided by Shimadzu GmbH, model “IR spirit”, shown in Figure 13. Working mode: resolution 4 and 64 scans.

Micro-IR analysis were performed using Nicolet iN10 machine (Thermo Fisher Scientific Inc.), shown in Figure 14. Working with sampling area equal to 150 μm, 256 scans and spectral range between 4000 and 675 cm^{-1}.

Micro Raman analysis were performed using LabRAM HR Evolution machine (Horiba Jobin Yvon GmbH), shown in Figure 15. Provided with green laser (532 nm) and 80x objective and working at two exposures of 30 seconds. The spectral range is between 4000-100 cm^{-1}.


Figure 13: ATR machine - Shimadzu IR Spirit


Figure 14: Micro IR machine - Thermo Fisher Scientific Nicolet iN10

Figure 15: Micro Raman machine - Horiba Jobin Yvon LabRAM HR Evolution

3.2 Surface treatments

In this paragraph are described the surface treatments which have been performed on PP specimens before bonding, for both thermosetting and thermoplastic adhesives.

Surface treatments for the specimens bonded with structural thermosetting adhesives are grouped together because both PUR and MA adhesives need a strongly polar surface of the PP substrate, rich in oxygen and functional polar groups.

3.2.1 Bonding with Polyurethane and Methacrylate adhesives

These kinds of structural adhesives are very difficult to be bonded with a strongly non-polar PP substrate since they are characterized by polar chemical composition. For this reason, plasma surface treatment of polypropylene substrates must be able to produce, on the surface, the highest amount of oxygen and FPGs which can enhance the adhesion with these kinds of adhesives.

Low-pressure plasma system can remove all the air present in the process chamber in order to reduce as much as possible the presence of oxygen on the final substrate surface.

Whereas, in the case of the CAPPJ system, the plasma gets in contact with the surrounding air, through the gap between the jet and the substrate, catching oxygen from the air and introducing on the surface a larger amount of oxygen and FPGs.

For this reason, the CAPPJ system was chosen in order to treat the PP substrates before bonding.

It was performed a preliminary surface chemical and optical characterization of the treated samples, as reported in paragraph 4.2, in order to define the most suitable process gas to be used for plasma treatments of PP samples to be bonded with the structural adhesives listed in paragraph 3.1 (PUR and MA adhesives).

From these characterizations, nitrogen (N_2) plasma resulted to be the most effective process gas in order to increase the amount of oxygen on the surface of PP substrates. Therefore, the plasma treatment configuration for bonding PUR and MA adhesives is performed using N_2; in Table 7 is reported the configuration adopted for the CAPPJ system. The results are reported in paragraph 4.7.1.

Type of plasma	Process gas	Power	WD	Jet speed	Pressure	Gas flow	Reference voltage	Plasma voltage	Plasma intensity
CAPPJ	N_2	512 W	10 mm	125 mm/s	12 mbar	20 l/min	100%	342 V	24 kHz

Table 7: CAPPJ treatment configuration for the use of structural adhesives

3.2.2 Bonding with Polyolefin HMA adhesive

Two different surface configurations of the substrates were analysed in order to find the correct way to prepare the substrate surface before the plasma treatment and the bonding procedure: surface cleaned just with a dry cloth and surface washed with n-heptane.

The results from the lap shear tensile test of the mentioned specimens (reported in paragraph 4.8.1) suggested that the best way to pre-treat the substrates is to wash them with n-heptane.

Low-pressure plasma system was chosen in order to investigate the effect of plasma on P samples to be bonded with the polyolefin HMA since this system is able to remove all the air present in the process chamber reducing as much as possible the presence of oxygen on the final surface of the substrate.

It was performed a preliminary surface chemical and optical characterization of the treated samples, as reported in paragraph 4.5, in order to define the process gas to be used for low-pressure vacuum plasma treatments that can lead to the best adhesion properties.

In this investigation, air and nitrogen resulted not to be suitable for our purpose because of their ability to strongly polarize the polymer surface by introducing a large amount of oxygen, which is counterproductive to the use of polyolefin HMAs (paragraph 4.5).

Therefore, it was decided to use Ar as process gas in order to treat PP substrates to be bonded with the polyolefin HMA, since the presence of oxygen on the surface resulted to be lower with respect to the other process gasses analysed in this study.

The bonding procedure was performed just after the treatment with plasma, avoiding as much as possible contact with the ambient air.

It was necessary to define a suitable plasma exposure time since the low-pressure plasma system admits the control of the exposure time instead of the working distance (as for the CAPPJ system),

Two process gasses were tested in the conditions reported in Table 8 in order to define which is the best plasma exposure time able to enhance the properties of PP using the low-pressure plasma technology. The results of this test are reported in paragraph 4.8.2.1.

Type of plasma	Process gas	Power	WD	Exposure time
Vacuum	Ar	200W	750 mm	2 min 5 min 10 min
Vacuum	N_2	200W	750 mm	2 min 5 min 10 min

Table 8: Explorative tests for the definition of the plasma exposure time for low-pressure vacuum plasma surface treatment

According to the results of the experimental procedure aimed at defining the correct plasma exposure time for the low-pressure plasma system (paragraph 4.8.2.1) and the results of the chemical surface characterizations (paragraph 4.5), it was decided to use Ar as process gas for 2 minutes of plasma exposure.

Table 9 reports the process configurations used to treat the PP substrates in order to be bonded with the polyolefin HMA, for both the vacuum and CAPPJ plasma systems. The results of these tests are reported in paragraph 4.8.2 .

The atmospheric plasma treatment with Ar was performed just for comparative purposes.

Type of plasma	Process gas	Power	WD	Exposure time
Vacuum	Ar	200W	750 mm	2 min

Type of plasma	Process gas	Power	WD	Jet speed	Pressure	Gas flow	Reference voltage	Plasma voltage	Plasma intensity
CAPPJ	Ar	114 W	8 mm	125 mm/s	12 mbar	19 l/min	100%	342 V	24 kHz

Table 9: Configurations adopted for the plasma treatments of PP in order to be bonded with the polyolefin HMA

3.3 Ageing procedures

The specimens bonded with thermosetting structural adhesives (PUR and MA adhesives) were subjected to three different accelerated ageing conditions in order to evaluate the strength of the bonded joints even in extreme conditions of temperature and relative humidity.

These ageing procedures were not used for the thermoplastic polyolefin hot-melt adhesive because of its intrinsic sensitivity to heat which would lead to a deterioration of the adhesion properties of the bonded joints.

The ageing procedures performed in this study are reported here below:

- **Ageing A**: 500 hours at 90°C ;
- **Ageing B**: 500 hours at 40°C and relative humidity ≥ 95% ;
- **Ageing C**: three thermal cycles in sequences 24 hours long each, in the following conditions:
    - 80°C;
    - 40°C and 95% relative humidity;
    - -40°C.

3.4 Bonding procedure

After the surface preparation and treatment of the substrates, described in paragraph 3.2, rectangular specimens of dimensions 100 mm × 20 mm × 3 mm were placed on a device (Figure 16) devoted to facilitate the correct alignment and overlap of the joint. This equipment ensured also a constant adhesive layer thickness of 1 mm.

The adhesive layer was applied by means of a dual-component adhesive variable-ratio pneumatic dispenser (paragraph 3.1) in the case of PUR and MA adhesives, covering an overlap area of 25 mm × 20 mm; the joint configuration is represented in Figure 17.

Whereas, in the case of polyolefin HMA, the adhesive layer was applied by means of the melting gun, covering an overlap area of 12.5 mm × 20 mm according to standard ASTM D3163; the joint configuration is represented in Figure 18.

After bonding, two weights were placed on the specimens to ensure a uniform pressure over the overlapped surface, as shown in Figure 19.

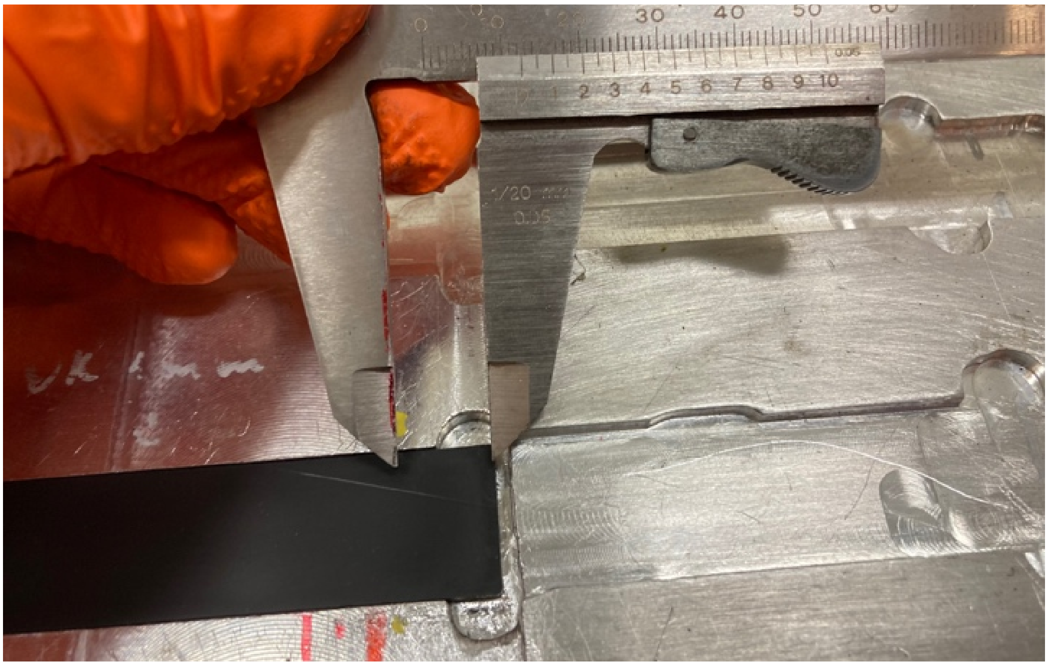

Figure 16: Positioning device for alignment and overlapping of the joint

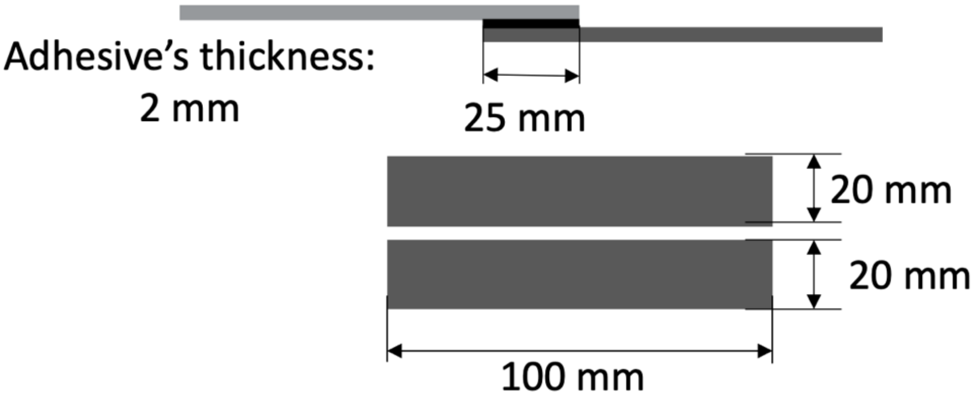

Figure 17: Single overlap joint configuration for the specimens bonded with the polyurethane adhesive and the methacrylate adhesive

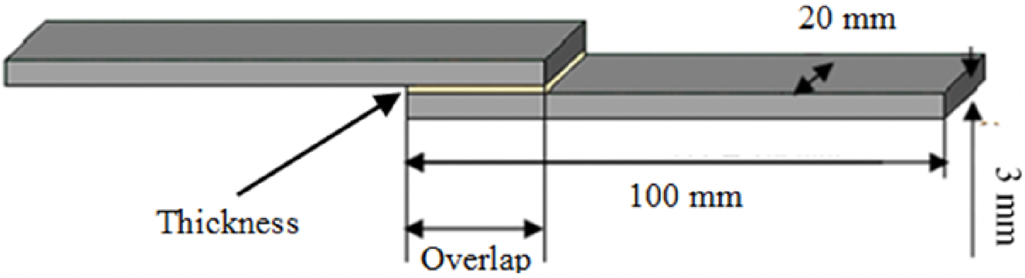

Figure 18: Single overlap joint configuration for the specimens bonded with the polyolefin HMA

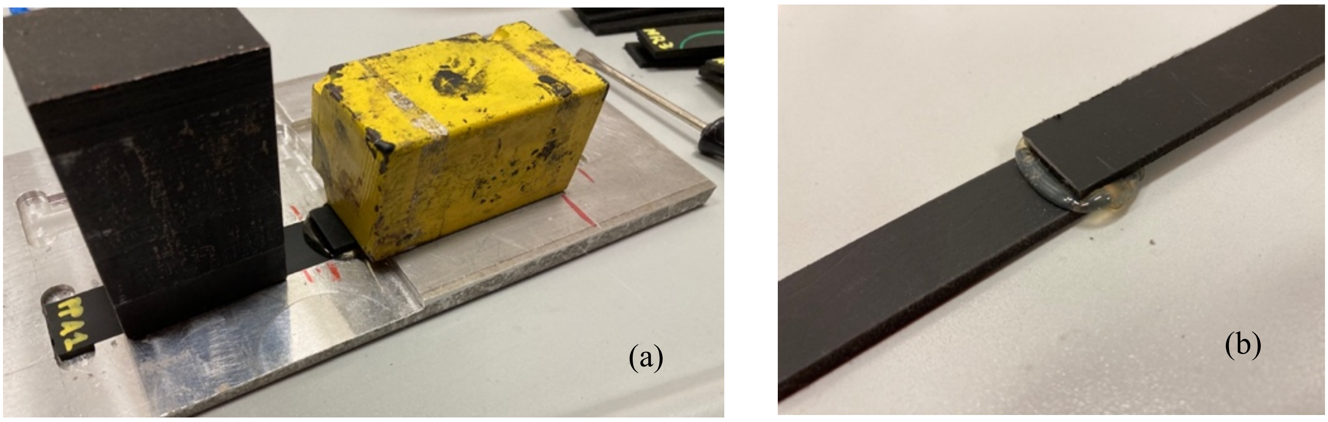

Figure 19: Joint layout after adhesive deposition (a) and after solidification (b)

Then, after the complete solidification of the adhesive, the excess adhesive was removed and lap shear tests were performed.

3.5 Lap shear test

A lap shear test was chosen in order to evaluate the influence of plasma treatments on the mechanical characteristics of single lap bonded joints, in particular, the shear strength and the adhesion properties variation.

For this study, an Instron test machine was used (paragraph 3.1) at a test speed of 5 mm/min (quasi-static test) and 100 mm/min (dynamic test). More than one sample were used for each treatment condition in order to have a statistical validation of the results.

The dynamic test was performed in order to evaluate the strain rate effect of the bonded joints. The strain rate effect is a phenomenon for which the yield strength of the specimen progressively increases by increasing the test velocity. Not all the materials are sensitive to strain rate effect (e.g., fibres in composite materials) but, in our case, the response is dominated by the adhesive which is a polymeric material and they are, by definition, sensitive to strain rate. In previous studies [45] it was demonstrated that a higher testing speed would lead to a more fragile behaviour of the joint and higher maximum loads since the adhesive is sensible to strain rate effect.

For this reason, it was decided to test the specimens treated with low-pressure Ar plasma (paragraph 4.8.2.2) at an higher test speed (more favourable condition of strain rate), in order to enhance a cohesive failure of the bonded joint.

The shear strength was computed considering the actual overlap area of each sample and the corresponding maximum load. The mean value for both shear strengths and maximum loads was taken as the resultant value.

The percentage standard deviation from the average was calculated for the maximum load values obtained from the lap shear test in order to have an idea about the repeatability of the results.

4 Results and discussion

In this study, two different production batches of substrate samples have been used, one for bonding the polyurethane and methacrylate adhesives, the other for bonding the polyolefin hot-melt adhesive.

The 1st production batch has been used for bonding the polyurethane and methacrylate adhesives, while the 2nd production batch has been used for bonding the polyolefin HMA.

The two production lots evidenced great differences in the chemical surface characterization probably due to a different use of release agents during the moulding production.

The treatments performed and analysed on the 1st production lot were focused on the use of air and nitrogen plasma at atmospheric pressure since, for bonding the polyurethane and methacrylate adhesives, the objective was to obtain the highest possible amount of oxygen on the PP surface and, theoretically, these gasses are the most suitable in order to reach this objective.

Whereas, low-pressure plasma system was used considering air, nitrogen and argon as process gasses in order to treat PP samples to be bonded with the polyolefin HMA.

4.1 Surface characterization of untreated samples (as received) –1st production lot

Such activity is aimed at discovering which are the chemical species present on the untreated surface of the substrate in order to understand whether they may affect the adhesion with the polyurethane and methacrylate adhesives considered in this study.

The characterization of the untreated substrates was performed on three samples in order to have statistically significant feedback.

Surfaces of the untreated samples were characterized by means of Scanning Electron Microscopy (SEM), Energy Dispersive X-Ray (EDX) and FTIR analysis in order to understand the base surface chemical properties of the substrates.

The two surfaces of the P sample do not show any difference one with respect to the other.

4.1.1 Scanning Electron Microscopy (SEM) analysis + EDX

Scanning electron microscopy (SEM) made it possible to view the morphology of the specimens at magnifications greater than optical microscopy and to carry out surface chemical analyses, by coupling with the EDX probe. Both secondary electrons (LFD) and backscattered electrons (DualBSD) were detected for the untreated substrates.

Figure 20 shows the images acquired on the untreated substrate at different magnifications. Whereas, the areal EDX analysis is represented in Figure 21.

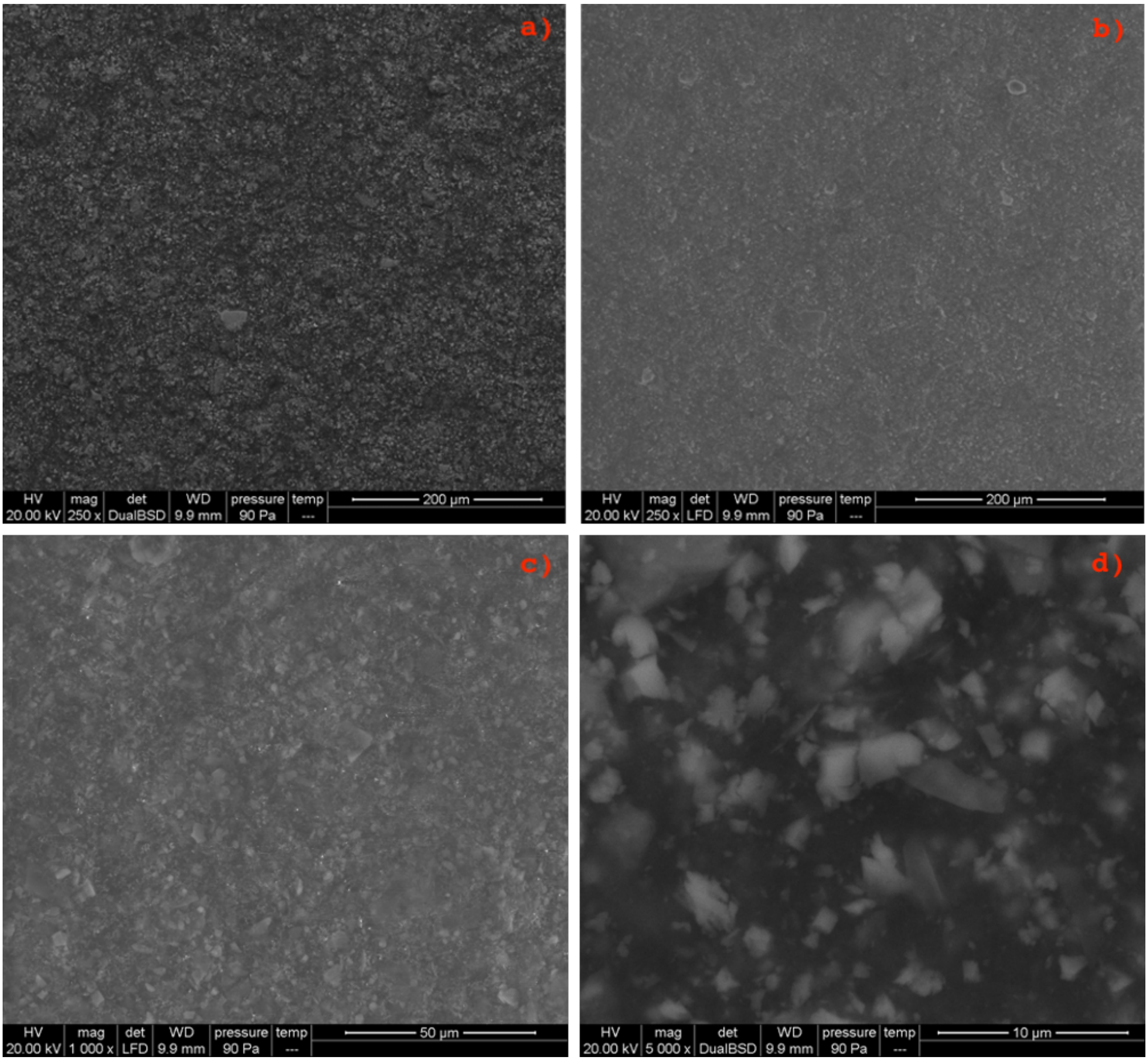

Figure 20: SEM images of untreated P sample - 1st lot:
a) 250x magnification (DualBSD), b) 250x magnification (LFD),
c) 1000x magnification (LFD), d) 5000x magnification (DualBSD)

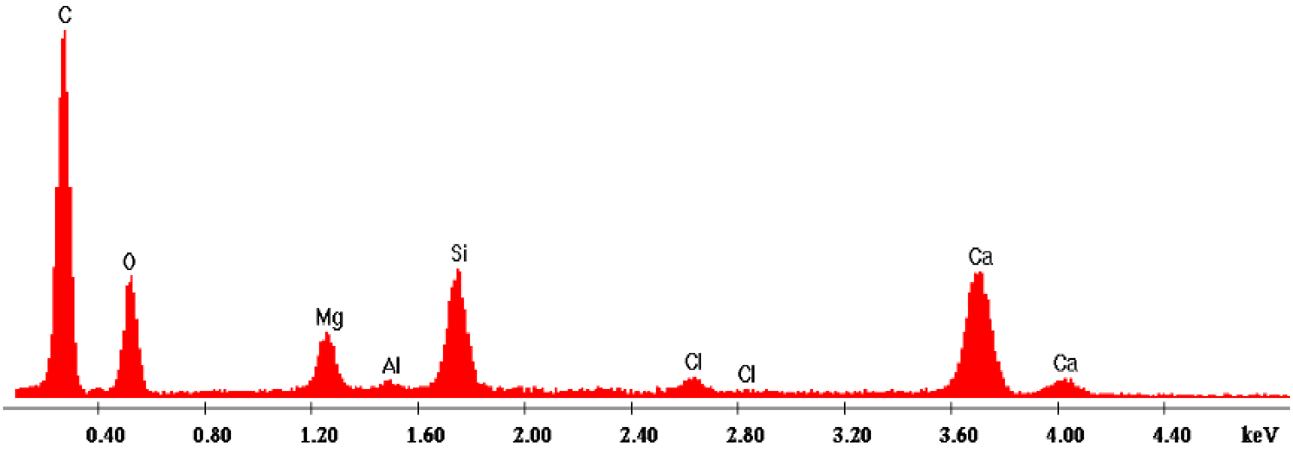

Element	***Wt. %***
C	62,67
O	21,08
Mg	2,38
Si	4,41
Ca	8,58
Al	0,36
Cl	0,52
TOTAL	100

Figure 21: Areal EDX analysis of untreated P sample - 1st lot

As can be seen, there is a great presence of magnesium (Mg) and silicon (Si), indicating the presence of a large quantity of talc. Moreover, a large amount of oxygen and calcium (Ca) is present, probably due to the massive use of release agents.

4.1.2 FTIR analysis

Considering all the three P samples, the acquired spectra are relatively identical, indicative of the fact that these specimens do not exhibit inhomogeneities. The infrared spectrum of untreated P sample in the range of 600-3500 cm^{-1} (Figure 22) covers the absorption due to the fundamental vibrations of the most common organic molecules.

It was acquired for P_1 but it is valid also for the other analysed specimens.

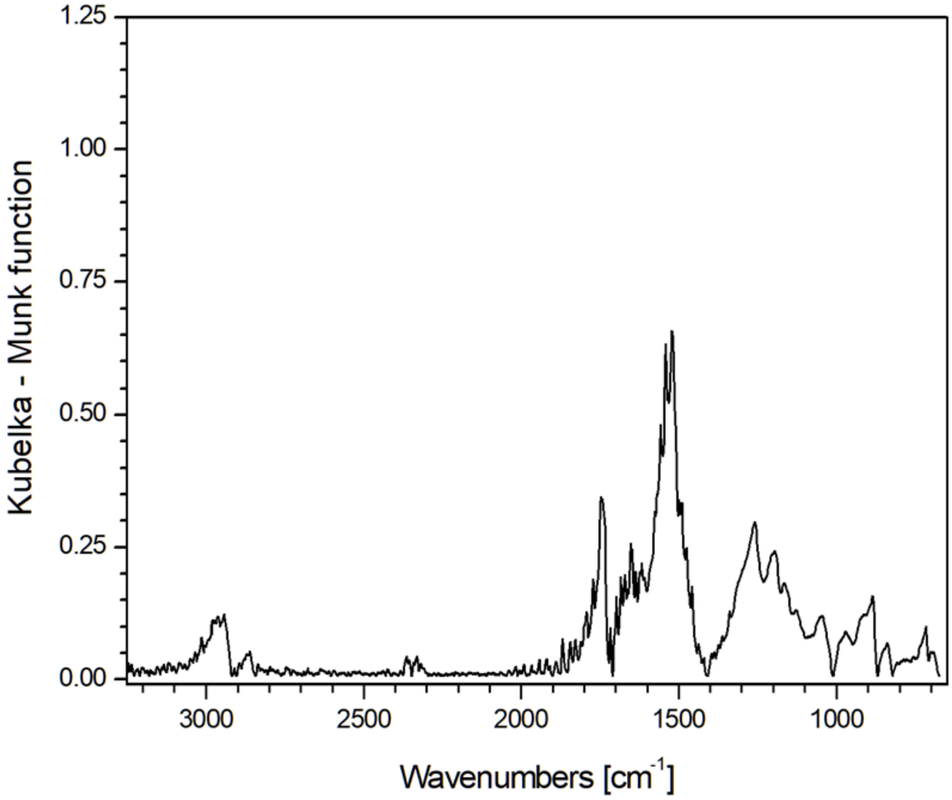

Figure 22: FTIR analysis of untreated P sample - 1st lot

4.2 Surface characterization of treated samples – 1st production lot

Such activity is aimed at understanding whether there are correlations between the adhesion properties and the surface functionalization after atmospheric pressure plasma treatment. More specifically, we want to know which are the chemical species that have been produced on the surface by the plasma treatment in order to understand whether they may affect the adhesion between the substrates and the polyurethane or methacrylate adhesives.

Surfaces of the treated samples were characterized by means of Scanning Electron Microscopy (SEM), Energy Dispersive X-Ray (EDX) analysis and FTIR analysis.

4.2.1 P samples treated with AIR plasma using CAPPJ system

4.2.1.1 SEM + EDX analysis

For this analysis, has been considered a lower magnification (125x) in order to evaluate also the macro-effect of the plasma exposure on the surface of the substrate.

The SEM images in Figure 23 evidence, considering the images at 125x magnification, more uniform morphology of the samples compared to the untreated ones. Whereas, higher magnifications do not show a significant change in the surface roughness.

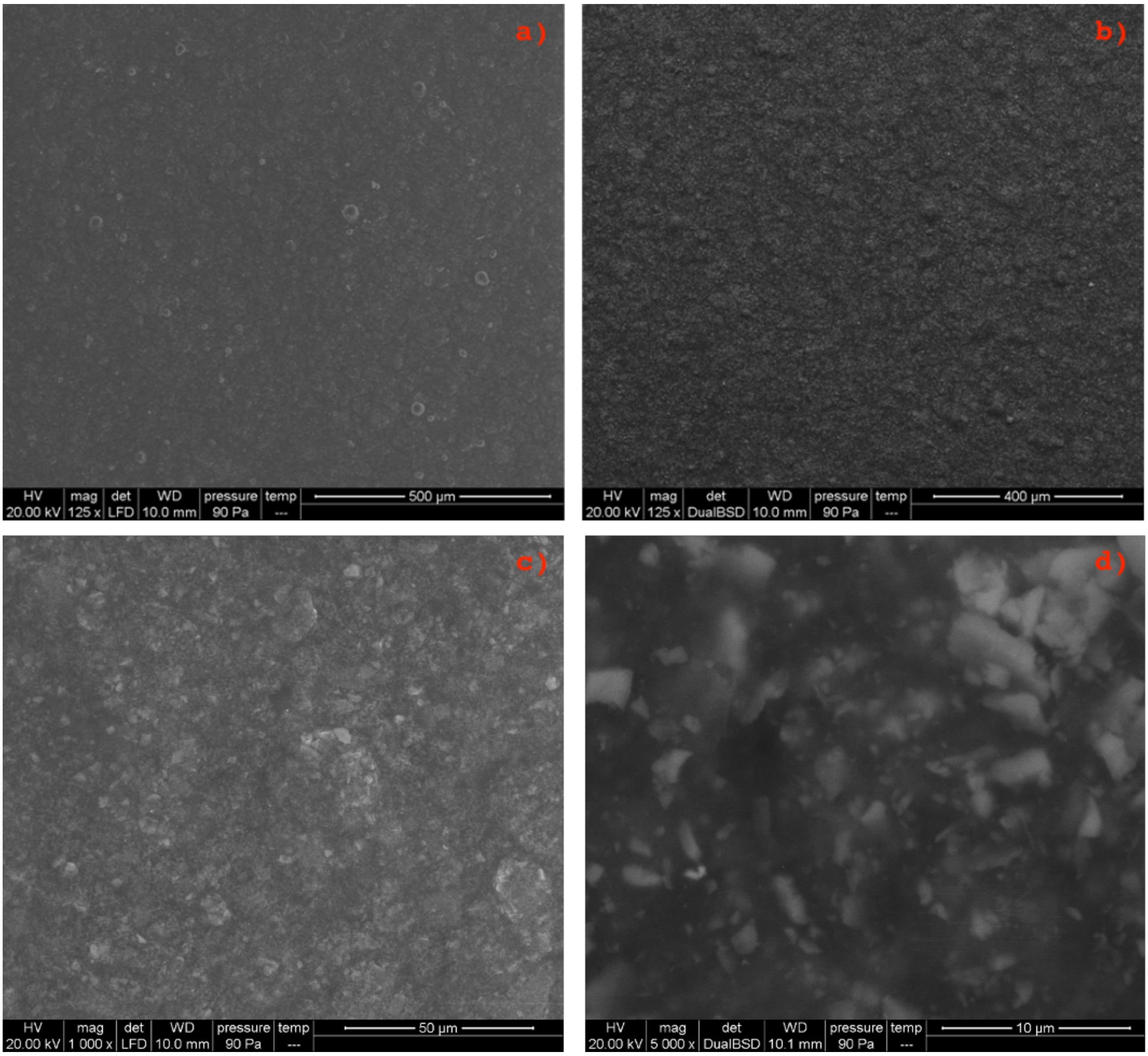

Figure 23: SEM images of atmospheric pressure air plasma treated P sample - 1st lot: a) 125x magnification (LFD), b) 125x magnification (DualBSD), c) 1000x magnification (LFD), d) 5000x magnification (DualBSD)

Figure 24 shows the areal EDX analysis. Comparing these results with the EDX analysis results of Figure 21, it is possible to say that the atmospheric pressure air plasma treatment does not show any significant change in the chemical surface composition with respect to the untreated substrate.

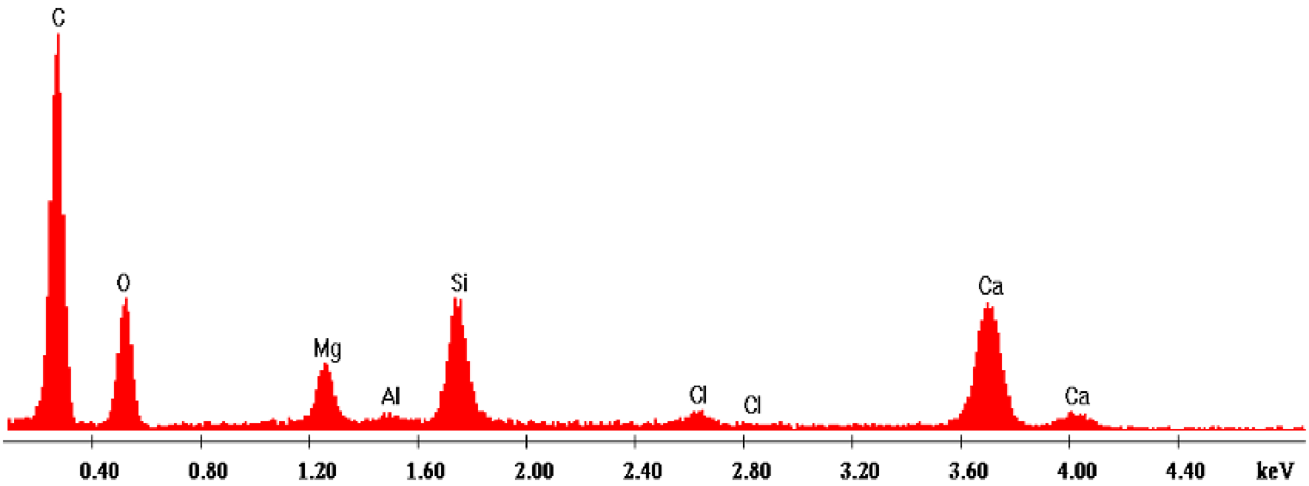

Element	***Wt. %***
C	62,88
O	21,77
Mg	2,36
Si	4,25
Ca	7,95
Al	0,28
Cl	0,51
TOTAL	100

Figure 24: Areal EDX analysis of atmospheric pressure air plasma treated P sample - 1st lot

4.2.1.2 FTIR analysis

The infrared spectrum of atmospheric pressure air plasma treated P sample in the range of 700-3300 cm^{-1} (Figure 25) covers the absorption due to the fundamental vibrations of the most common organic molecules. It shows that there is not a significant change in the spectrum of the treated specimen (blue curve) with respect to the untreated one (black curve).

There is a slightly increased functionality of C=O groups (band 1647, 1747 cm^{-1}). It is also possible to see an increase of the signal at 1100 cm^{-1} which is characteristic of the C-O functional group. Moreover, at 1380 – 1420 cm^{-1}, it is possible to see a less marked variation of the O-H vibrations (probably associated with C-OH (Alcohols) groups).

On the contrary, there is no increase of the signals at 3200 cm^{-1}, which is the characteristic wavenumber of the hydroxyl groups (-OH).

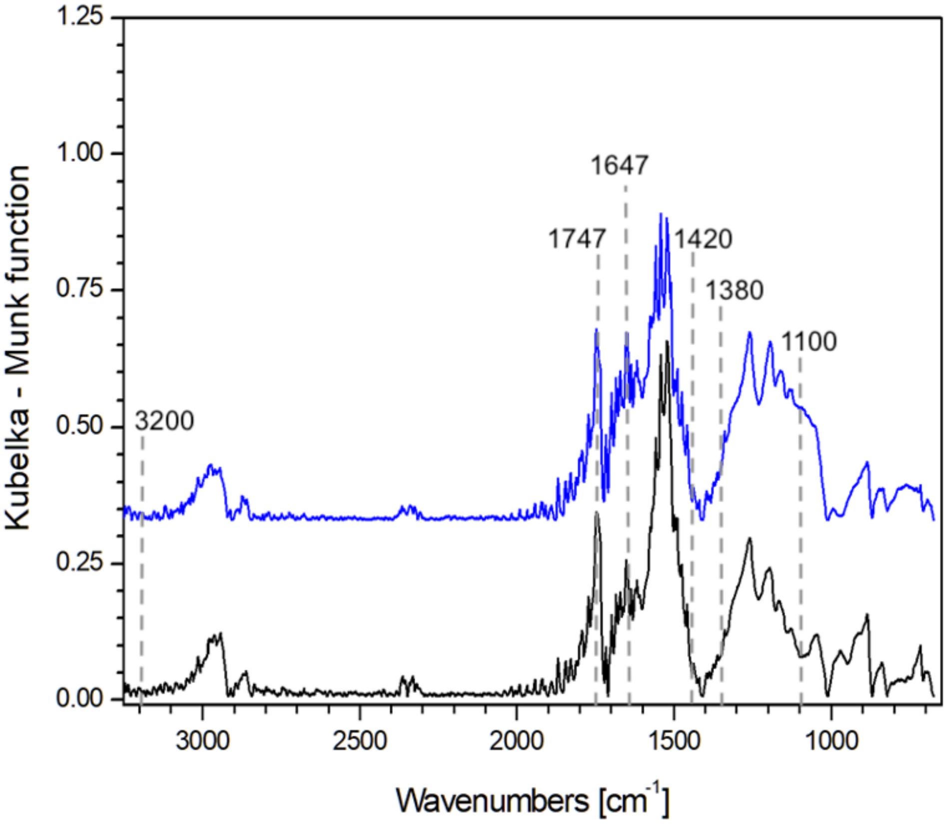

Figure 25: FTIR analysis of atmospheric pressure air plasma treated P sample - 1st lot

4.2.2 P samples treated with NITROGEN plasma using CAPPJ system

4.2.2.1 SEM + EDX analysis

The macro-effect of atmospheric pressure nitrogen plasma exposure on the surface of the substrate is slightly higher compared to the air plasma treatment. Indeed, from the SEM images in Figure 26, it is possible to see that, considering the images at higher magnification, the samples show a slight increment of the surface roughness.

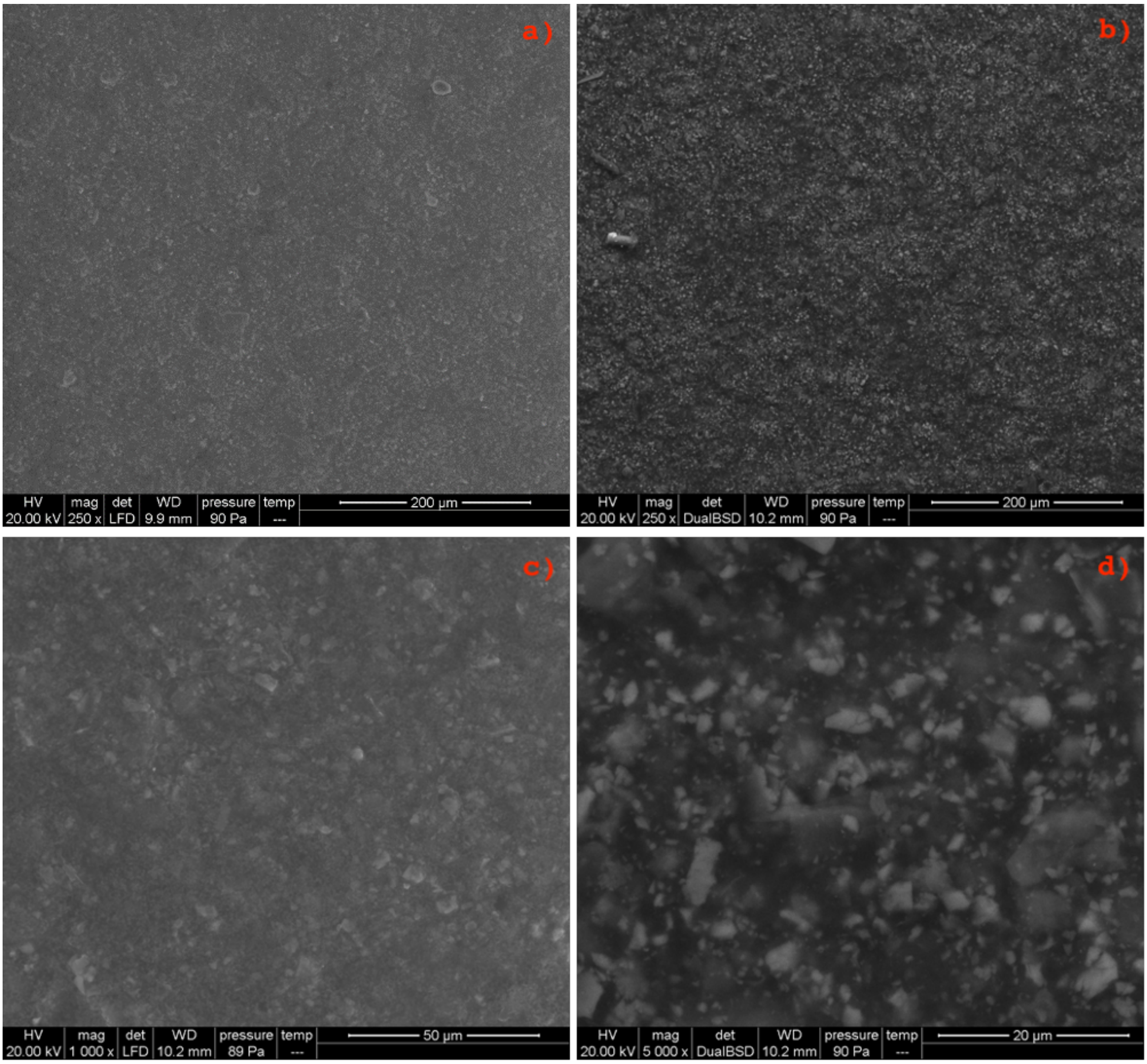

Figure 26: SEM images of atmospheric pressure nitrogen plasma treated P sample - 1st lot:
a) 250x magnification (LFD), b) 250x magnification (DualBSD),
c) 1000x magnification (LFD), d) 5000x magnification (DualBSD)

For what concerns the areal EDX analysis in Figure 27, this plasma treatment shows a sensible increase in oxygen concentration. Meaning that nitrogen plasma treatment has improved the polarity of the surface, making the substrate more suitable for bonding with the polyurethane or methacrylate adhesives.

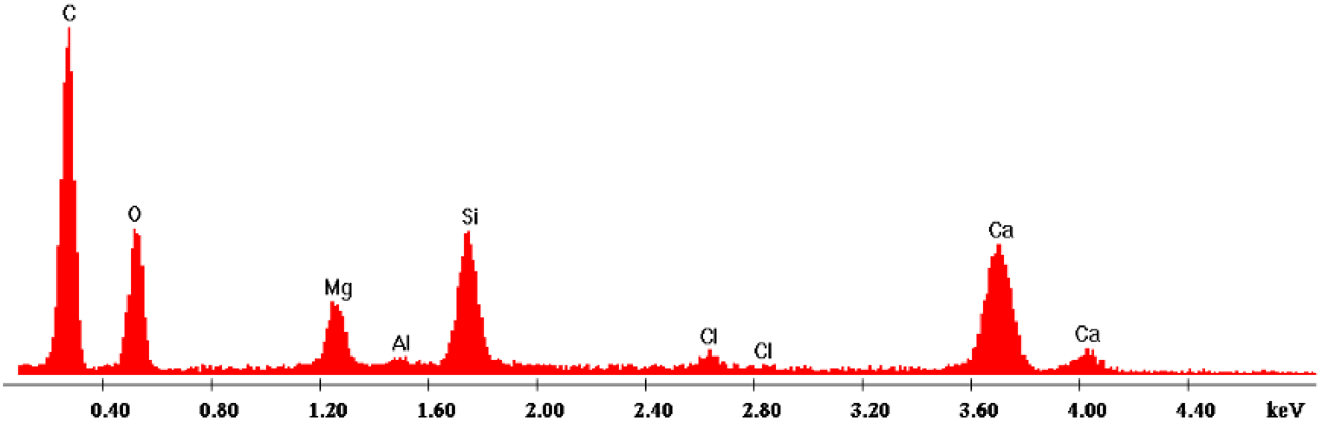

Element	***Wt. %***
C	56,3
O	26,28
Mg	2,77
Si	4,91
Ca	8,94
Al	0,25
Cl	0,55
TOTAL	100

Figure 27: Areal EDX analysis of atmospheric pressure nitrogen plasma treated P sample - 1st lot

This result is interesting since, even if the air contains oxygen itself, nitrogen plasma can produce a higher amount of it on the polypropylene surface.

This can be ascribed to the CAPPJ system which works in contact with the ambient air, allowing nitrogen to interact with the oxygen contained in the surrounding air.

4.2.2.2 Micro-IR spectroscopy

The infrared spectrum of atmospheric pressure N_2 plasma-treated P sample in the range of 700-3300 cm^{-1} (Figure 28) covers the absorption due to the fundamental vibrations of the most common organic molecules. It shows that there is a significant change in the spectrum of the treated specimen (red curve) with respect to the untreated ones (black curve).

There is an increased functionality of carbonyl (C=O) functional groups (band 1647, 1747 cm^{-1}). It is also possible to see an increase of the signal at 1100 cm^{-1} which is characteristic of the C-O functional group. Moreover, at 1380 – 1420 cm^{-1}, it is possible to see a great increase of the O-H vibrations (probably associated with C-OH (Alcohols) groups).

Contrary to what happened with air plasma, for nitrogen plasma we can see a sharp increase of the signal at 3200 cm^{-1}, which is the characteristic wavenumber of the hydroxyl groups (-OH).

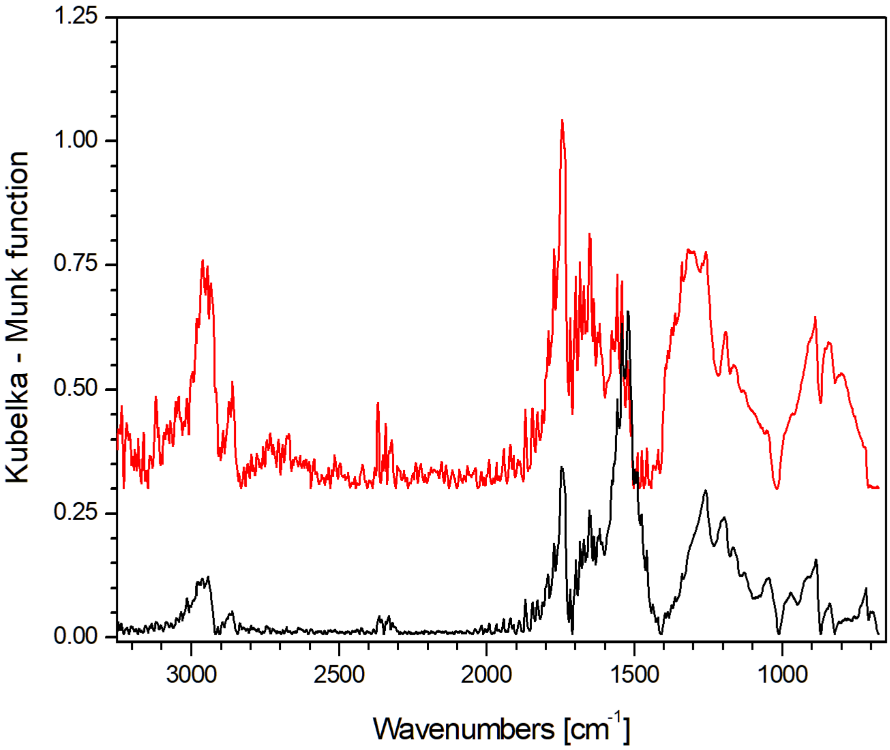

Figure 28: FTIR analysis of atmospheric pressure nitrogen plasma treated P sample - 1st lot

We can conclude that, atmospheric pressure nitrogen plasma treatment is a good solution in order to increase the surface energy of the polypropylene substrate, and so to effectively activate the surface before bonding.

4.3 Surface characterization of untreated samples (cleaned with cloth) – 2nd production lot

Such activity is aimed at assessing which are the chemical species present on the untreated surface of the substrate in order to understand whether they may affect the adhesion with the polyolefin hot-melt adhesive.

Also in this case, the characterization of the untreated substrates was performed on three samples in order to have statistically significant feedback.

Surfaces of the untreated samples were characterized by means of Optic Microscopy, Scanning Electron Microscopy (SEM) + EDX, Micro-Raman spectroscopy, Micro-IR spectroscopy and Attenuated Total Reflection (ATR) analysis in order to understand the base surface chemical properties of the substrates.

The two surfaces of the P sample do not show any difference one with respect to the other.

4.3.1 Optic microscopy

Through the use of optical microscopy, it was possible to visualize the morphology of the samples. Untreated substrates were optically analysed with a 10x magnification, as shown in Figure 29.

Lighter particles are present in all three samples, most likely due to the presence of talc and magnesite. The surface is smooth and it presents a non-uniform roughness.

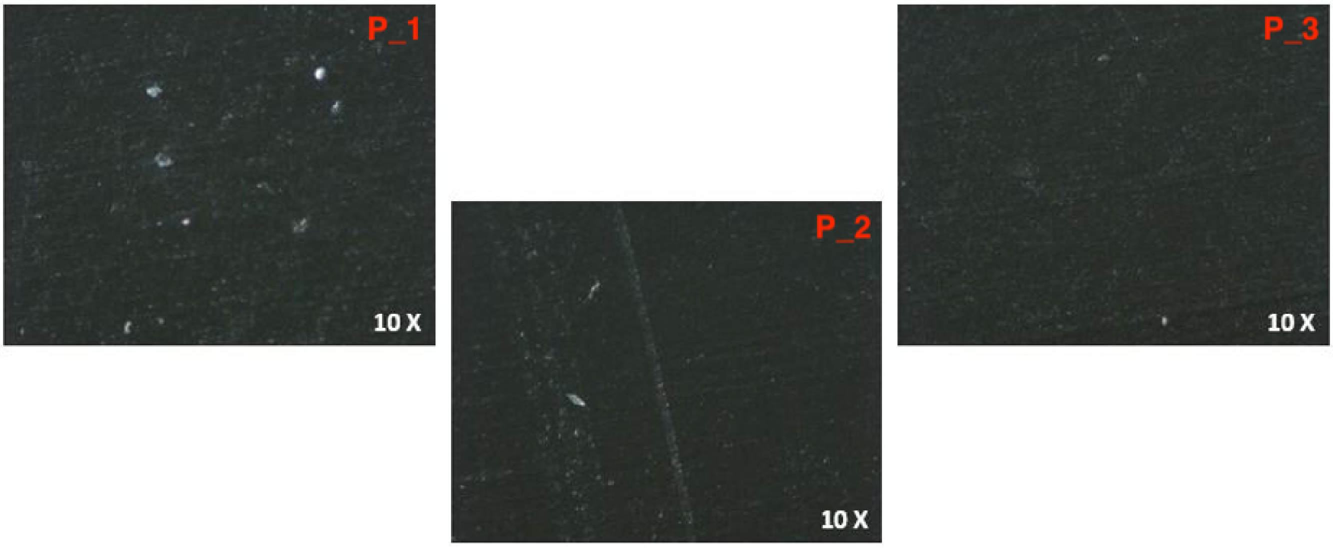

Figure 29: Untreated substrate surface magnification with optical microscopy (10x) – 2nd lot

4.3.2 Scanning Electron Microscopy (SEM) analysis + EDX

Scanning electron microscopy (SEM) makes it possible to see the morphology of the specimens at magnifications greater than optical microscopy and to carry out surface chemical analyses, by coupling with the EDX probe.

Both secondary electrons (LFD) and backscattered electrons (DualBSD) were detected for the untreated substrates.

Figure 30 shows the image acquired on the untreated substrate (P sample) at 500x magnification, with relative areal chemical analysis. As can be seen, there is the presence of magnesium and silicon, indicating the presence of talc on the surface.

Whereas, the magnification at 5000x, considering two specific punctual chemical analyses, is represented in Figure 31. In the analysis of "Point 2", in addition to magnesium (Mg) and silicon (Si) due to the presence of talc, sodium (Na) and chlorine (Cl) are also present, due to impurities or, more likely, to the use of release agents during the production.

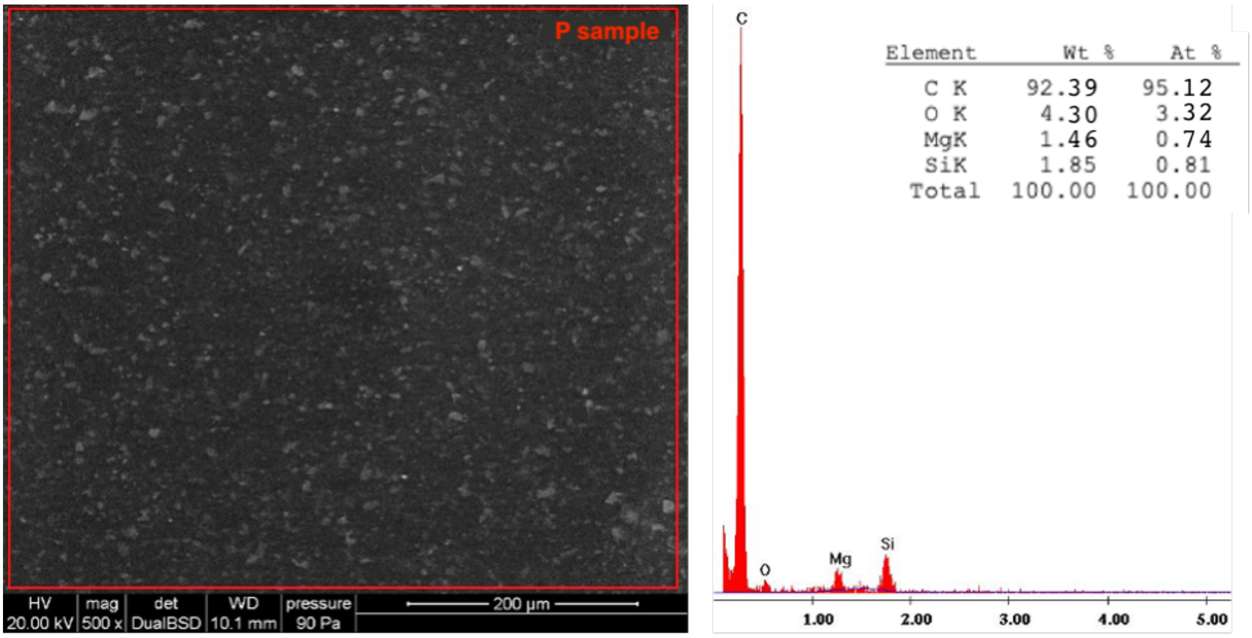

Element	Wt %	At %
C K	92.39	95.12
O K	4.30	3.32
MgK	1.46	0.74
SiK	1.85	0.81
Total	100.00	100.00

Figure 30: SEM image with 500x magnification and areal EDX analysis of untreated P sample (cleaned with cloth) – 2nd lot

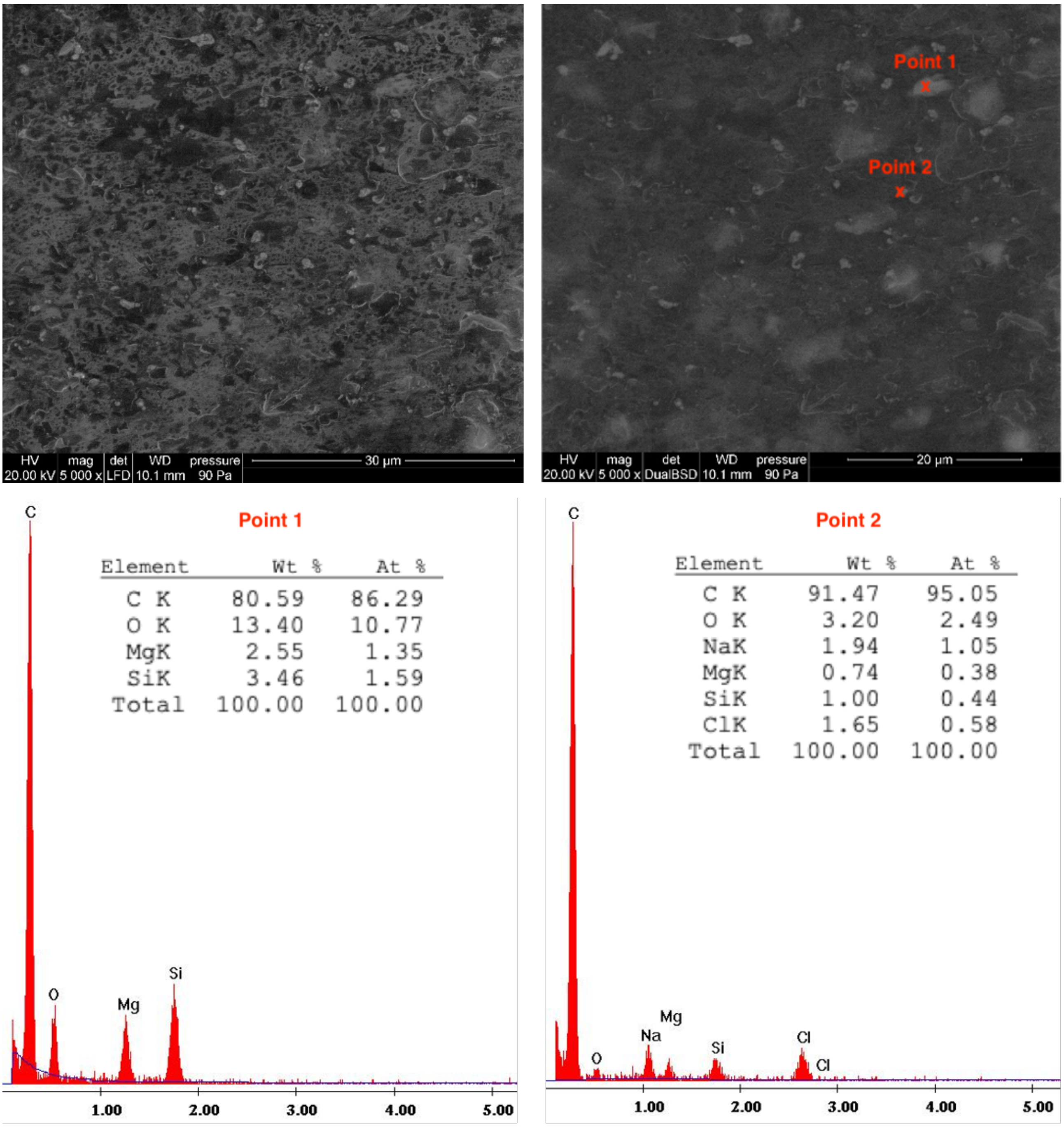

Point 1

Element	Wt %	At %
C K	80.59	86.29
O K	13.40	10.77
MgK	2.55	1.35
SiK	3.46	1.59
Total	100.00	100.00

Point 2

Element	Wt %	At %
C K	91.47	95.05
O K	3.20	2.49
NaK	1.94	1.05
MgK	0.74	0.38
SiK	1.00	0.44
ClK	1.65	0.58
Total	100.00	100.00

Figure 31: SEM images with 5000x magnification and punctual EDX analysis of untreated P samples (cleaned with cloth) – 2nd lot

4.3.3 Micro-IR spectroscopy

Considering all the three P samples, the acquired spectra are relatively identical, indicative of the fact that these specimens do not exhibit inhomogeneities. The infrared spectrum of untreated P sample in the range of 700-4000 cm^{-1} is shown in Figure 32. It was acquired for P_1 but it is valid also for the other analysed specimens.

Micro-IR characterization of P samples was performed in three different positions on the surface of the specimen in order to visualize any differences attributable to inhomogeneity of the sample: on the right (red line), in the middle (green line) and on the left (blue line). It shows the typical spectrum of polypropylene with the addition of talc and Carbon Black pigment.

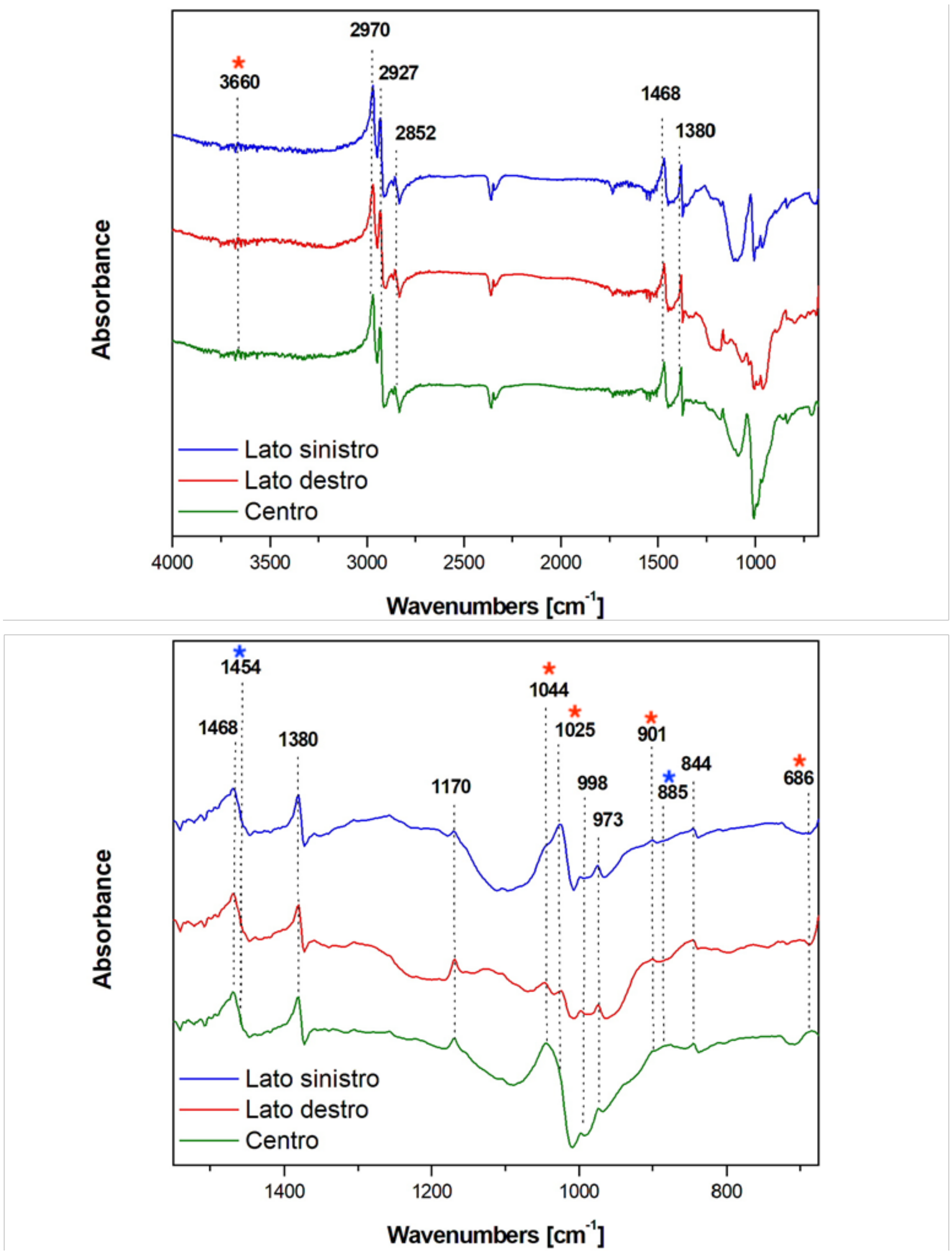

Figure 32: Micro-IR spectrum of untreated P sample – 2nd lot

From the spectrum it is possible to see some bands that are marked with an asterisk. The bands related to the presence of surface magnesite are highlighted in blue, whereas the bands relating to the presence of talc are highlighted in red.

Table 10 reports the main absorption peaks associated with the relative characteristic group vibrations for pure PP [46].

Wavenumbers [cm^{-1}]	Vibrational assignment
844	ν C-CH_3
973, 998, 1170	r -CH_3
1025	ν Si-O
1044	ν Si-O-Si
1380	δ_s -CH_3
1468	δ_s -CH_2-
2852	ν_s -CH_2-
2927	ν_{as} -CH_2-
2970	ν_{as} -CH_3

Table 10: Vibrational assignment for Micro-IR absorption peaks of untreated PP

In our spectrum represented in Figure 32, the absorption peak located at 844 cm^{-1} is assigned to C–CH_3 stretching vibration (ν). Absorption peaks displayed at 973, 998 and 1170 cm^{-1} are assigned to –CH_3 rocking vibration (r). Symmetric bending vibration mode (δ_s) of –CH_3 group is detected at 1380 cm^{-1}. The absorption peak observed at 2970 cm^{-1} is related to –CH_3 asymmetric stretching vibration (ν_{as}). All the previously referred absorption peaks are related to methyl group presence in the polypropylene. The peaks at 1468, 2852 and 2927 cm^{-1} are attributed to –CH_2– symmetric bending, –CH_2– symmetric stretching (ν_s) and –CH_2– asymmetric stretching, respectively [47, 48, 49]. The region of the infrared spectrum ranging from 3500 cm^{-1} and 600 cm^{-1} covers the absorption due to the fundamental vibrations of the most common organic molecules.

The goal is to verify both the grafting of oxygen-based functionalities and the increase in the degree of hydrophilia.

4.3.4 Attenuated Total Reflection (ATR) spectroscopy

The ATR characterization has been performed on three specimens and, as can be seen from the spectra in Figure 33, there are no particular differences between the three P samples analysed.

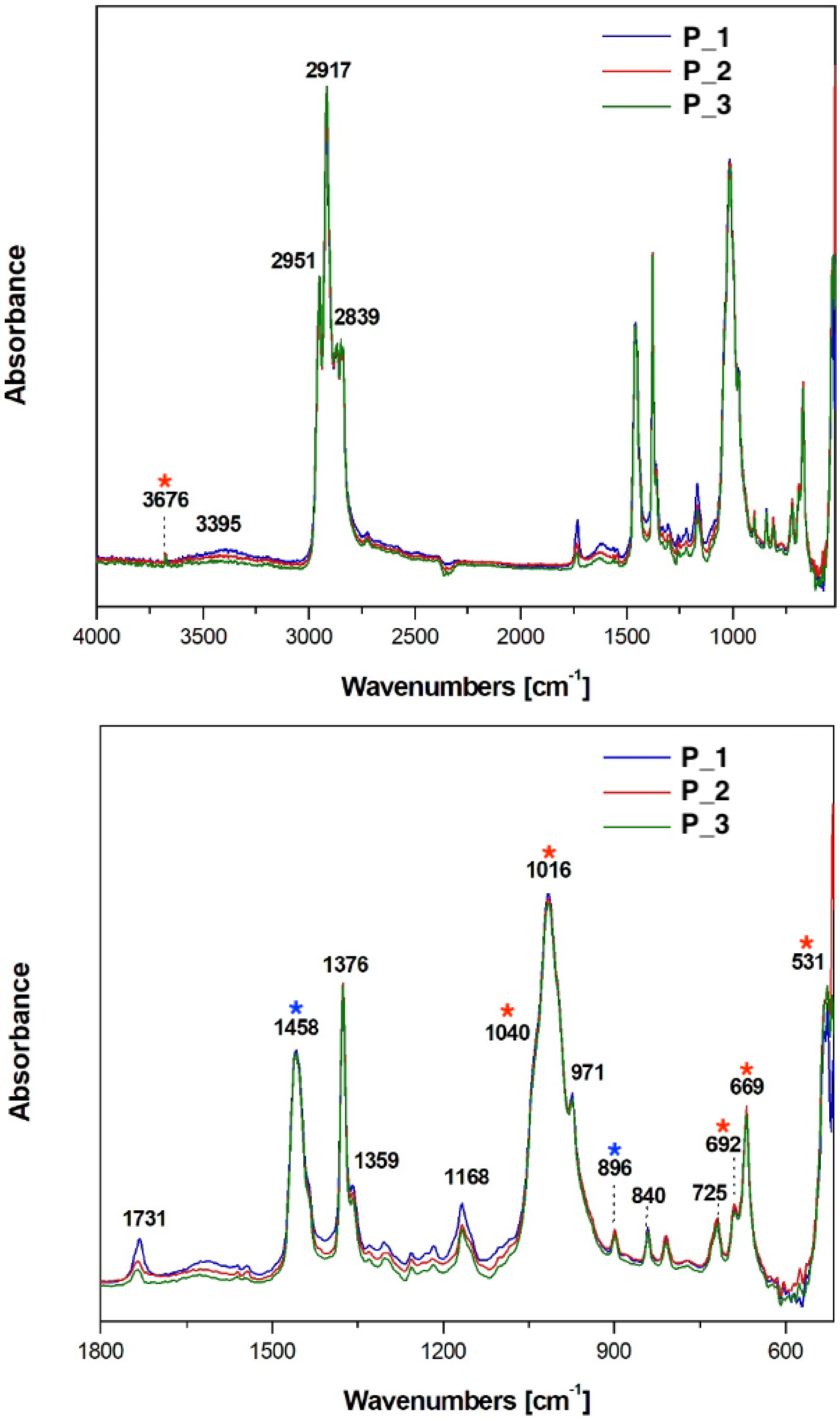

Figure 33: ATR characterization of untreated P samples – 2nd lot

From the spectrum, it is possible to see some bands that are marked with an asterisk. The bands related to the presence of surface magnesite are highlighted in blue, whereas the bands relating to the presence of talc are highlighted in red.

Table 11 reports the assignment of the bands of the ATR spectra. The assignments relative to the main talc bands are highlighted.

Wavenumbers [cm^{-1}]	**Vibrational assignment**
669	OH libration
840	ν C-CH_3
971, 997, 1168	r -CH_3
1016	ν Si-O
1040	ν Si-O-Si
1376	δ_s -CH_3
1458	δ_s -CH_2-
2839	ν_s -CH_2-
2917	ν_{as} -CH_2-
2951	ν_{as} -CH_3

ν = stretching vibration
r = rocking vibration
δ = bending vibration
s = symmetric
as = asymmetric

Table 11: Assignment of the main bands of the ATR spectra of untreated P samples

4.3.5 Micro-Raman spectroscopy

Micro-Raman characterization of untreated P samples was performed on three specimens and, also in this case, the results showed good repeatability and consistency with the previous analysis. Micro-Raman spectra of untreated P samples in the range of 300-4000 cm^{-1} are shown in Figure 34. The vibrational assignments of the Raman peaks of isotactic PP are given in Table 12 for comparative purposes [46, 50]. As can be noted in the resultant PP spectra, also Micro-Raman spectroscopy confirms the results obtained in the previous characterizations.

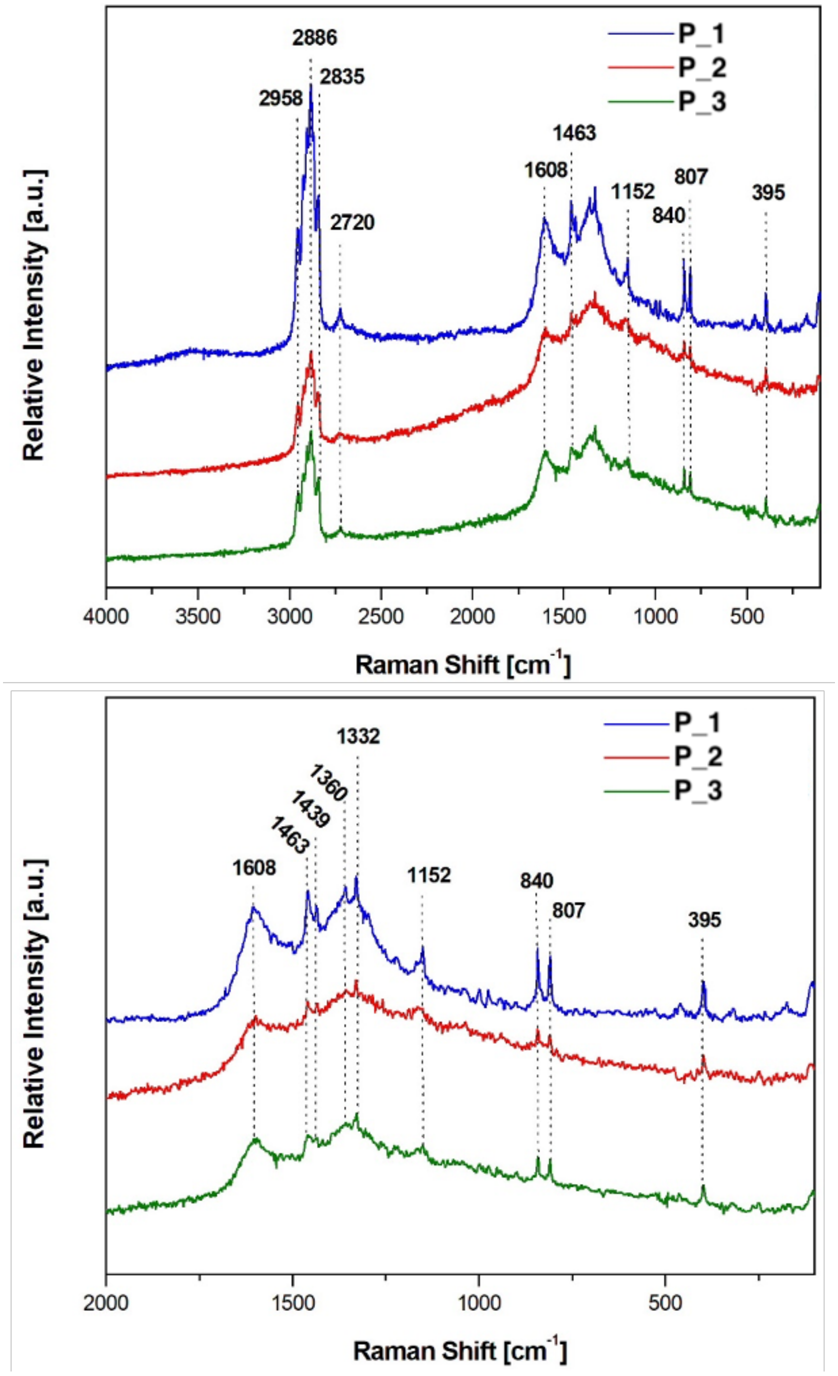

Figure 34: Micro-Raman spectra of untreated P samples – 2nd lot

Raman Shift [cm^{-1}]	**Vibrational assignment**
808	r (CH_2), ν (C-C)
841	r (CH_2)
972	r (CH_3), ν (C-C)
998	r (CH_3)
1151	ν (C-C), δ (CH)
1168	ν (C-C), r (CH_3), w (C-C)
1220	t (CH_2), w (CH), ν (C-C)
1330	δ (CH), t(CH_2)
1360	δ_s (CH_3)
1435	δ_{as} (CH_3)
1459	δ (CH_2)
2840	δ_s (CH_2)
2885	ν_s (CH_3), ν_s (CH_2)
2905	ν (CH)
2953	ν_{as} (CH_3), ν_{as} (CH_2)

Table 12: Vibrational assignments for Raman bands of isotactic polypropylene

Raman spectrum of pure PP from 500 to 1500 cm^{-1} includes C–C backbone stretching vibrations (ν), –CH2– deformation and –CH3 deformation vibrations whereas from 2600 to 3000 cm^{-1} it includes –CH2– and –CH3 stretching vibration modes [46].

Referring to Figure 34, Raman peaks at 808 and 840 cm^{-1} are due to the vibrations of molecules in the crystalline phase (rocking vibration of –CH2– and C–C stretching vibration) and the vibrations of helical molecules contained in the amorphous regions, respectively.

Raman peaks at 975, 999, 1152 and 1170 cm^{-1} are assigned to the rocking vibration mode (r) of –CH3 group. The bands at 1170 and 1220 cm^{-1} are ascribed to the stretching of C–C, which is related to the stress-sensitive molecular deformation [47, 51, 50, 52].

Moreover, the peak at 1170 cm^{-1} represents also the wagging vibration (w) of C–C, whereas the peak at 1220 cm^{-1} is ascribed also to the wagging vibration of CH and the twisting vibration (t) of –CH2– groups.

The peak at 1332 cm^{-1} is associated with the bending mode of the CH and the twisting mode of –CH2– groups. Bands sited at 2886 cm^{-1} and 2953 cm^{-1} are ascribed to the CH_3 symmetric stretching (ν_s) and asymmetric stretching (ν_{as}) vibration mode, respectively. Symmetric and asymmetric stretching vibration modes of –CH2– group are associated with the peaks at 2886 and 2953 cm^{-1}, respectively. The band at 2905 cm^{-1} corresponds to CH stretching vibration mode.

Raman band displayed at 1360 cm^{-1} is related to –CH3 symmetric bending (δ_s) vibration mode. Raman peaks at 1439 and 1463 cm^{-1} region can be assigned to the asymmetric bending (δ_{as}) vibration mode of –CH3 group [53, 49].

The differences between the assignments of the peaks present in Table 12 and those shown in Figure 34 can be considered negligible.

4.4 Surface chemical characterization of untreated samples washed with n-heptane – 2nd production lot

Such activity is aimed at understanding whether there are variations in the chemical composition on the untreated P sample surface after the washing with n-heptane. More specifically, we want to know which are chemical species present on the surface in order to understand whether they may affect the adhesion between the substrates and the polyolefin hot-melt adhesive.

Surfaces of the untreated samples washed with n-heptane were characterized by means of Scanning Electron Microscopy (SEM), Energy Dispersive X-Ray (EDX) analysis and Attenuated Total Reflection (ATR) spectroscopy in order to understand the base surface chemical properties variation of the substrates.

After washing with n-heptane, the surface of the substrate appears lighter, as shown in Figure 35, probably due to the removal of the carbon black pigment and the contaminants on the surface.

Figure 35: Surface of the untreated P sample after washing with n-heptane

4.4.1 SEM + EDX analysis

Scanning electron microscopy (SEM) analysis made it possible to see differences in morphology and chemical composition of the substrate's surface after the surface pre-treatment with n-heptane.

Both secondary electrons (LFD) and backscattered electrons (DualBSD) were detected for the untreated substrates.

Figure 36 displays the images acquired on the untreated substrate (P sample) washed with n-heptane at different magnifications.

Whereas, Figure 37 shows the areal EDX analysis based on the red area of Figure 36,b).

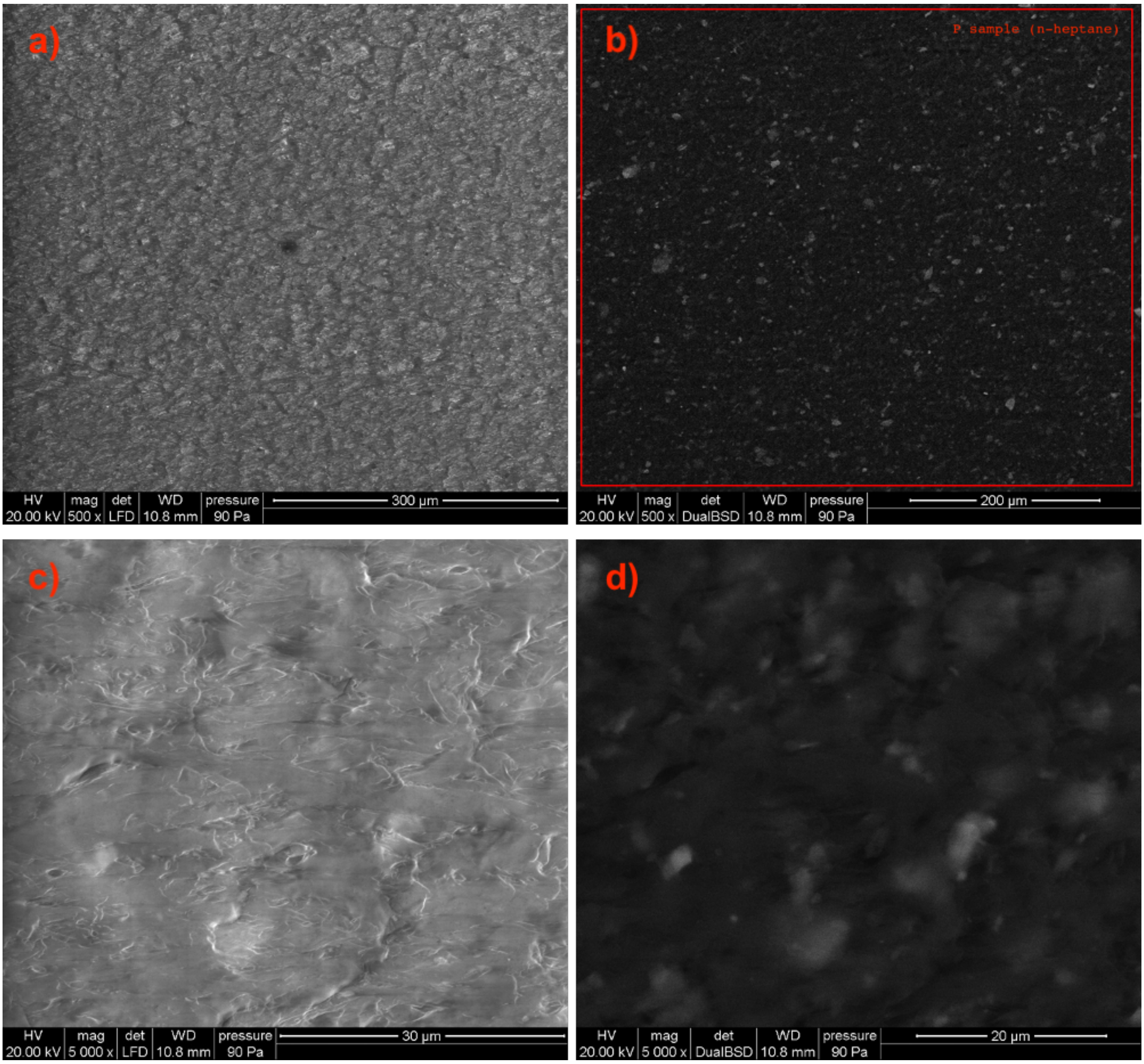

Figure 36: SEM images of untreated P sample (washed with n-heptane) – 2nd lot:
a) 500x magnification (LFD); b) 500x magnification (DualBSD);
c) 5000x magnification (LFD); d) 5000x magnification (DualBSD)

As can be noted from the EDX areal analysis, the presence of oxygen is sharply decreased with respect to the sample cleaned with just a cloth (paragraph 4.3.2).

This phenomenon can be ascribed to the removal of releasing agent waxes/contaminants or of the carbon black pigments from the surface.

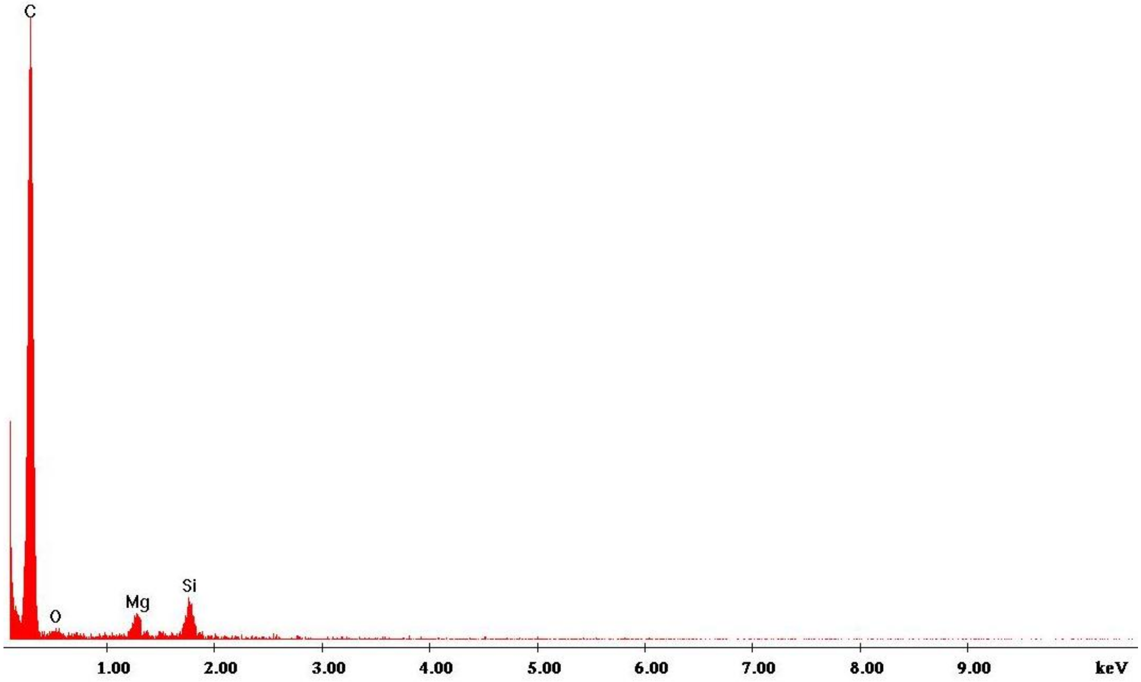

Element	Wt %	At %
C K	93.58	96.05
O K	3.11	2.40
MgK	1.42	0.72
SiK	1.88	0.83
Total	100.00	100.00

Figure 37: Areal EDX analysis of untreated P samples washed with n-heptane

This result led us to think that this pretreatment can improve the adhesion of the substrates with the polyolefin hot-melt adhesive considered in this study.

4.4.2 ATR spectroscopy

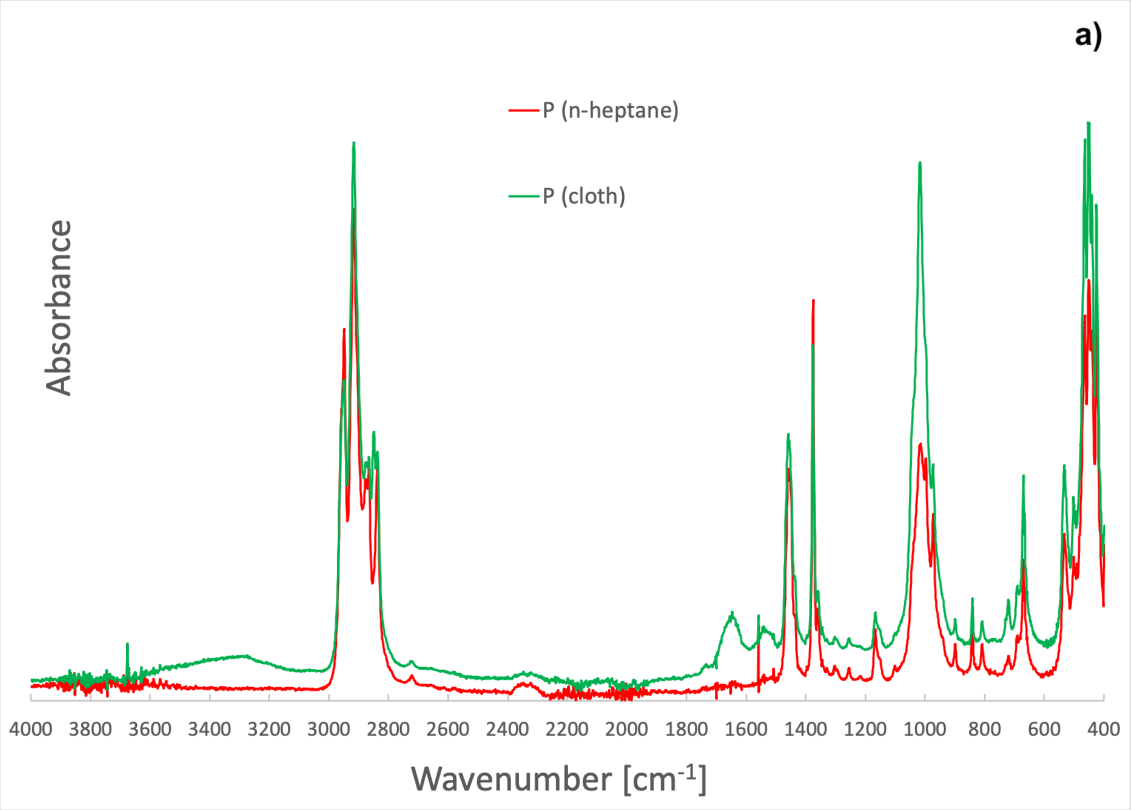

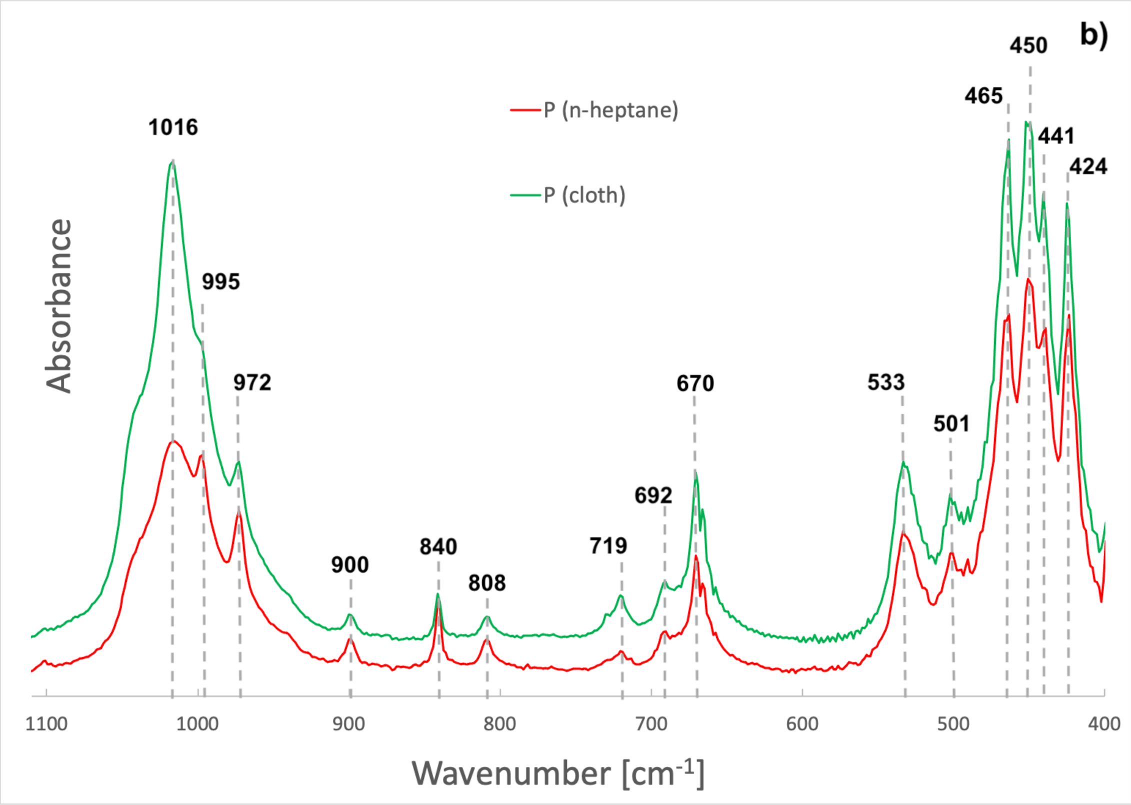

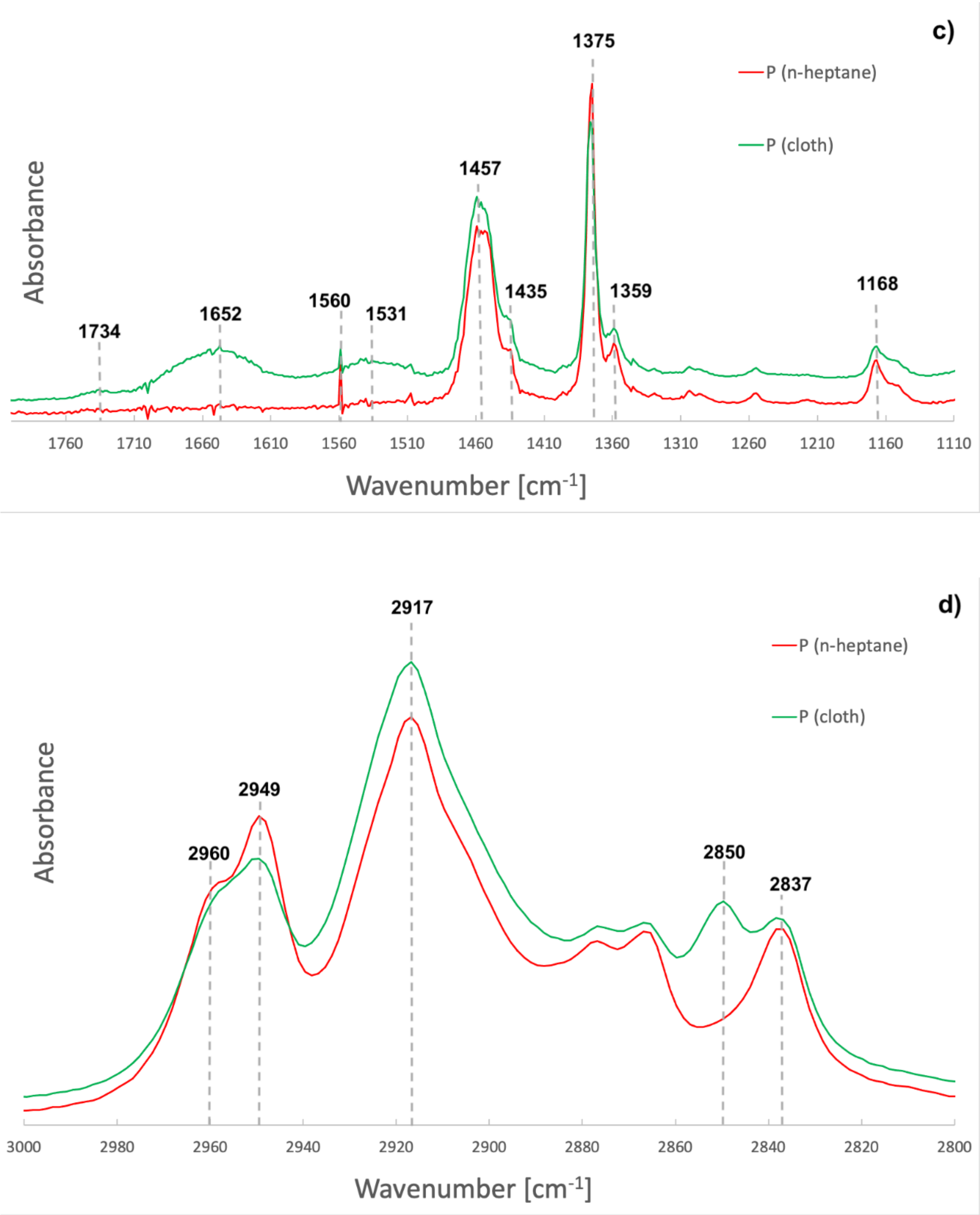

Figure 38: ATR analysis for untreated P samples before and after pretreatment with n-heptane – 2^nd^ lot: a) complete diagram from 400 to 4000 cm^{-1}; b) diagram from 400 to 1110 cm^{-1}; c) diagram from 1110 to 1800 cm^{-1}; d) diagram from 2800 to 3000 cm^{-1};

The main absorption peaks associated with the relative characteristic group vibrations of polypropylene have been already presented in paragraph 4.3 .

The ATR analysis shows that a simple cleaning with a cloth is not sufficient to remove the pollutants present on the surface. On the contrary, the use of n-heptane has allowed the almost total elimination of pollutants (most likely waxes used as release agents). Indeed, the characteristic peaks of polypropylene are visible.

4.5 Surface characterization of treated samples – 2nd production lot

Such activity is aimed at understanding whether there are correlations between the adhesion properties and the surface functionalization after low-pressure plasma treatment.

More specifically, we want to know which are the chemical species that have been produced on the surface by the plasma treatment in order to understand whether they may affect the adhesion between the components and the polyolefin hot-melt adhesive.

Surfaces of the treated samples were characterized by means of Scanning Electron Microscopy (SEM), Energy Dispersive X-Ray (EDX) analysis and Attenuated Total Reflection (ATR) spectroscopy.

4.5.1 P samples treated with AIR plasma using Low-Pressure Plasma system

4.5.1.1 SEM + EDX analysis

Scanning electron microscopy (SEM) analysis made it possible to see differences in morphology and chemical composition of the substrate's surface after the plasma treatment using low-pressure air plasma. Both secondary electrons (LFD) and backscattered electrons (DualBSD) were detected for the plasma-treated substrates.

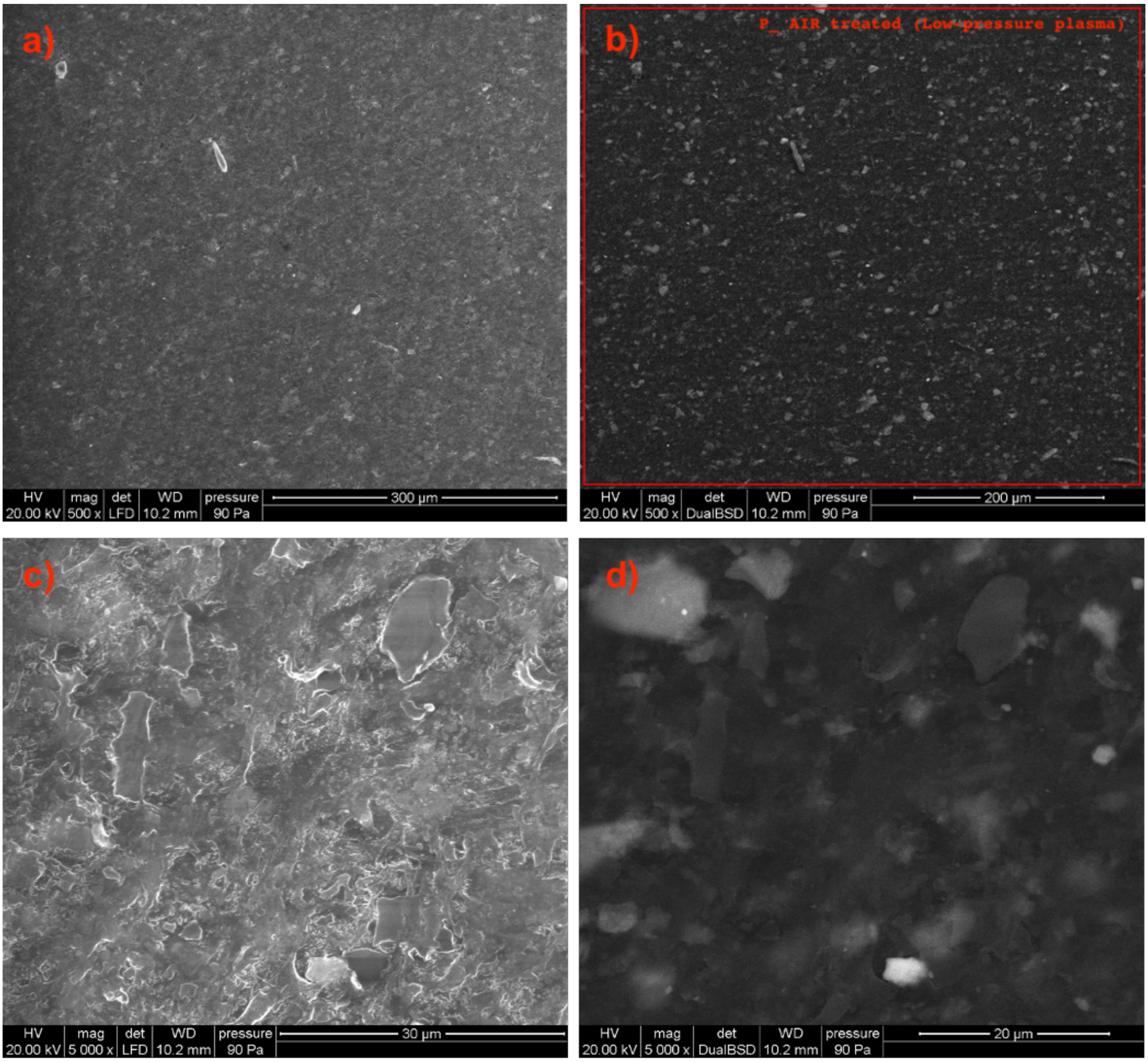

Figure 39: SEM images of low-pressure air plasma-treated sample (cleaned with a cloth before treatment):
a) 500x magnification (LFD); b) 500x magnification (DualBSD);
c) 5000x magnification (LFD); d) 5000x magnification (DualBSD)

Figure 39 displays the images acquired on the plasma-treated substrate (simply cleaned with a cloth before treatment) at different magnifications.

Whereas, Figure 40 shows the areal EDX analysis based on the red area of Figure 39,b).

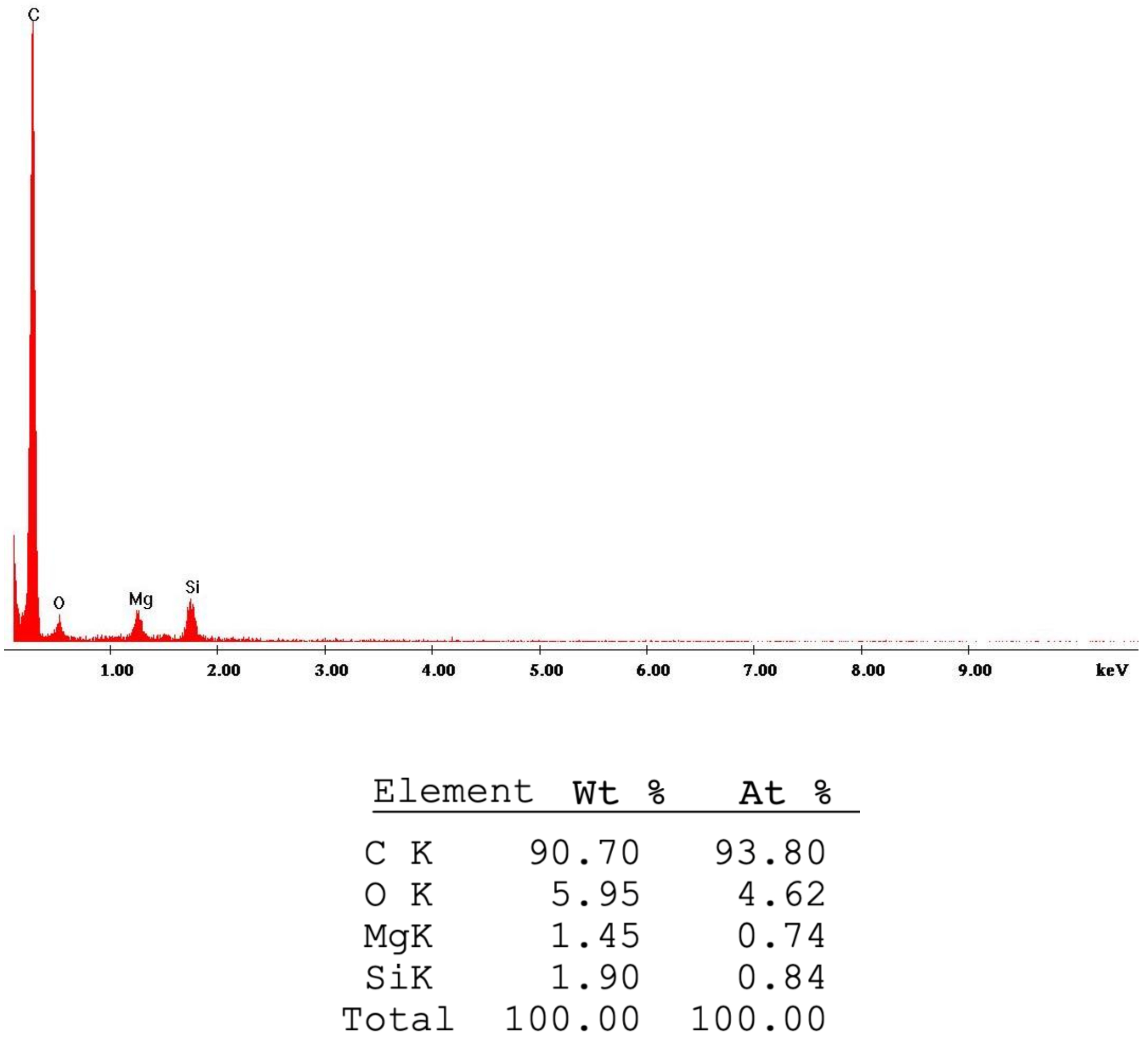

Element	Wt %	At %
C K	90.70	93.80
O K	5.95	4.62
MgK	1.45	0.74
SiK	1.90	0.84
Total	100.00	100.00

Figure 40: Areal EDX analysis of low-pressure air plasma-treated samples (cleaned with a cloth before treatment)

From the areal EDX analysis, it is possible to see that low-pressure air plasma treatments lead to a sharp increase in the amount of oxygen on the surface with respect to the untreated samples.

Compared to the untreated sample simply cleaned with a cloth (paragraph 4.3.2) we have an increase in the amount of oxygen on the surface of about the 40% more.

Whereas, compared to the untreated sample pre-treated with n-heptane (paragraph 4.4.1) we have an increase in the amount of oxygen on the surface of about the 93% more.

This result suggests that this treatment is not suitable for bonding the PP substrates with the polyolefin hot-melt adhesive.

4.5.1.2 ATR spectroscopy

From the comparison between the ATR analysis performed on untreated P samples simply cleaned with a cloth (Figure 38) and on the surface of the P sample after the low-pressure plasma treatment using air as process gas, shown in Figure 41, it is possible to see that there not relevant variation in the chemical composition after the plasma treatment.

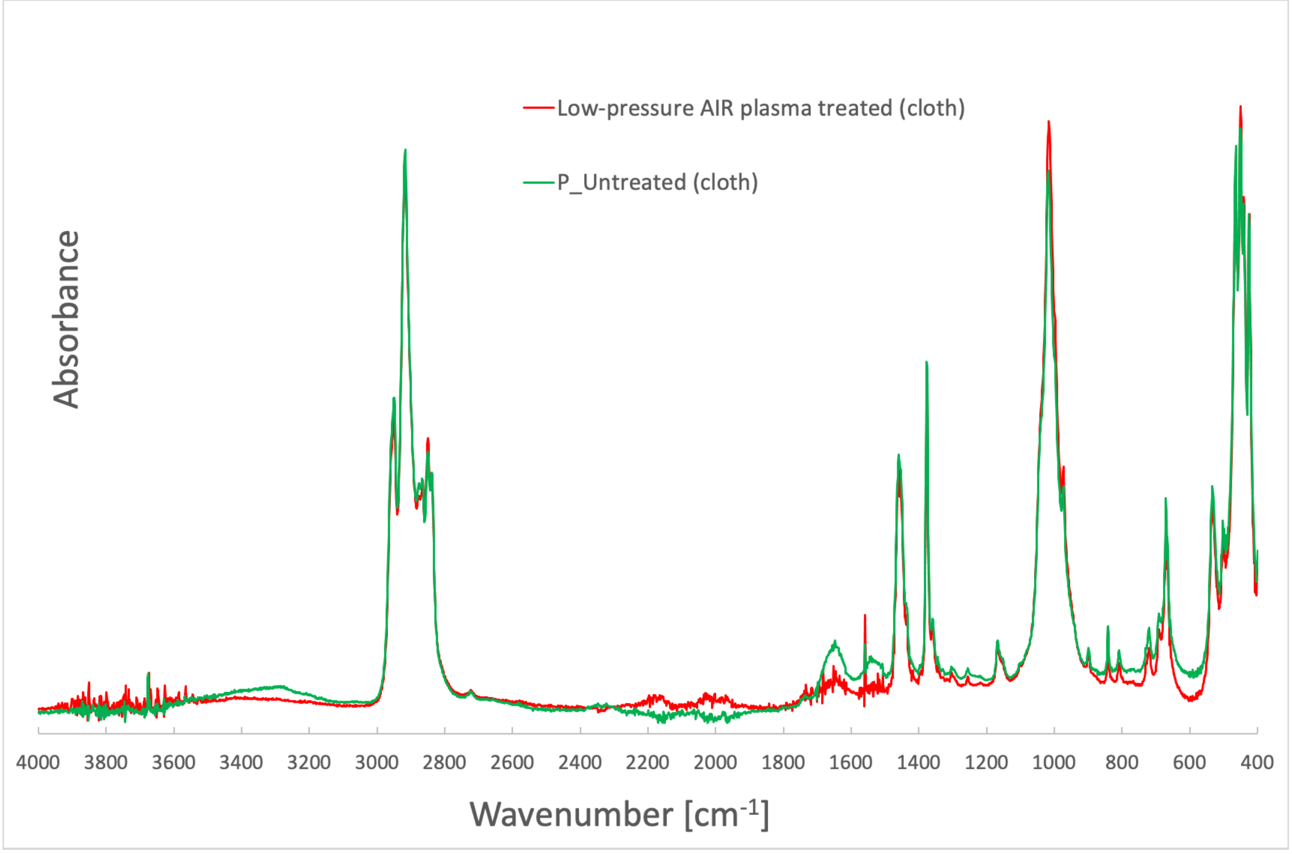

Figure 41: ATR analysis of low-pressure air plasma-treated samples (cleaned with a cloth before treatment)

4.5.2 P samples treated with NITROGEN plasma using Low-Pressure Plasma system

4.5.2.1 SEM + EDX analysis

Scanning electron microscopy (SEM) analysis made it possible to see differences in morphology and chemical composition of the substrate's surface after the plasma treatment using low-pressure N_2 plasma. Both secondary electrons (LFD) and backscattered electrons (DualBSD) were detected for the plasma-treated substrates.

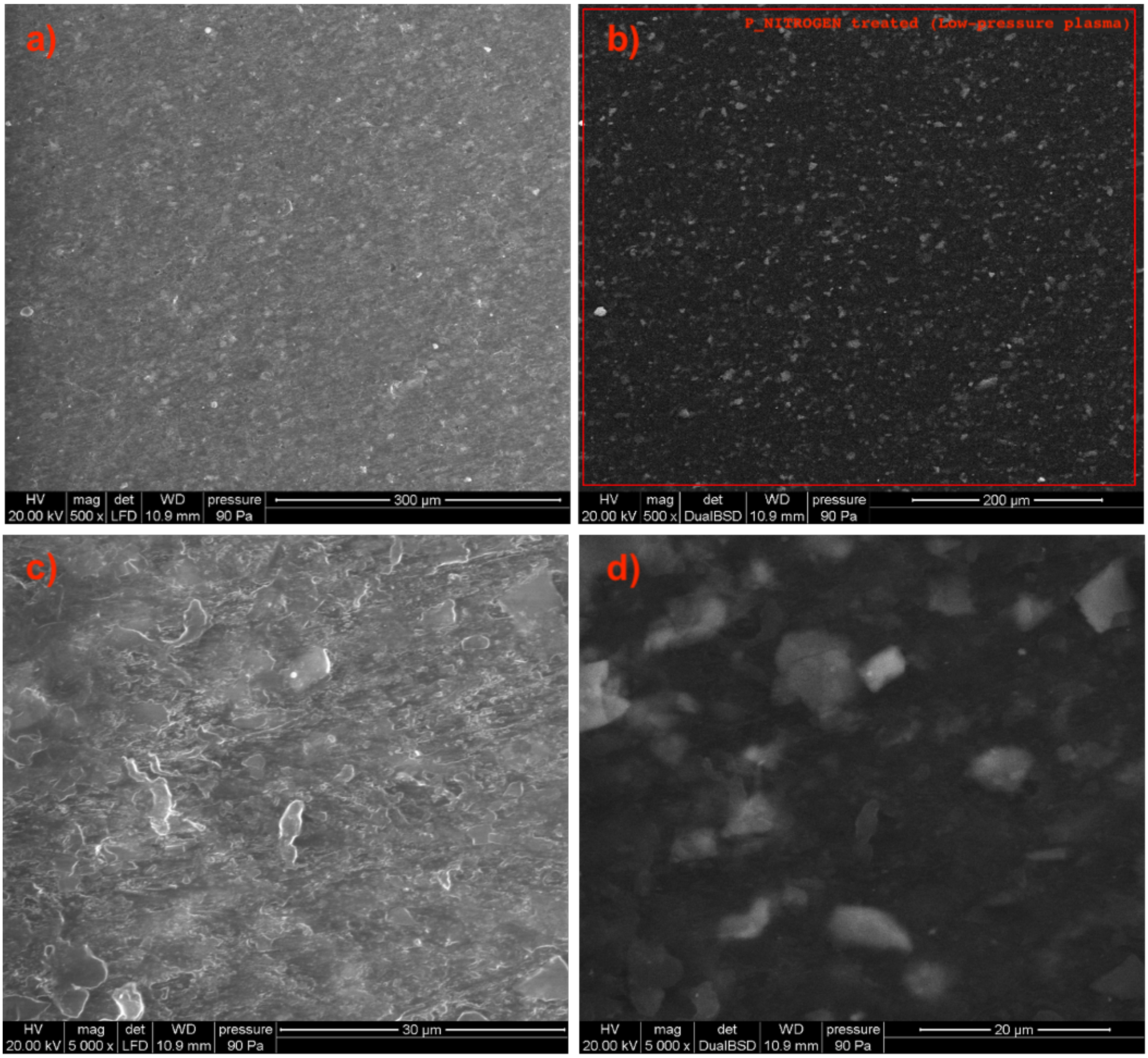

Figure 42: SEM images of low-pressure nitrogen plasma-treated sample (cleaned with a cloth before treatment) – 2nd lot:
a) 500x magnification (LFD); b) 500x magnification (DualBSD);
c) 5000x magnification (LFD); d) 5000x magnification (DualBSD)

The images acquired on the plasma-treated substrate (simply cleaned with a cloth before treatment) at different magnifications are represented in Figure 42. Whereas, the areal EDX analysis based on the red area of Figure 42,b) is represented in Figure 43.

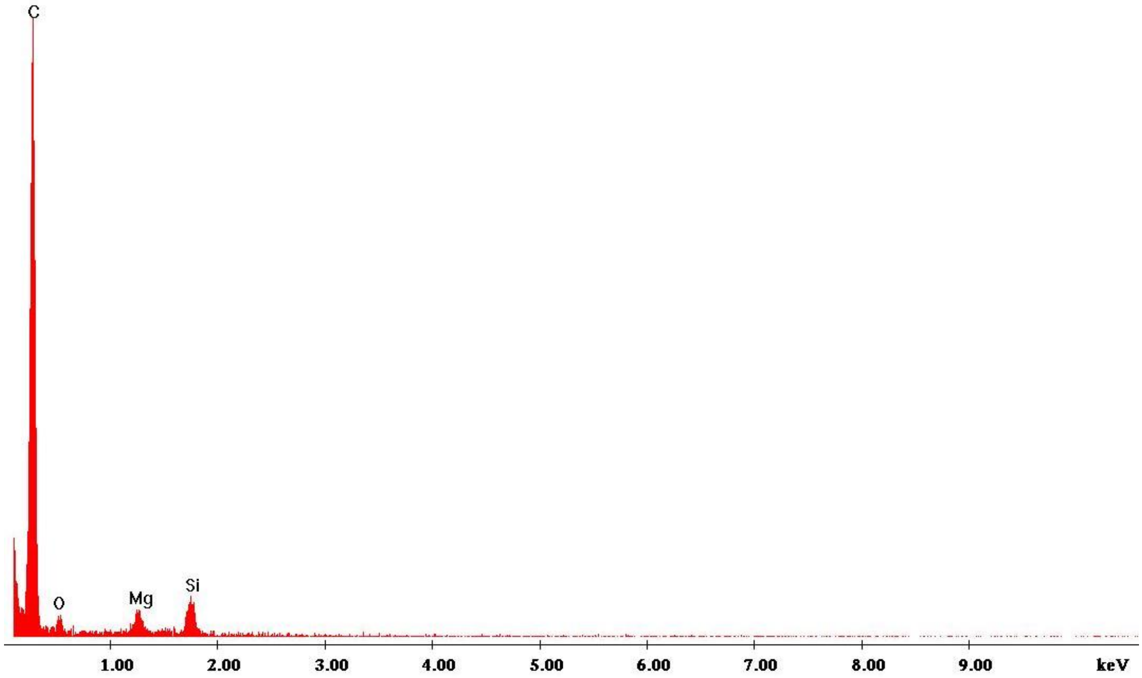

Element	Wt %	At %
C K	91.33	94.22
O K	5.63	4.36
MgK	1.23	0.63
SiK	1.80	0.79
Total	100.00	100.00

Figure 43: Areal EDX analysis of low-pressure nitrogen plasma-treated samples (cleaned with a cloth before treatment)

From the areal EDX analysis, it is possible to see that low-pressure N_2 plasma treatments lead to a sharp increase in the amount of oxygen on the surface with respect to the untreated samples.

Compared to the untreated sample simply cleaned with a cloth (paragraph 4.3.2) we have an increase in the amount of oxygen on the surface of about the 30% more.

Whereas, compared to the untreated sample pre-treated with n-heptane (paragraph 4.4.1) we have an increase in the amount of oxygen on the surface of about the 82% more.

This result suggests that this treatment is not suitable for bonding the PP substrates with the polyolefin hot-melt adhesive.

4.5.2.2 ATR spectroscopy

From the comparison between the ATR analysis performed on untreated P samples simply cleaned with a cloth (Figure 38) and on the surface of the P sample after the low-pressure plasma treatment using N_2 as process gas, shown in Figure 44, it is possible to see that there not relevant variation in the chemical composition after the plasma treatment.

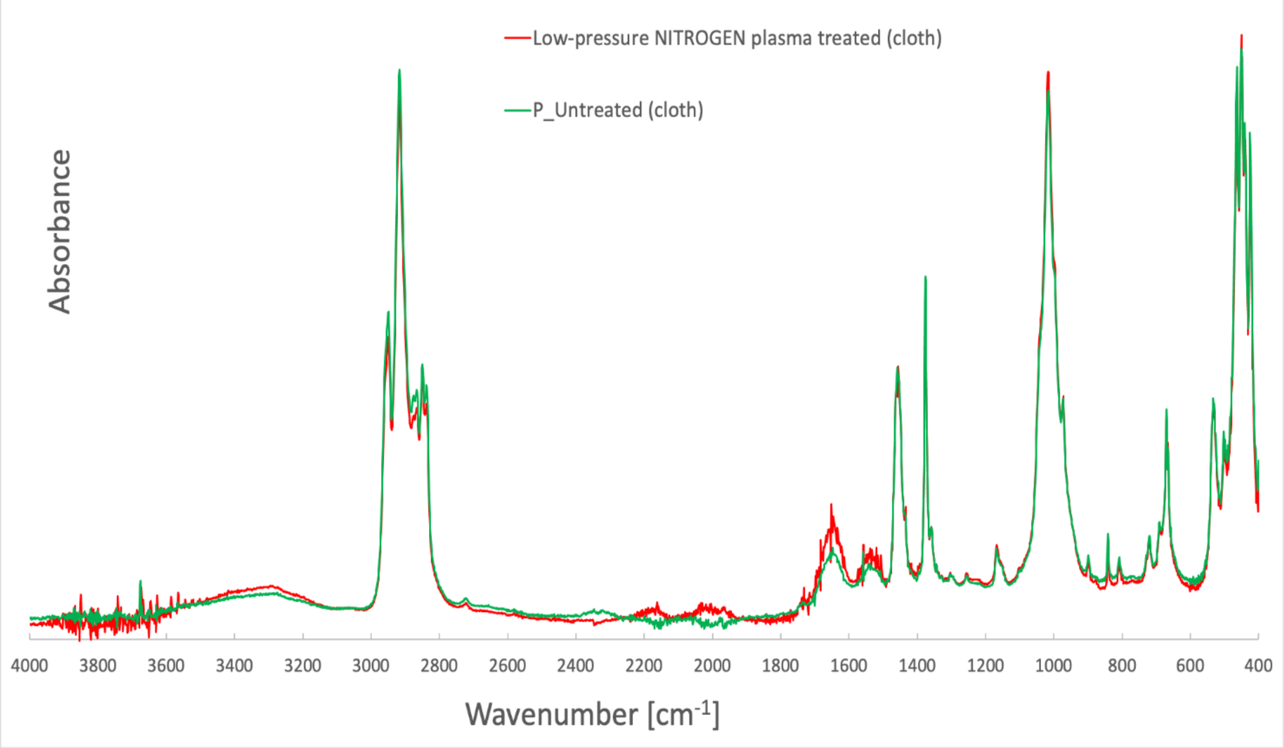

Figure 44: ATR analysis of low-pressure nitrogen plasma-treated samples (cleaned with a cloth before treatment)

4.5.3 P samples treated with ARGON plasma using Low-Pressure Plasma system

4.5.3.1 SEM + EDX analysis

Scanning electron microscopy (SEM) analysis made it possible to see differences in morphology and chemical composition of the substrate's surface after the plasma treatment using low-pressure Ar plasma. Both secondary electrons (LFD) and backscattered electrons (DualBSD) were detected for the plasma-treated substrates.

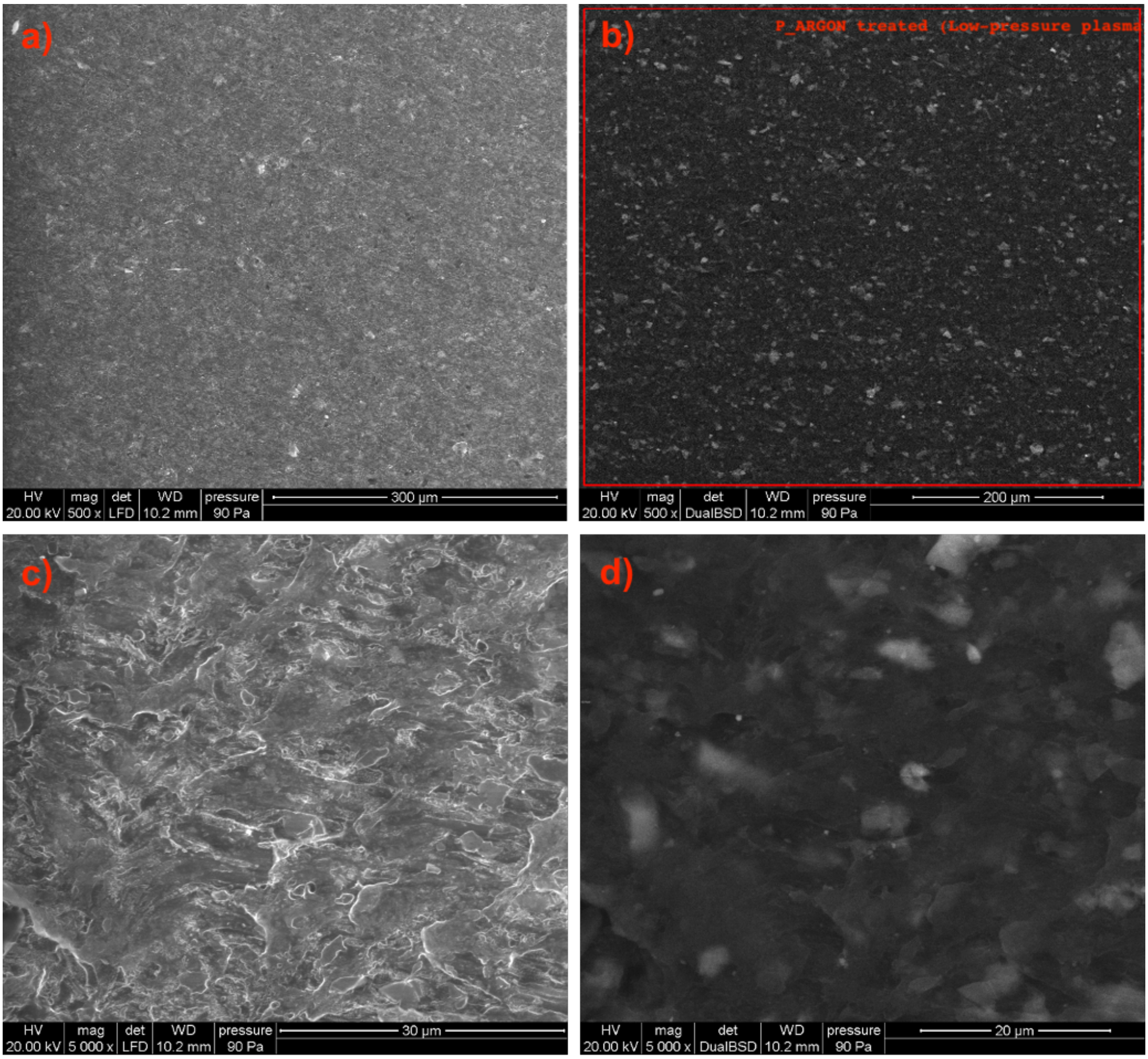

Figure 45: SEM images of low-pressure argon plasma-treated sample (cleaned with a cloth before treatment) – 2nd lot:
a) 500x magnification (LFD); b) 500x magnification (DualBSD);
c) 5000x magnification (LFD); d) 5000x magnification (DualBSD)

The images acquired on the plasma-treated substrate (simply cleaned with a cloth before treatment) at different magnifications are represented in Figure 45. Whereas, the areal EDX analysis based on the red area of Figure 45,b) is represented in Figure 46.

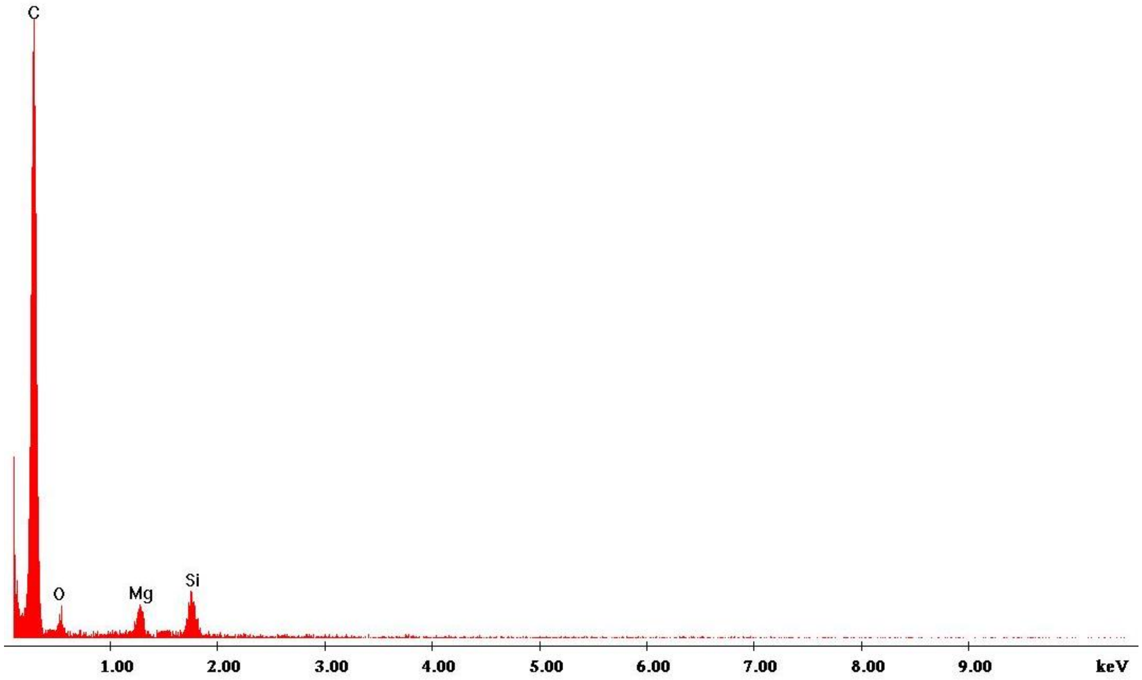

Element	Wt %	At %
C K	91.27	94.30
O K	5.21	4.04
MgK	1.52	0.78
SiK	2.00	0.88
Total	100.00	100.00

Figure 46: Areal EDX analysis of low-pressure argon plasma-treated samples (cleaned with a cloth before treatment)

From the areal EDX analysis, it is possible to see that low-pressure Ar plasma treatments lead to a lower increase in the amount of oxygen on the surface with respect to the samples treated with air and nitrogen. Compared to the untreated sample simply cleaned with a cloth (paragraph 4.3.2) we have an increase in the amount of oxygen on the surface of about the 20% more.

Whereas, compared to the untreated sample pre-treated with n-heptane (paragraph 4.4.1) we have an increase in the amount of oxygen on the surface of about the 68% more.

This result suggests that this treatment is still not suitable for bonding the PP substrates with the polyolefin hot-melt adhesive, but it is the best solution compared to the other process gasses analysed.

4.5.3.2 ATR spectroscopy

From the comparison between the ATR analysis performed on untreated P samples simply cleaned with a cloth (Figure 38) and on the surface of the P sample after the low-pressure plasma treatment using Ar as process gas, shown in Figure 47, it is possible to see that there not relevant variation in the chemical composition after the plasma treatment.

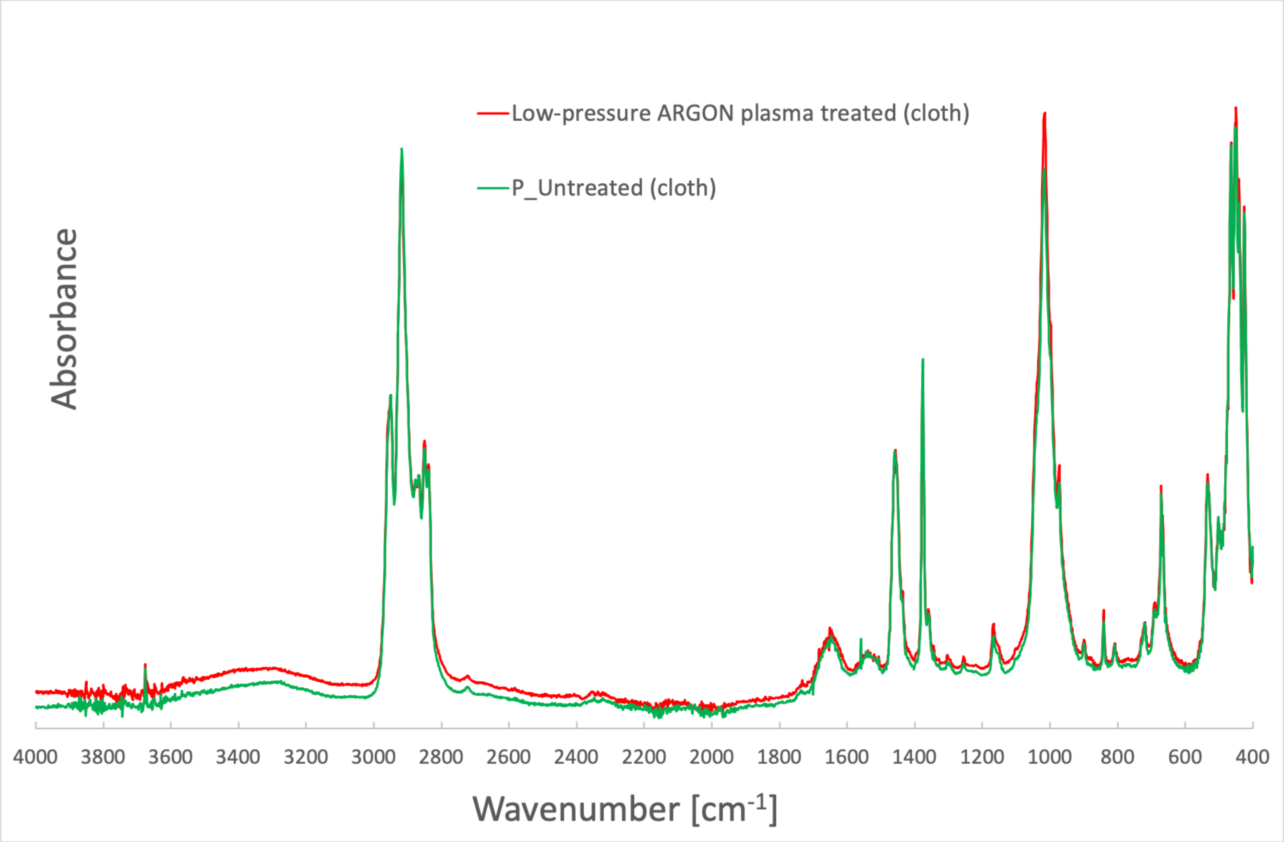

Figure 47: ATR analysis of low-pressure argon plasma-treated samples (cleaned with a cloth before treatment)

4.6 Chemical characterization of the Polyolefin Hot-Melt Adhesive

At a first sight, the surfaces of the adhesive blocks appear to be slightly different: one is smooth and shiny (Figure 48,a), the other is rougher and matte (Figure 48,b).

Such activity is aimed at understanding the chemical composition of polyolefin hot-melt adhesive considered in this study (paragraph 3.1). More specifically, we want to know which are the chemical species present on the surfaces in order to understand whether they may affect the adhesion between the substrates.

Surfaces of the polyolefin hot-melt adhesive were characterized by means of Scanning Electron Microscopy (SEM), Energy Dispersive X-Ray (EDX) analysis and Attenuated Total Reflection (ATR) spectroscopy in order to understand the base surface chemical properties.

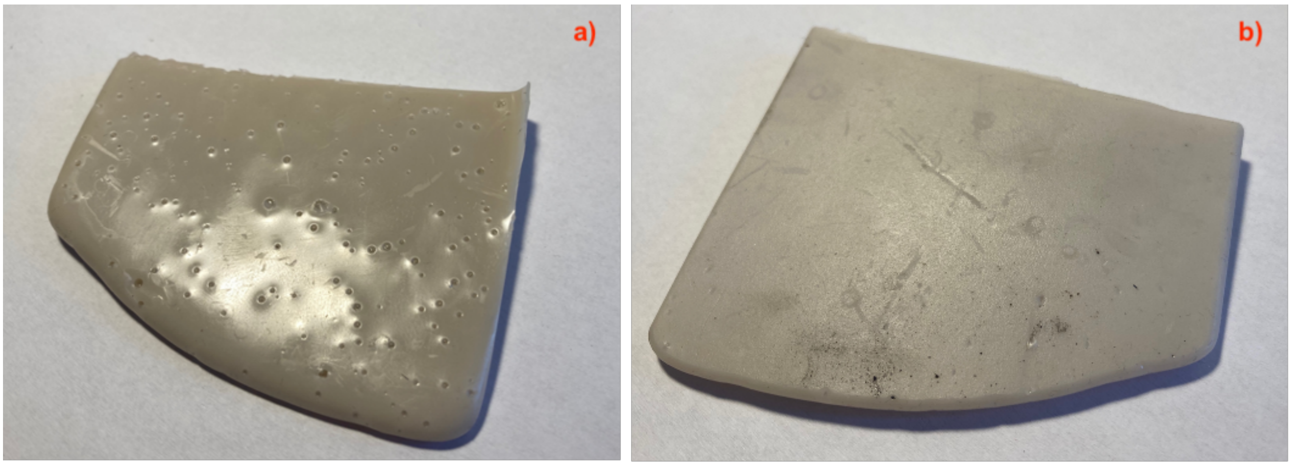

Figure 48: Surfaces of the polyolefin HMA before melting:
a) smooth and shiny surface; b) rough and matte surface

4.6.1.1 SEM + EDX analysis

Scanning electron microscopy (SEM) analysis made it possible to see differences in morphology and chemical composition of the adhesive before the melting and the deposition on the substrate.

Both secondary electrons (LFD) and backscattered electrons (DualBSD) were detected.

Figure 49 shows the SEM images acquired on the smooth surface at different magnifications. Whereas, the areal EDX analysis based on the red area of Figure 49,c) is represented in Figure 50.

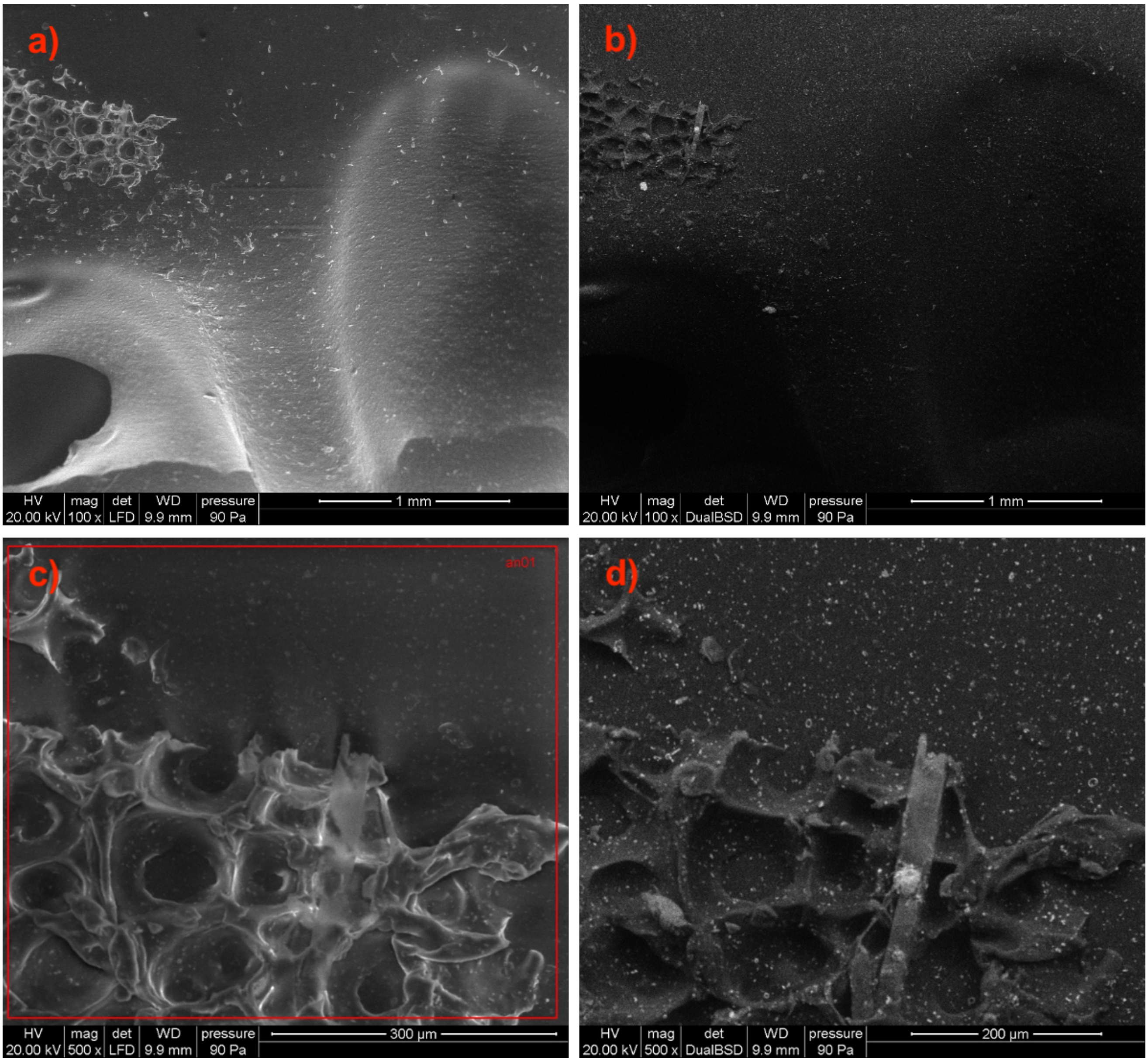

Figure 49: SEM images of the polyolefin hot-melt adhesive used in this study:
a) 100x magnification (LFD); b) 100x magnification (DualBSD);
c) 500x magnification (LFD); d) 500x magnification (DualBSD)

From the SEM analysis, it can be seen that the adhesive has an irregular surface. Whereas, from the areal EDX analysis of the smooth surface, it is possible to see that the composition of the adhesive is very poor of contaminants.

Only a small fraction of calcium is present, probably due to the presence of waxes used as release agents or to avoid the blocks to stick together when they are stocked.

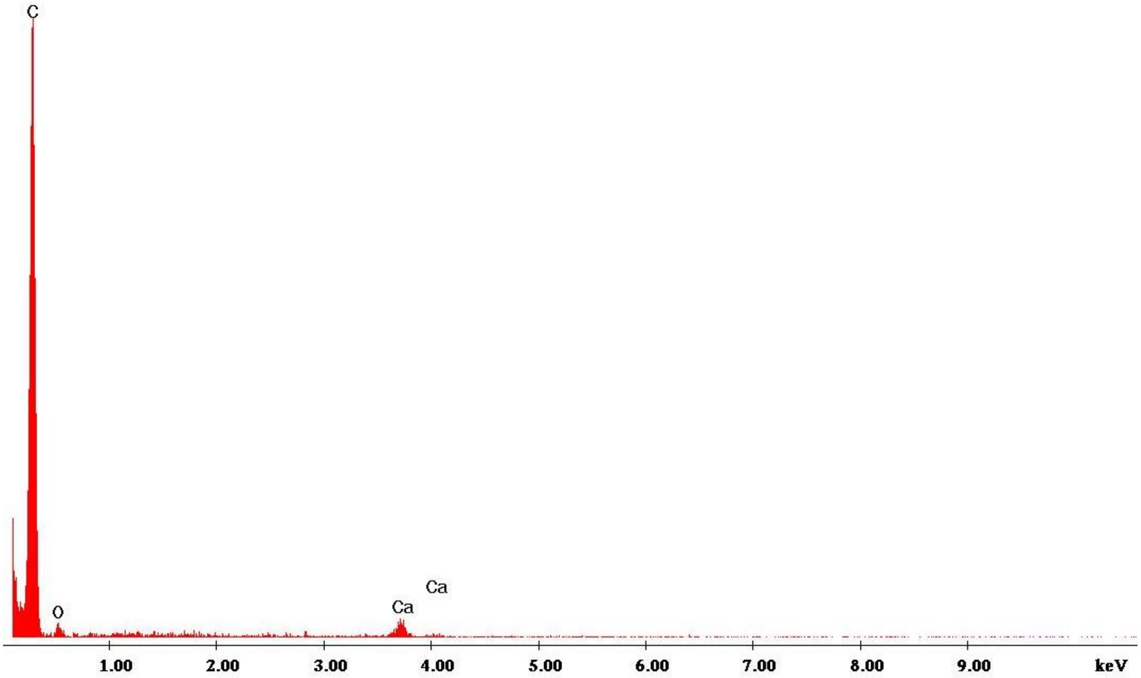

Element	Wt %	At %
C K	93.29	95.61
O K	5.04	3.88
CaK	1.66	0.51
Total	100.00	100.00

Figure 50: Areal EDX analysis of the polyolefin hot-melt adhesive

4.6.1.2 ATR spectroscopy

The comparison between the ATR analysis performed on the two different surfaces of the adhesive (Figure 51) evidenced slightly different chemical composition.

The smother surface shows a more intense vibration from 500 to 1500 cm^{-1} associated with C–C backbone stretching vibrations, –CH2– deformation and –CH3 deformation vibrations.

Anyway, there not relevant variation in the chemical composition.

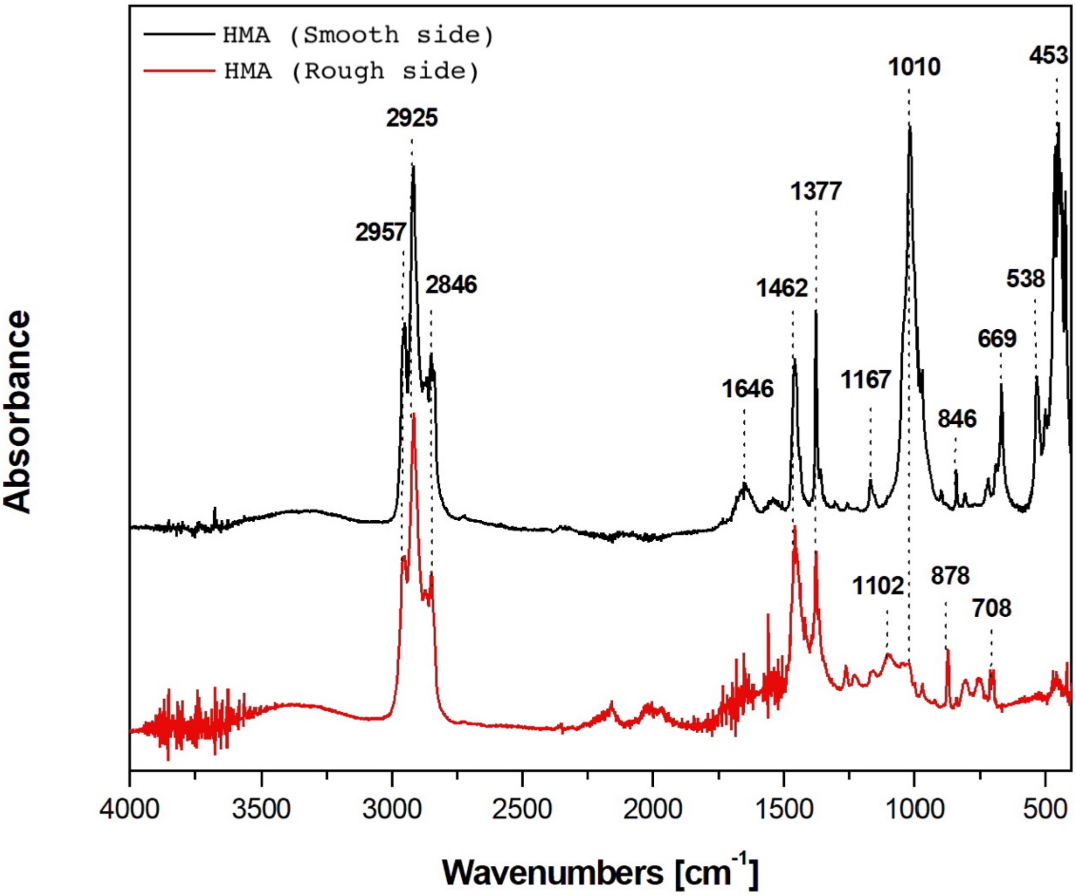

Figure 51: ATR analysis of the polyolefin hot-melt adhesive performed on both sides

4.7 *Mechanical characterization for Polyurethane and Methacrylate adhesive bonding*

Referring to paragraph 3.2.1, the results of lap shear tests after the plasma treatments are here presented in order to discuss the outcomes and analyse the results. The treatments and the nomenclature adopted for the tests are reported in Table 13.

Treatment	P sample
NOT treated	PP
N_2 plasma	PP_N_x

Table 13: Adopted treatments and nomenclature for the mechanical characterization of structural adhesives

Where the term "x" is substituted with the ageing procedure to which the bonded joints were subjected.

The comparison with the untreated bonded joints is not shown in the presentation of the results since, as can be seen from the fracture surfaces in Figure 52 and Figure 53, in the absence of plasma surface treatments, bonding with both adhesives (PUR and MA adhesives) resulted impossible.

Maximum load and shear stress values were computed as the average value of the three specimens for each treatment condition. Moreover, the shear stress was computed by measuring the actual bonding area.

Figure 52: Fracture surface of untreated bonded joint with polyurethane adhesive (Betaforce)

Figure 53: Fracture surface of untreated bonded joint with methacrylate adhesive (Plexus)

4.7.1 Surface treatment for bonding Polyurethane and Methacrylate adhesives

According to the results of the chemical surface characterization of the PP substrates treated with CAPPJ system, N_2 was selected as process gas for this plasma treatment, for the reasons already discussed in paragraph 3.2.1 .

In this case, the comparison of the plasma-treated SLJs has been performed between the simply treated bonded joints and the ones that have undergone the ageing processes described in paragraph 3.3 since the bonding with the untreated substrates was impossible.

The atmospheric plasma treatment using N_2 with CAPPJ system led to a sharp increase of the adhesion of the PP substrates with the adhesive. This is due to the activation effect of nitrogen plasma which produce, on the surface of the non-polar substrate, a large amount of oxygen and FPGs that are much more compatible with the polar composition of these kinds of adhesives.

The load-displacement curves of the treated bonded joints using the polyurethane adhesive and the methacrylate adhesive are shown, respectively, in Figure 54 and Figure 55.

PUR adhesive led to slightly lower maximum loads with respect to the ones obtained with the MA adhesive. Anyway, both of them showed a very good mechanical strength improvement with respect to the untreated bonded joint.

The elongation corresponding to the maximum load is about 5 mm, in the case of PUR adhesive, and it does not change significantly with the ageing process.

Whereas in the case of MA adhesive, the maximum elongation reaches about 7 mm and, after the ageing processes, it increases until almost 12 mm (~70% more) for ageing condition “C” (Figure 55). Moreover, the curves show larger deformations of the SLJs after the ageing processes, contrary to what happens in the case of PUR adhesive.

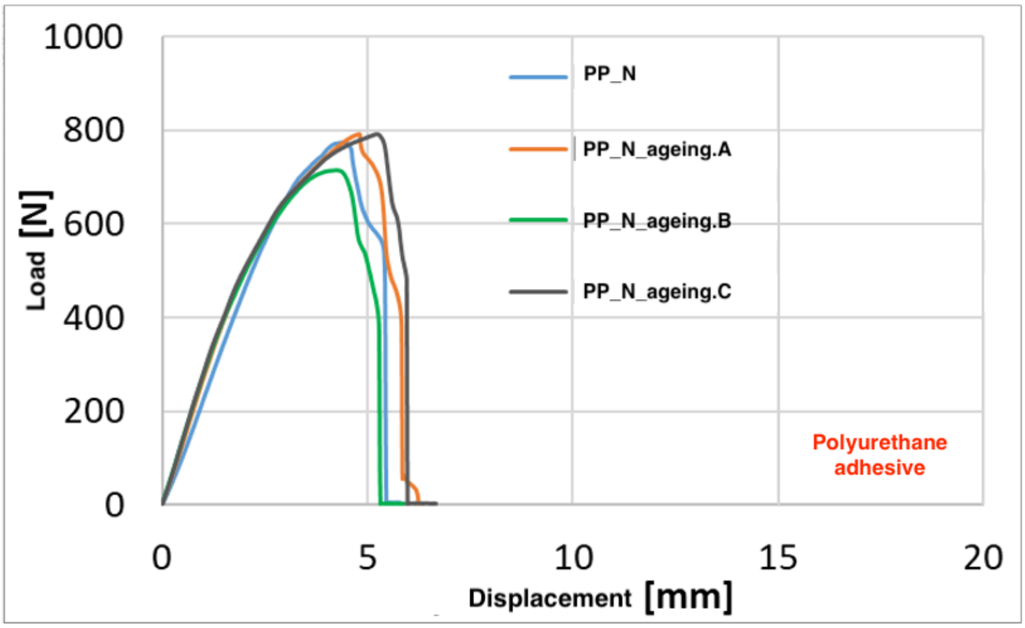

Figure 54: Load-displacement curves for atmospheric pressure nitrogen plasma treated bonded joints using polyurethane adhesive

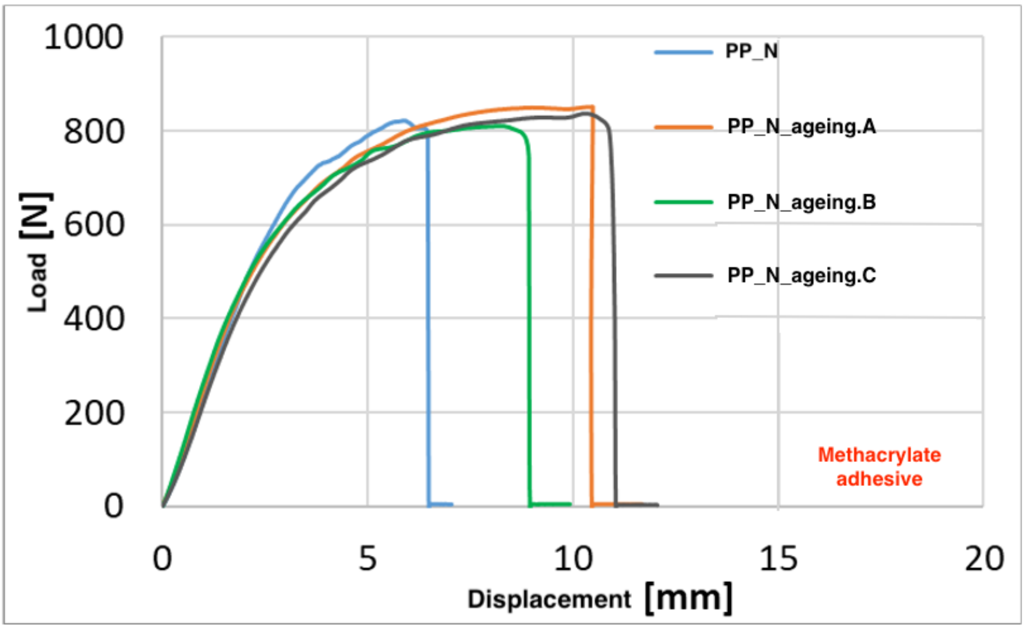

Figure 55: Load-displacement curves for atmospheric pressure nitrogen plasma treated bonded joints using methacrylate adhesive

The bar charts representing the mean maximum shear stress for the SLJs prepared with the treated specimens, before and after ageing, are represented in Figure 56.

The shear strength of the bonded joints prepared using the MA adhesive is always slightly higher with respect to the ones prepared using the PUR adhesive, especially for those subjected to ageing processes.

Moreover, no significant change in maximum shear stress was evidenced between the simply treated bonded joints and those also subjected to the thermal ageing cycles “A” or “C”. Whereas, the bonded joints subjected to the wet cycle (ageing process “B”) show a slight decrease in maximum stress.

From the analysis of the fracture surfaces, there were no particular differences between the single lap joints prepared using the two different adhesives. Both of them showed the failure of the adherent, in all the case studies. In Figure 57 is shown the fracture surface obtained after the tensile test of the plasma-treated bonded joints.

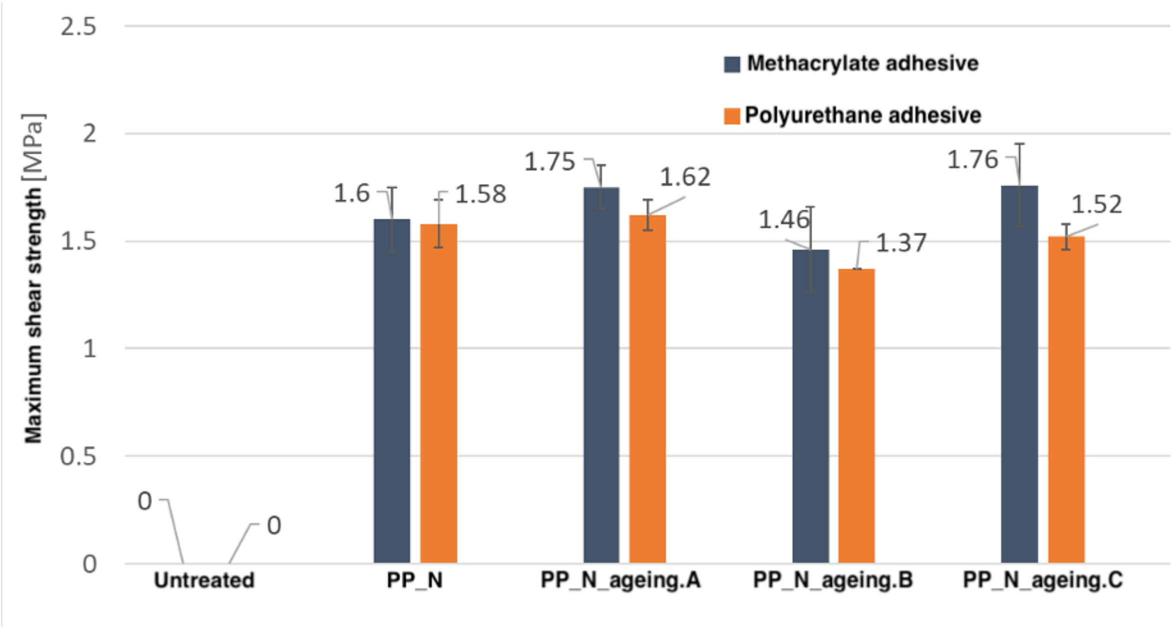

Figure 56: Maximum shear stress variation for PP bonded joints treated with atmospheric pressure nitrogen plasma and subjected to different ageing conditions

Therefore, we can conclude that, in order to bond polypropylene with these kinds of structural adhesives, the use of plasma treatments is essential.

The bond that is created between the two PP substrates is very strong so that the failure of the PP is reached sooner with respect to the adhesives. Moreover, even when subjected to extreme ageing conditions, the bonded joints maintain almost all their strength.

Methacrylate adhesive resulted to be more sensitive to the ageing processes with respect to the polyurethane one, both in terms of maximum elongation and maximum shear stress.

Whereas, polyurethane adhesive showed a more fragile mechanical behaviour compared to the methacrylate one.

Figure 57: Fracture surface of atmospheric pressure nitrogen plasma treated bonded joints

Plasma treatment using CAPPJ system working with nitrogen as process gas resulted to be effective in order to reach our objective.

4.8 Mechanical characterization for the Polyolefin Hot-Melt Adhesive bonding

4.8.1 Surface pre-treatment definition for bonding the polyolefin HMA

It was performed a chemical analysis of the untreated bonded joints subjected to two different surface pre-treatments (paragraph 4.3 and 4.4) in order to choose the more effective method to prepare the specimen before plasma treatments and bonding.

The mechanical properties derived from the lap shear test (performed at 5 mm/min) of the untreated SLJs bonded using the polyolefin HMA whose surfaces of the substrates were subjected to two different pre-treatments (paragraph 3.2.2) are reported in Table 14. Whereas, the load-displacement curves derived from the lap shear test of the untreated bonded joints pre-treated with a cloth and with n-heptane are reported, respectively, in Figure 58 and Figure 59.

These results evidenced that the most effective pre-treatment of the substrates consists of a surface washing with n-heptane.

All the bonded joints tested by lap shear tests showed an adhesive failure of the joint (Figure 60 and Figure 61), meaning that, without any plasma treatment, the adhesion with the PP substrate is not strong enough to exploit the maximum strength of the adhesive.

P SAMPLE surface	**Cleaned with cloth**	**Washed with n-heptane**
Maximum Load [N]	257	317
Standard Deviation [N]	40	21
Maximum shear strength [MPa]	1.06	1.25
Increment/Decrement on shear strength [%]	---	+12%

Table 14: Mechanical characterization of P sample surface pre-treatments

The definition of a baseline, in order to make comparisons with the treated joints, has been done by making an average curve, as shown in Figure 58 and Figure 59.

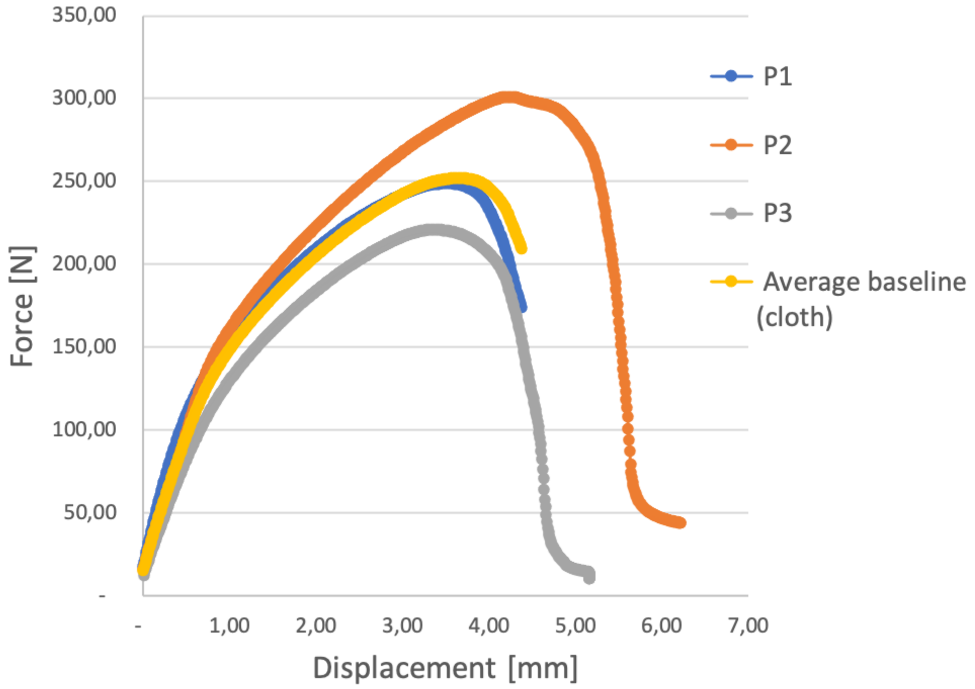

Figure 58: Load-displacement curves and baseline for untreated specimens (surfaces cleaned with a dry cloth)

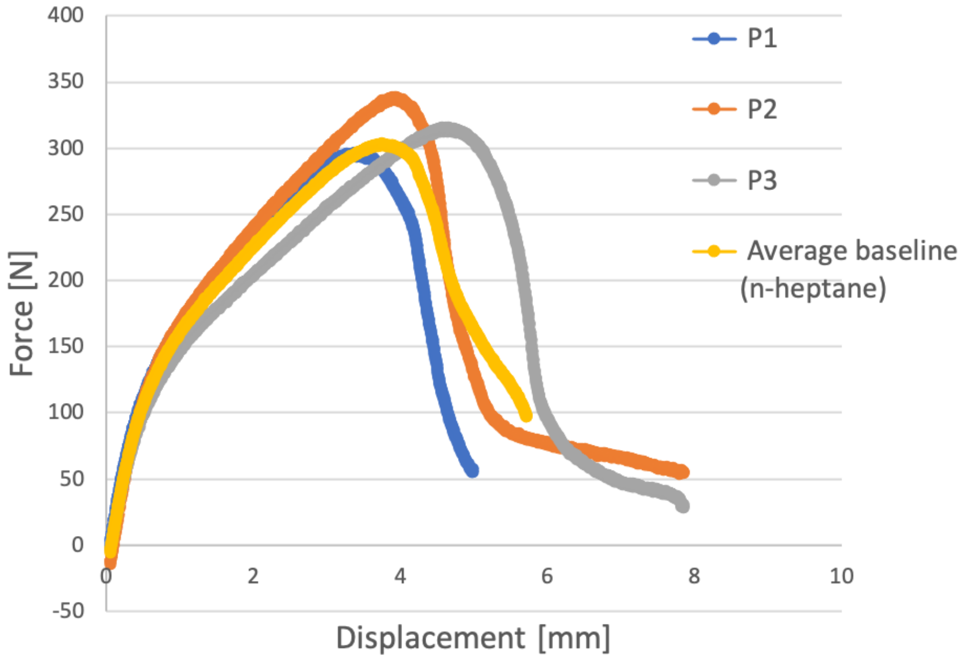

Figure 59: Load-displacement curves and baseline for untreated specimens (surfaces washed with n-heptane)

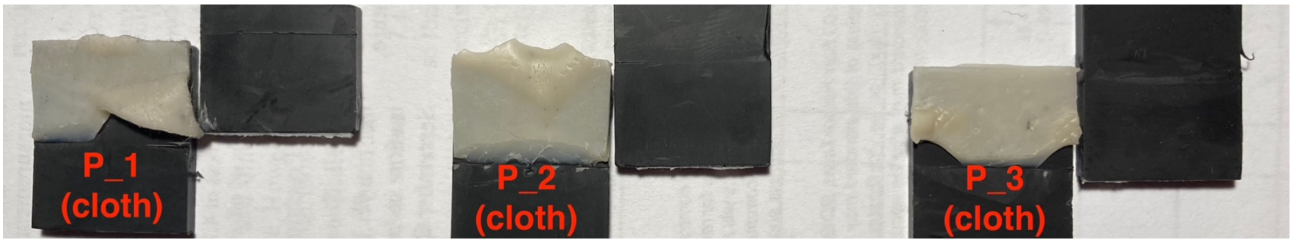

Figure 60: Fracture surfaces for untreated P specimens pre-treated by cleaning with a dry cloth

Figure 61: Fracture surfaces for untreated P specimens pre-treated by washing the surface with n-heptane

Given these results, it was decided to pre-treat the specimens by washing the surfaces with n-heptane before the plasma treatment and the subsequent bonding procedure.

4.8.2 Surface treatment for bonding the polyolefin HMA

Referring to paragraph 3.2.2, the results of lap shear tests after the plasma treatments are here presented in order to discuss the different outcomes and define the most efficient configuration of the process. The treatments and the nomenclature adopted for the tests are reported in Table 15.

Treatment	P sample
NOT treated	P
Ar plasma	PA_x_y
N_2 plasma	PN_x_y

Table 15: Adopted treatments and nomenclature for the mechanical characterization of the polyolefin HMA

Where the term "x" is substituted with letter "V" for low-pressure vacuum plasma treatments or with letter "A" for the atmospheric pressure plasma treatment. The term "y" represents the time exposure value (for vacuum plasma system) or the working distance used (for atmospheric plasma system).

For each treatment, a comparison with the untreated bonded joints was performed.

Maximum load and shear stress values were computed as the average value of the three specimens for each treatment condition. Moreover, the shear stress was computed by measuring the actual bonding area. The standard deviation values give an idea about the repeatability of the results coming from the testing machine for what concerns the maximum load values.

4.8.2.1 Definition of the exposure time for Low-Pressure Plasma treatments

It was necessary to define a suitable plasma exposure time since the low-pressure plasma system admits the control of the exposure time instead of the working distance (for the CAPPJ system).

Two process gasses (Ar and N_2) were tested in order to define which is the best plasma exposure time able to enhance the properties of PP using the low-pressure plasma technology.

The baseline used for this test was given by the tensile tests performed on SLJs prepared with untreated P sample cleaned using just a cloth, as described in paragraph 4.8.1.

The lap shear test was performed at 5 mm/min in order to evaluate the effect of the plasma treatment in the worst-case scenario for the adhesive. Since the adhesive is sensible to the strain rate effect, higher test velocities would lead to a more brittle behaviour, enhancing the cohesive failure of the adhesive.

Considering the different process gas admixtures in Table 8, the numerical results from the lap shear tests of the bonded joints treated with low-pressure plasma working with Ar and N_2 are reported, respectively, in Table 16 and Table 17.

It is worth to state that for this preliminary and explorative experimental test just one specimen was tested for each plasma treatment, whereas, for the untreated baseline, it was considered the average curve obtained by testing 3 joints whose results are reported in paragraph 4.8.1 (specimens cleaned with just a cloth).

Using Ar as process gas with the low-pressure plasma system, we obtain a slight increment of the adhesion properties with respect to the untreated bonded joints. The maximum shear strength increases by 20% with respect to the untreated joint strength and it also reaches a higher maximum displacement corresponding to the peak load.

Whereas, increasing the plasma exposure time the adhesion properties decrease and remain almost constant at a lower strength. The load-displacement curves which allow comparing the effect of three different plasma exposure times for the low-pressure Ar plasma treatment are shown in Figure 62.

The analysis of the fracture surfaces in Figure 63 did not evidence substantial differences between the different treatments carried out. All the plasma exposure times led to an adhesive failure, hence they resulted ineffective to reach our objective.

P SAMPLE (Ar plasma-treated)	**Not treated**	**2 min**	**5 min**	**10 min**
Maximum Load [N]	257	320	272.5	277
Maximum shear strength [MPa]	1.06	1.27	1.13	1.12
Increment/Decrement on shear strength [%]	---	+20%	+7%	+5.5%

Table 16: Mechanical properties of bonded joints treated with low-pressure argon plasma at different exposure times

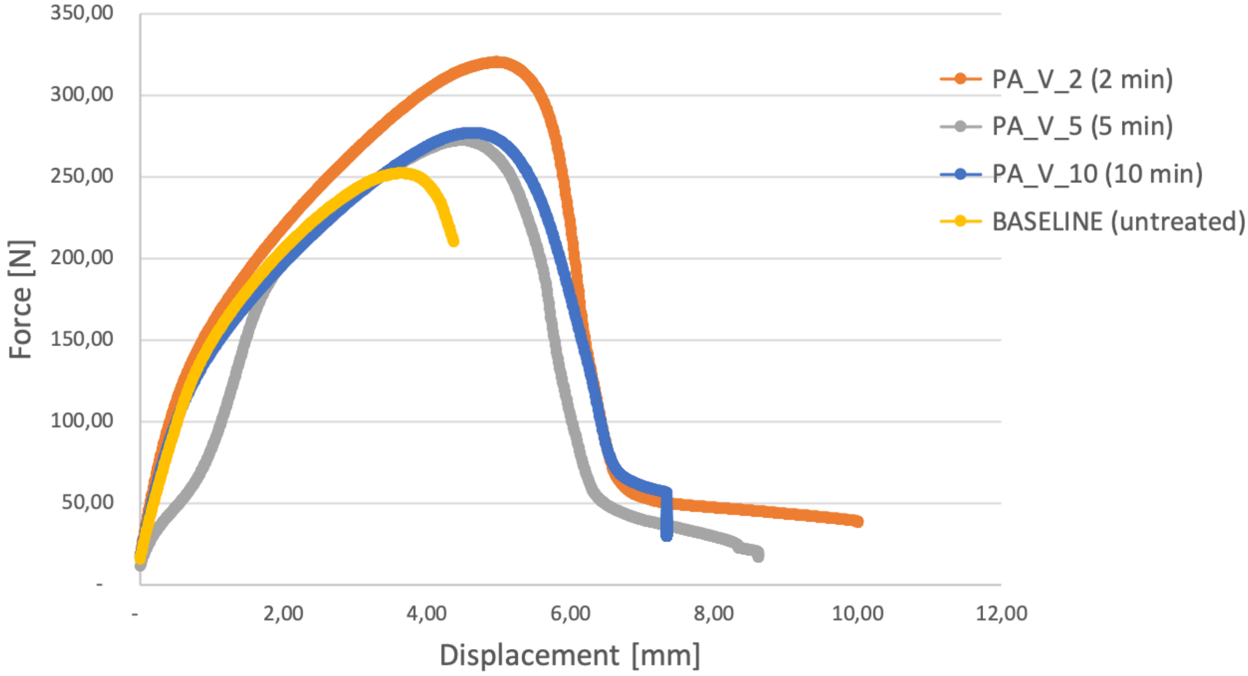

Figure 62: Load-displacements curves for low-pressure argon plasma treatments

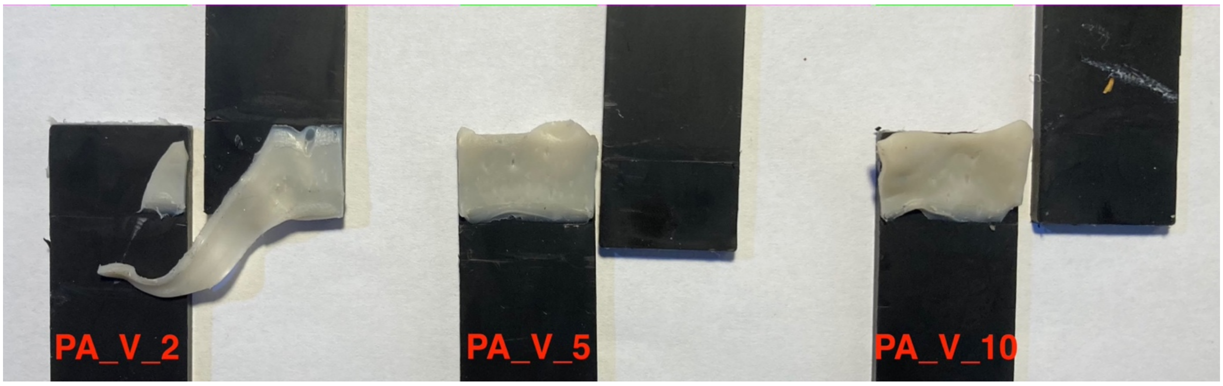

Figure 63: Fracture surfaces of bonded joints treated with low-pressure argon plasma with different exposure times

Using N_2 as process gas with the low-pressure plasma system, we obtained a slight increment of the adhesion properties with respect to the untreated bonded joint for 2 minutes of plasma exposure, as shown in Table 17. Also in this case, increasing the plasma exposure time, the adhesion properties decrease and remain almost constant for exposure times higher than 5 minutes.

The load-displacement curves which allow comparing the effect of the same three different plasma exposure times are shown in Figure 64.

In this case, the elongation corresponding to the maximum load is quite similar to the one of the untreated baseline, for all the considered exposure times.

P SAMPLE (N_2 plasma-treated)	**Not treated**	**2 min**	**5 min**	**10 min**
Maximum Load [N]	257	275	250	248
Maximum shear strength [MPa]	1.06	1.18	1.04	1.09
Increment/Decrement on shear strength [%]	---	+11%	-1.5%	+2.8%

Table 17: Mechanical properties of bonded joints treated with low-pressure nitrogen admixture plasma at different exposure time

The analysis of the fracture surfaces did not evidence substantial differences between the different plasma exposure times, as shown in Figure 65.

Moreover, all the treatments led to an adhesive failure of the SLJs. Specimen PN_V_5 showed an adhesive-cohesive failure but it can be considered mostly adhesive; therefore, also this treatment resulted ineffective to reach our objective.

Therefore, we can conclude that these treatments resulted to be ineffective in order to reach the rupture of the adhesive and so a cohesive failure of the bonded joint.

Anyway, from this explorative experience it was possible to notice which is the most effective plasma exposure time for what concerns plasma treatments of PP using a low-pressure vacuum plasma system.

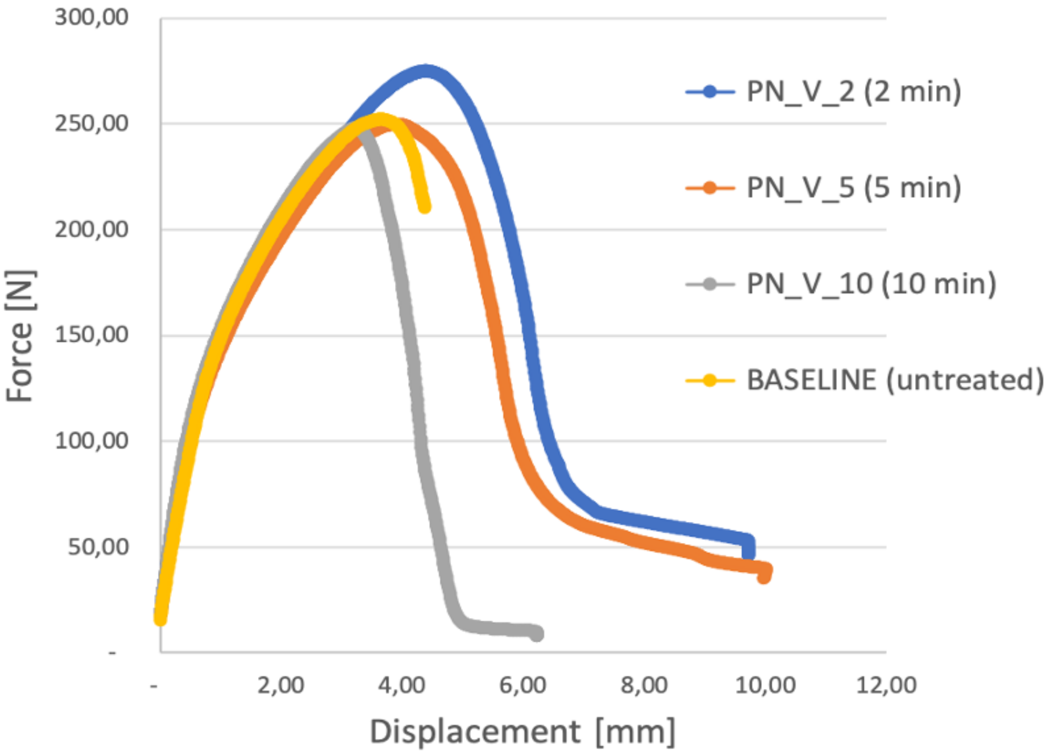

Figure 64: Load-displacements curves for low-pressure nitrogen plasma treatments

The decreasing trend of shear strength with respect to the plasma exposure time for the process gas admixture studied in this paragraph has been reported in Figure 66. Noteworthy is the behaviour which characterize each plasma treatment using a specific gas.

After 2 minutes of plasma exposure, the shear strength tends to reach a plateau at a value close to the one of the untreated bonded joint.

Argon plasma treatment shows the best results for what concerns the increase of the maximum shear strength. Low-pressure plasma treatment resulted to be more effective for 2 minutes of plasma exposure in any case.

According to these results, in the present study, it was planned to analyse the effect of low-pressure plasma on PP substrates treating the samples for 2 minutes, since this plasma exposure time has shown to better enhance the mechanical properties of the bonded joint.

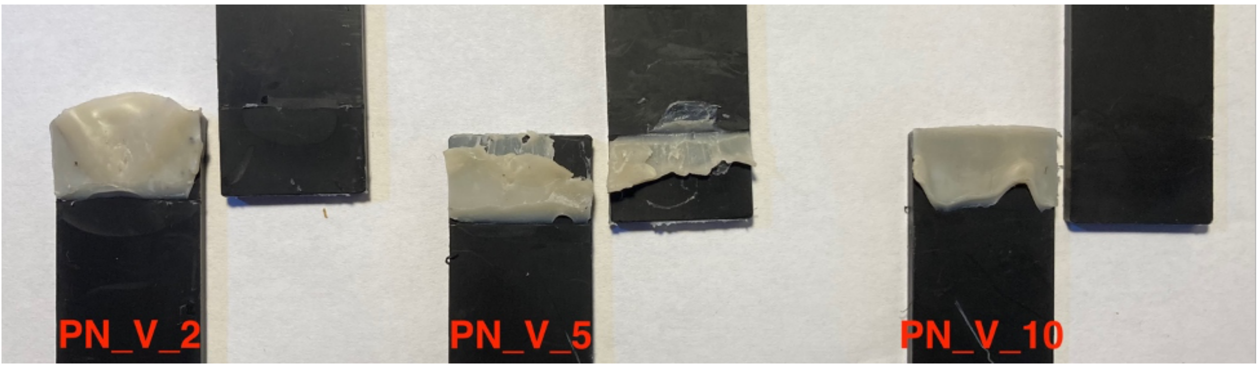

Figure 65: Fracture surfaces of bonded joints treated with low-pressure nitrogen plasma with different exposure times

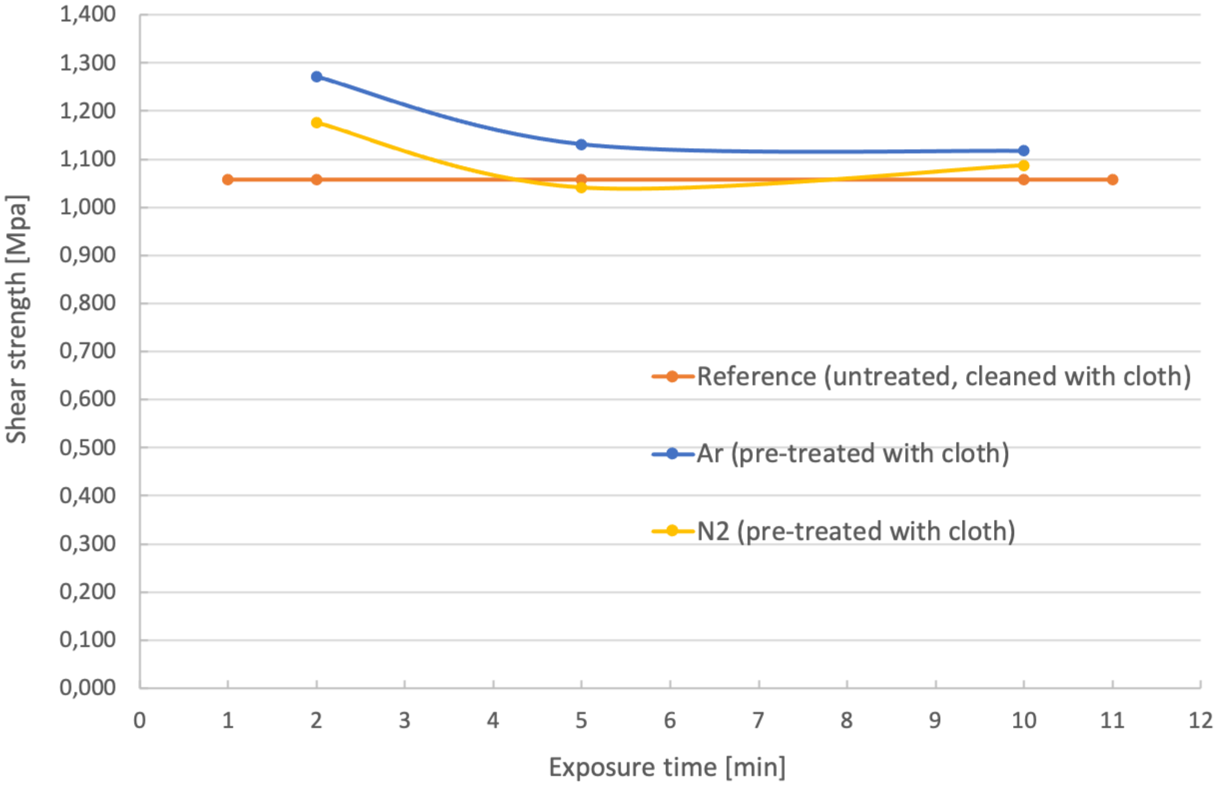

Figure 66: Shear strength variation with exposure time for low-pressure vacuum plasma treatments

4.8.2.2 Low-pressure argon plasma treatment on P samples

(Dynamic lap shear test – 100 mm/min)

According to the results of the chemical surface characterization of the PP substrates treated with low-pressure plasma system (paragraph 4.5.3), low-pressure plasma treatment using Ar for 2 min of plasma exposure was selected for this treatment, for the reasons already specified in paragraph 3.2.2.

Conducting the tensile test at 5 mm/min in the preliminary test for the definition of the exposure time, we obtained a totally adhesive failure of the bonded joint. Therefore, in this case, it was decided to evaluate the strain rate effect on treated joints, performing the lap shear tensile test at 100 mm/min.

The baseline used for the comparison between the untreated bonded joints and the joints treated with plasma is referred to the untreated SLJs prepared with samples washed with n-heptane before bonding, as suggested in paragraph 4.8.1 .

Load-displacement curves and the average baseline curve of the untreated bonded joints used as reference for this test performed at 100 mm/min are reported in Figure 67.

Maximum loads and shear strength values obtained from the lap shear test are reported in Table 18. Obviously, given the sensitivity of the adhesive to strain rate effect, the maximum load values are higher with respect to the ones obtained for the quasi-static test performed in paragraph 4.8.2.1. Moreover, the mechanical behaviour of the treated SLJs resulted to be less ductile (Figure 68).

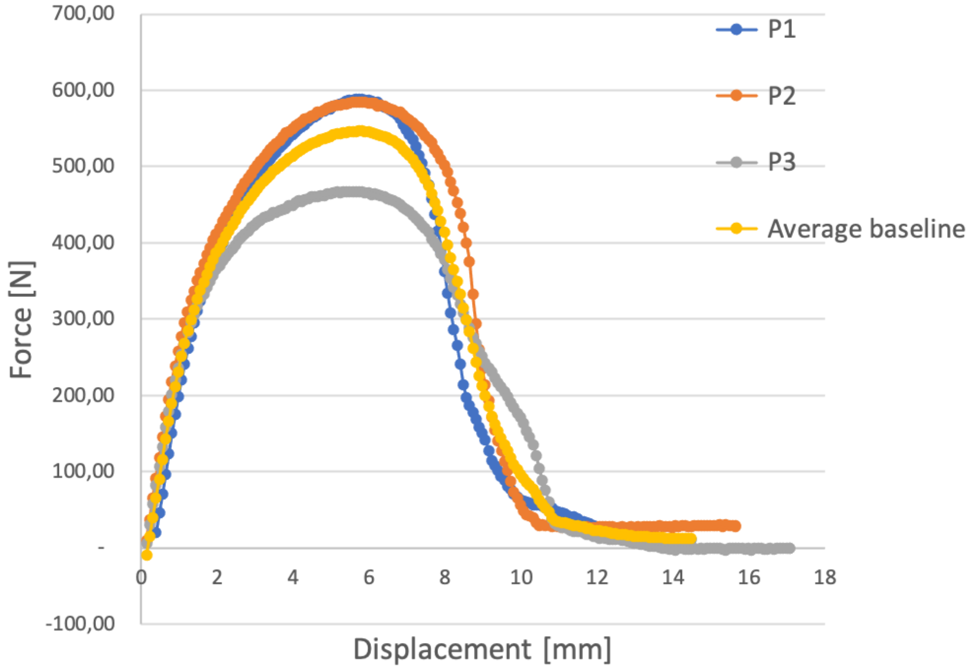

Figure 67: Load-displacement curves for untreated specimens washed with n-heptane before joining tested at 100 mm/min

Noteworthy is the effect of the pre-treatment performed on the substrates before the plasma treatments and the bonding. The samples that were not washed with n-heptane showed a sharp reduction of the maximum shear strength of about 28% with respect to the untreated one.

Whereas, the specimens washed with n-heptane showed a much lower shear strength reduction. Anyway, plasma treatment resulted ineffective in improving the adhesion.

The load-displacement curves shown in Figure 68 and Figure 69 evidenced that plasma treatments decrease the adhesion properties of the bonded joints with respect to the untreated ones. Moreover, it is clear that, without washing the surface with n-heptane before plasma treatments, the mechanical properties of the bonded joints decreased.

P SAMPLE	**Not treated** **washed with n-heptane**	**Ar treated 2 min** **cleaned with cloth**	**Ar treated 2 min** **washed with n-heptane**
Maximum Load [N]	547	399	487
Standard Deviation [N]	68	9	30
Maximum shear strength [MPa]	2.2	1.6	1.9
Increment/Decrement on shear strength [%]	---	-28%	-11%

Table 18: Results from the lap shear test performed at 100 mm/min for low-pressure argon plasma treatment

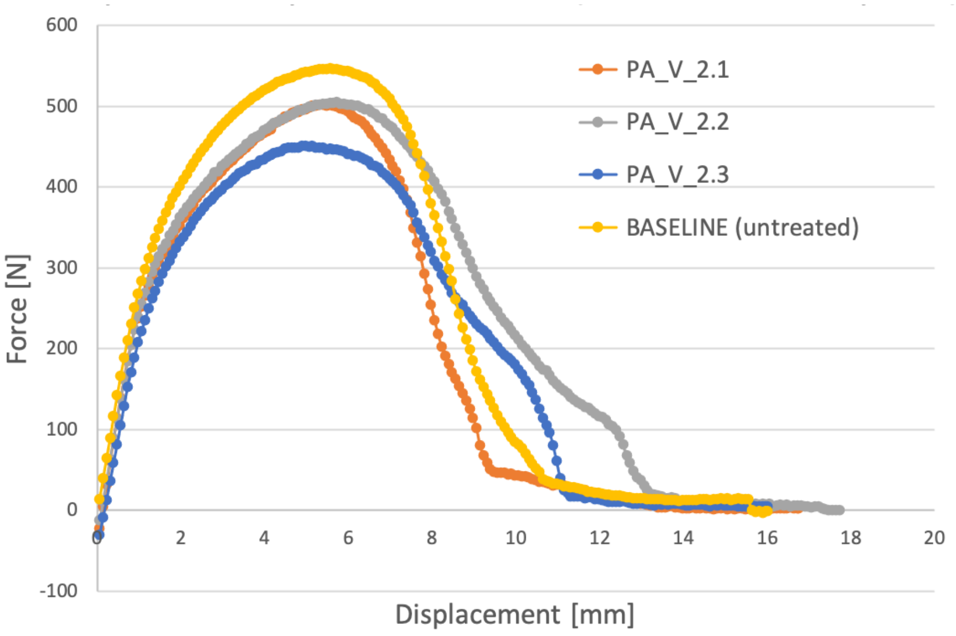

Figure 68: Load-displacement curves for low-pressure argon plasma treated specimens (pre-treated by washing the substrates with n-heptane)

The displacement corresponding to maximum load, obtained in the case of pre-treated substrates with n-heptane (Figure 68), is about 6.5 mm and the mechanical behaviour of the curves is very similar to the one corresponding to the untreated baseline.

Whereas, in the case of pre-treatment using just a cloth (Figure 69), the maximum displacement corresponding to maximum load reaches about 4 mm before failure and the mechanical behaviour of the curves appears to be more fragile with respect to the case in Figure 68.

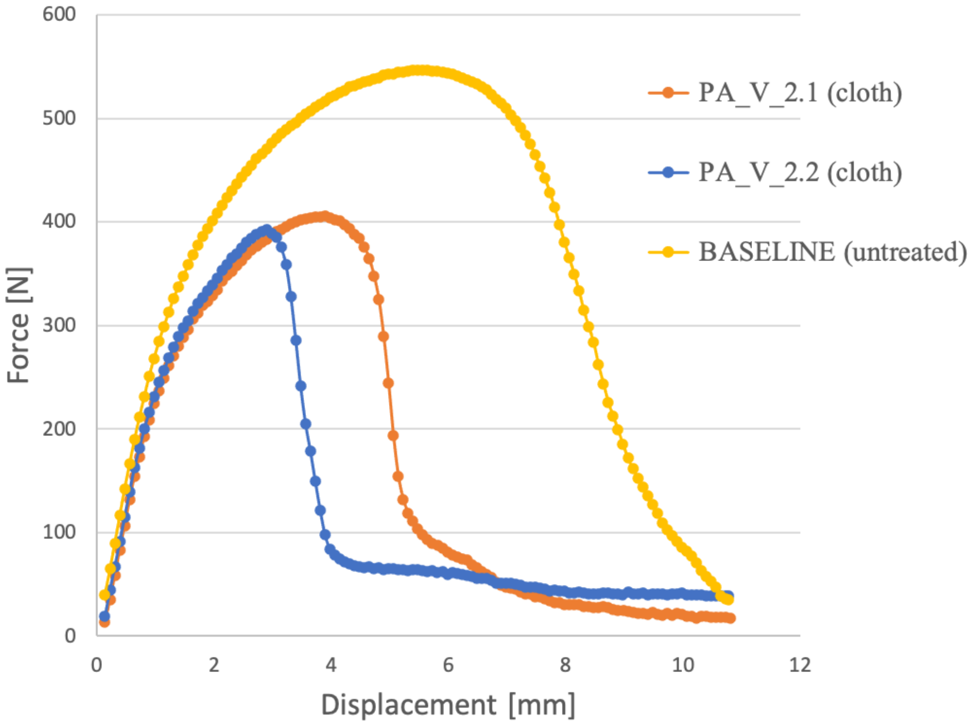

Figure 69: Load-displacement curves for low-pressure argon plasma treated specimens (pre-treated by cleaning the substrates with a dry cloth)

This behaviour is evident also from the analysis of the fracture surfaces, reported in Figure 70. The fracture surfaces of the untreated baseline tested at 100 mm/min (Figure 70,a) show an adhesive/cohesive failure since it can be seen a rupture in the adhesive together with a detachment of the adhesive from the substrate.

Even the fracture surfaces of the low-pressure Ar plasma treated bonded joints pre-treated with n-heptane (Figure 70,b) show an adhesive/cohesive failure.

Noteworthy are the fracture surfaces of the treated bonded joints pre-treated with just a cloth (Figure 70,c). They show a totally adhesive failure and this reflects perfectly the results reported in Table 18 and the ones from the chemical characterization of the bonding surfaces (paragraph 4.4).

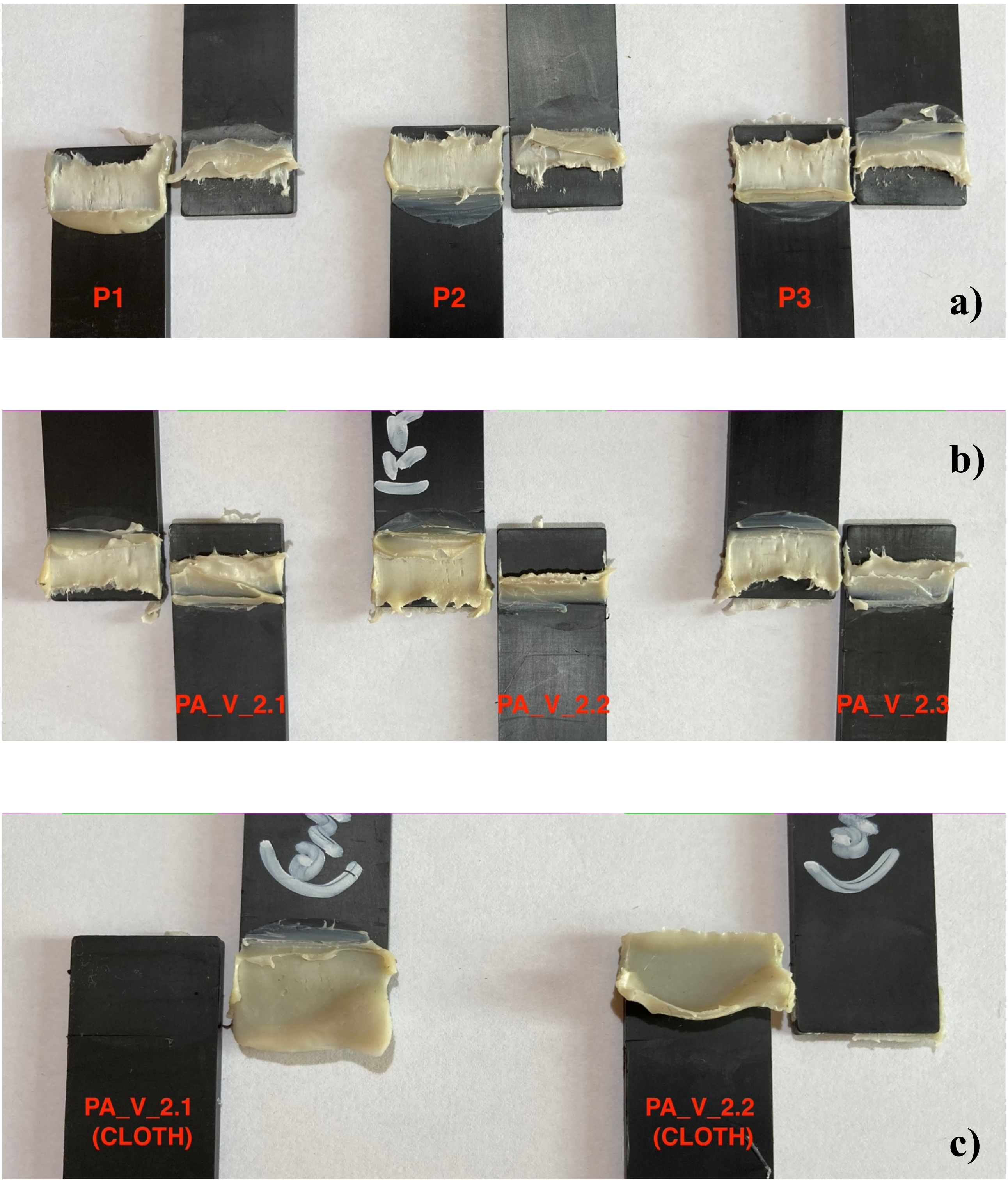

Figure 70: Fracture surfaces of: a) untreated specimen washed with n-heptane, b) low-pressure argon plasma treated specimen for 2 min of plasma exposure (washed with n-heptane), c) low-pressure argon plasma treated specimen for 2 min of plasma exposure (cleaned with a dry cloth)

Therefore, according to these results, we can conclude that, in the case of low-pressure plasma treatments using Ar as process gas, a short plasma treatment, in the range of few minutes, produced a maximum bond strength compared to other exposure times. The maximum shear strength after 2 minutes of plasma exposure was 20% higher with respect to a longer plasma treatment in the range of 5 to 10 minutes.

Low-pressure argon plasma treatments resulted to improve the mechanical properties of the joints only in the case of substrates that have not been subjected to the pre-treatment with n-heptane. This is probably due to the plasma etching effect that may lead to the removal of contaminants present on the surface, as the washing with n-heptane would do.

Low-pressure plasma treatment using Ar for 2 min of plasma exposure resulted ineffective to reach a complete cohesive failure, also in more favourable condition of strain rate.

Plasma treatments showed a detrimental behaviour for the adhesion of the polyolefin hot-melt adhesive with the PP substrates.

The only parameter that is effective in improving the adhesive properties is washing the substrates with n-heptane before plasma treatments.

4.8.2.3 Atmospheric pressure argon plasma treatment on P samples (Quasi-static lap shear test – 5 mm/min)

Just for comparative purposes, it was performed an atmospheric pressure plasma treatment using Ar as process gas also for the 2nd production batch of samples.

In this case, the baseline used for the comparison between the untreated and plasma treated bonded joints is referred to the SLJs prepared with untreated P samples washed with n-heptane before bonding, whose mechanical properties are reported in Table 14.

The working distance chosen for this treatment was 8 mm because, from a preliminary analysis, it resulted to be the lowest WD that did not lead to damage of the adherent surface.

The atmospheric plasma treatment using Ar with CAPPJ system, led to a reduction of the adhesion properties with respect to the untreated bonded joint of about 4%, as shown in Table 19.

The load-displacement curves shown in Figure 71 allow to compare the effect of the plasma treatment using pure Ar with respect to the untreated baseline.

In this case, the elongation corresponding to the maximum load does not undergo relevant variations with respect to the untreated joint.

The analysis of the fracture surfaces showed no evident differences between the treated specimen in Figure 72 and the untreated baseline specimens in Figure 61. Moreover, the treatments led to a complete adhesive failure of the bonded joint. Therefore, this treatment is not suitable in order to reach our objective.

P SAMPLE	**Not treated** **washed with n-heptane**	**Ar plasma treated** **WD = 8 mm**
Maximum Load [N]	317	305
Standard Deviation [N]	21.2	6.14
Maximum shear strength [MPa]	1.25	1.2
Increment/Decrement on shear strength [%]	---	-3.7%

Table 19: Mechanical properties of bonded joints treated with atmospheric pressure argon plasma at WD = 8 mm

The behaviour of the load-displacement curves is repeatable and shows a mostly ductile behaviour for both the treated and untreated bonded joints.

Therefore, we can conclude that atmospheric plasma treatment using Ar as process gas is ineffective in order to reach the rupture of the adhesive and so a cohesive failure of the bonded joint.

It is meaningless to study the effect also for an higher lap shear test velocity since the low-pressure plasma treatment using Ar led to a similar conclusion.

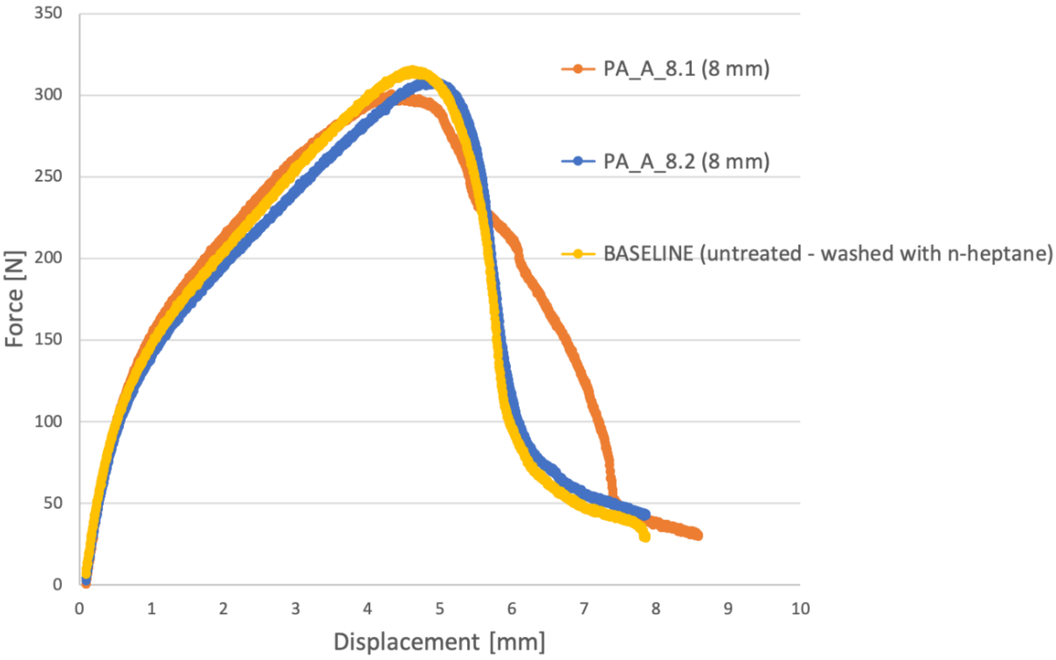

Figure 71: Load-displacement curves for CAPPJ argon plasma treatment at WD = 8 mm

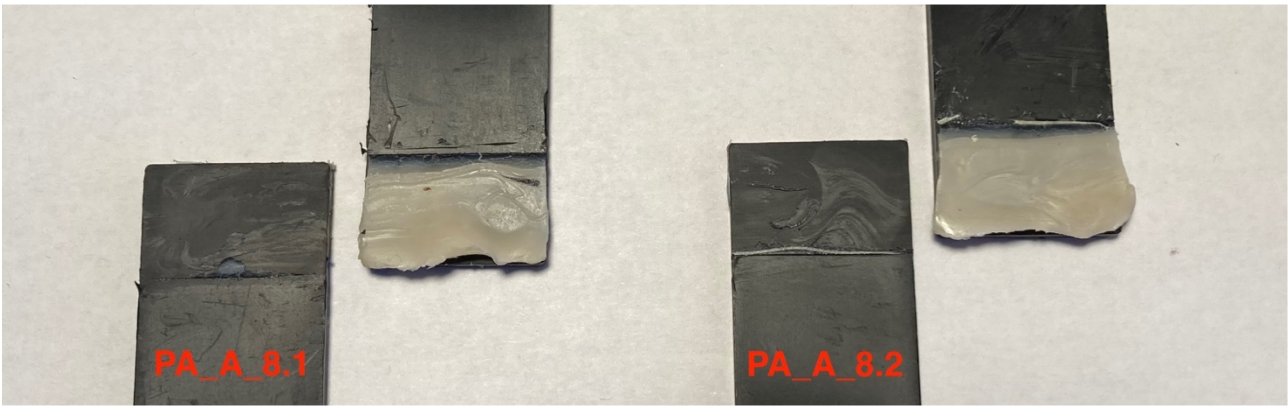

Figure 72: Fracture surfaces for the CAPPJ argon plasma treatment tested at 5 mm/min

5 Conclusions

Primarily, the optical and chemical characterization of the polypropylene substrates evidenced large differences between the two production batches used in this study.

The chemical analysis of the treated and untreated surfaces of the PP substrates used for bonding the polyurethane and methacrylate adhesive (belonging to the first production batch) highlighted a very high amount of oxygen compared to the PP substrates belonging to the second production batch (used for bonding the polyolefin HMA).

For what concerns the 1st production lot used for bonding PUR and MA adhesives, after atmospheric plasma treatments, the weight and atomic percentages of oxygen increase of about 20% more using N_2 as process gas, leading to a strongly polar surface.

Atmospheric plasma treatments using air plasma also increased the presence of oxygen but, even if the gas itself contains more oxygen with respect to N_2, it does not show a substantial difference from the untreated sample. This is probably due to the fact that, along the gap between the plasma jet and the substrates present in the CAPPJ system, N_2 reacts with the ambient air binding with the oxygen present in the surrounding.

Therefore, regarding the results of the tensile tests after the plasma treatments for bonding the structural adhesives (PUR and MA adhesives) considered in this study, we can conclude that, in order to bond polypropylene substrates, the use of plasma treatments is essential.

Plasma treatments are able to improve the adhesion of the substrates with the adhesives so that the failure of the adherent occurred for both single lap joints prepared using the two different adhesives, meaning that the forces involved in adhesion are greater than the resistance of the substrate itself.

Moreover, even when subjected to extreme ageing conditions, the bonded joints maintain almost all their strength. Methacrylate adhesive resulted to be more sensitive to the ageing processes with respect to the polyurethane one, both in terms of maximum elongation and maximum shear stress.

For what concerns the 2nd production lot used for bonding the polyolefin HMA, the chemical and optical surface analysis of the treated and untreated surfaces of the PP substrates highlighted that the presence of oxygen is not uniformly distributed (Figure 31).

After low-pressure plasma treatments, the weight and atomic percentages of oxygen increase of about 20% more using Ar as process gas, compared to the untreated sample simply cleaned with a cloth (paragraph 4.3.2). Whereas, compared to the untreated sample pre-treated with n-heptane (paragraph 4.4.1) it increases of about 68% more.

These results were confirmed by the lap shear tests on bonded joints treated with low-pressure Ar plasma treatment (paragraph 4.8.2.2) since it did not show any improvement in the mechanical properties of the treated SLJs bonded using the polyolefin hot-melt adhesive.

Therefore, regarding the results of the tensile tests after the plasma treatments for bonding the polyolefin HMA, this study has highlighted that, for the use of this specific polyolefin adhesive (paragraph 3.1), low-pressure plasma treatments (using the considered process gasses) is ineffective in increasing the adhesion properties of the polypropylene substrates.

However, it is interesting to note that an accurate surface preparation of the substrate, consisting in washing the surface with n-heptane, it is able to increase the mechanical properties of the SLJs bonded with the polyolefin HMA.

Anyway, none of the tested specimens led to a cohesive failure of the joints or a failure of the substrates, as happened in the case of structural adhesives bonding.

It can be concluded that atmospheric pressure N_2 plasma treatment of polypropylene creates a polar surface with excellent adhesion properties to improve, or even make possible, the adhesion in case of polyurethane and methacrylate adhesive bonding.

This is possible given the ability of plasma to activate the surface of the polyolefin polymer by the production of a larger amount of oxygen and functional polar groups on the substrate, making the surface compatible with the chemical structure of the adhesive.

Given the obtained results, space is left for future studies aimed to find an atmospheric or, more likely, a low-pressure plasma treatment that is able to activate the surface of the polypropylene maintaining, as much as possible, the polarity of the surface in order to further increase the mechanical properties of the joints bonded with polyolefin hot-melt adhesives. A solution can be to treat the substrates using a plasma deposition technology, in which a monomer is converted by the plasma in reactive fragments that will recombine to polymers in the gas phase. These polymers can be deposited on the substrate, thus creating a more suitable plasma-deposited polymer coating on the surface.

6 Acknowledgements

Having come to the end of this work, I would like to thank Prof. Giovanni Belingardi and Prof. Davide Salvatore Paolino for having given me the opportunity to be part of this research activity.

A particular thanks goes to Ing. Raffaele Ciardiello who, with patience and passion, has followed my work also through some difficulties, allowing me to develop my interests and teaching me important things for my future life.

An heartfelt thanks goes to Domenico D’Angelo who has given me the possibility to make a delightful working experience introducing me to the world of plasma technologies, with great professionalism and experience, showing interest in my studies and helping me when I needed.

A thanks also to Alessandro Croce and his research group of the UPO university, who contributed with their precise and clear chemical characterizations.

7 References

[1] J.Rowe, Advanced materials in automotive engineering, Woodhead Publishing Limited, 2012.

[2] "European Aluminium," March 2018. [Online]. Available: https://www.european-aluminium.eu/media/2434/european-aluminium_lightweighting-a-solution-for-low-carbon-mobility_position-paper-march-2018.pdf. [Accessed 19 March 2021].

[3] B.Chang, Y.Shi and S.Dong, "Comparative studies on stresses in weld-bonded, spot-welded and adhesive-bonded joints," *Journal of Materials Processing Technology,* vol. 87, p. 230– 236, 1999.

[4] G.Belingardi and G.Chiandussi, "Stress flow in thin walled box beams obtained by adhesive bonding joining technology," *International Journal of Adhesion & Adhesives,* vol. 24, p. 423–439, 2004.

[5] E.M.Petrie, Handbook of Adhesives and Sealants, McGraw-Hill, 2000.

[6] L.F.M.daSilva, A.Öchsner and R.D.Adams, Handbook of Adhesion Technology, Berlin: Springer-Verlag Berlin Heidelberg, 2011.

[7] M.Kehrer, A.Rottensteiner, W.Hartl, J.Duchoslav, S.Thomas and D.Stifter, "Cold atmospheric pressure plasma treatment for adhesion improvement on polypropylene surfaces," *Surface & Coatings Technology,* vol. 403, no. 126389, 2020.

[8] K.G.Kostov, T.M.C.Nishime, A.H.R.Castro, A.Toth and L.R.O.Hein, "Surface modification of polymeric materials by cold atmospheric plasma jet," *Applied Surface Science,* vol. 314, pp. 367-375, 2014.

[9] P.Sundriyal, M.Pandey and S.Bhattacharya, "Plasma-assisted surface alteration of industrial polymers for improved adhesive bonding," *International Journal of Adhesion and Adhesives,* vol. 101, no. 102626, 2020.

[10] Y.Kusano, "Atmospheric Pressure Plasma Processing for Polymer Adhesion: A Review," *The Journal of Adhesion,* vol. 90, no. 9, pp. 755-777, 2014.

[11] C.Maier and T.Calafut, Polypropylene - The Definitive User's Guide and Databook, Plastics Design Library, 1998.

[12] M.Noeske, J.Degenhardt, S.Strudthoff and U.Lommatzsch, "Plasma jet treatment of five polymers at atmospheric pressure: surface modifications and the relevance for adhesion," *International Journal of Adhesion & Adhesives,* vol. 24, pp. 171-177, 2004.

[13] R.Kawakami, Y.Yoshitani, K.Mitani, M.Niibe, Y.Nakano, C.Azuma and T.Mukai, "Effects of air-based nonequilibrium atmospheric pressure plasma jet T treatment on characteristics of polypropylene film surfaces," *Applied Surface Science,* vol. 509, no. 144910, 2020.

[14] N.V.Bhat and D.J.Upadhyay, "Plasma-Induced Surface Modification and Adhesion Enhancement of Polypropylene Surface," *Journal of Applied Polymer Science,* vol. 86, no. 4, pp. 925-936, 2002.

[15] M.Kehrer, J.Duchoslav, A.Hinterreiter, A.Mehic, T.Stehrer and D.Stifter, "Surface functionalization of polypropylene using a cold atmospheric pressure plasma jet with gas water mixtures," *Surface and Coatings Technology,* vol. 384, no. 125170, 2020.

[16] E.C.Dell'Orto, A.Vaccaro and C.Riccardi, "Morphological and chemical analysis of PP film treated by Dielectric Barrier Discharge," *Journal of Physics: Conference Series,* vol. 550, 2014.

[17] V.Jones, M.Strobel and M.J.Prokosch, "Development of Poly(propylene) Surface Topography During Corona Treatment," *Plasma Processes and Polymers,* vol. 2, no. 7, pp. 547-533, 2005.

[18] R.M.Overney, R.Lüthi, H.Haefke, J.Frommer, E.Meyer, H.J.Güntherodt, S.Hild and J.Fuhrmann, "An atomic force microscopy study of corona-treated polypropylene films," *Applied Surface Science,* vol. 64, no. 3, pp. 197-203, 1993.

[19] M.Strobel and C.S.Lyons, "The role of low-molecular-weight oxidized materials in the adhesion properties of corona-treated polypropylene film," *Journal of Adhesion Science and Technology,* vol. 17, no. 1, pp. 15-23, 2003.

[20] M.Strobel, C.Dunatov, J.M.Strobel, C.S.Lyons, S.J.Perron and M.C.Morgen, "Low-molecular-weight materials on corona-treated polypropylene," *Journal of Adhesion Science and Technology,* vol. 3, no. 1, pp. 321-335, 1989.

[21] M.Green, F.J.Guild and R.D.Adams, "Characterisation and comparison of industrially pre-treated homopolymer polypropylene, HF 135M," *International Journal of Adhesion & Adhesives,* vol. 22, pp. 81-90, 2002.

[22] R.Dorai and M.J.Kushner, "A model for plasma modification of polypropylene using atmospheric pressure discharges," *Journal of Physics D: Applied Physics,* vol. 36, no. 6, pp. 666-685, 2003.

[23] D.K.Owens and R.C.Wendt, "Estimation of the surface free energy of polymers," *Journal of Applied Polymer Science,* vol. 13, no. 8, pp. 1741-1747, 1969.

[24] Y.Yuan and T.R.Lee, "Contact Angle and Wetting Properties," *Surface Science Techniques. Springer,* pp. 3-34, 2013.

[25] S.Bhattacharya, A.Datta, J.M.Berg and S.Gangopadhyay, "Studies on Surface Wettability of Poly(Dimethyl) Siloxane (PDMS) and Glass Under Oxygen-Plasma Treatment and Correlation With Bond Strength," *Journal of Microelectromechanical Systems,* vol. 14, no. 3, pp. 590 - 597, 2005.

[26] D.Shaw, A.West, J.Bredin and E.Wagenaars, "Mechanisms behind surface modification of polypropylene film using an atmospheric-pressure plasma jet," *Plasma Sources Science and Technology,* vol. 25, no. 065018 , 2016.

[27] H.B.Baniya, R.P.Guragain, B.Baniya and D.P.Subedi, "Cold Atmospheric Pressure Plasma Jet for the Improvement of Wettability of Polypropylene," *International Journal of Polymer Science,* vol. 2020, no. 3860259, 2020.

[28] X.L.Deng, A.Y.Nikiforov, P.Vanraes and C.Leys, "Direct current plasma jet at atmospheric pressure operating in nitrogen and air," *Journal of Applied Physics,* vol. 113, no. 023305, p. 1–9, 2013.

[29] H.Yoshiki, "Generation of air microplasma jet and its application to local etching of polyimide films," *Journal of Applied Physics,* vol. 45, p. 5618–5623, 2006.

[30] M.Vishnuvarthanan and N.Rajeswari, "Effect of mechanical, barrier and adhesion properties on oxygen plasma surface modified PP," *Innovative Food Science and Emerging Technologies,* vol. 30, pp. 119-126, 2015.

[31] A.VanDeynse, P.Cools, C.Leys, N.DeGeyter and R.Morent, "Surface activation of polyethylene with an argon atmospheric pressure plasma jet: Influence of applied power and flow rate," *Applied Surface Science,* vol. 328, pp. 269-278, 2015.

[32] J.C.Vickerman and I.S.Gilmore, Surface analysis: the principal techniques, John Wiley & Sons, 2011.

[33] G.Binnig, C.F.Quate and C.Gerber, "Atomic Force Microscope," *PHYSICAL REVIEW LETTERS,* vol. 56, no. 9, 1986.

[34] G.Meyer and N.M.Amer, "Novel optical approach to atomic force microscopy," *Applied Physics Letters,* vol. 53, no. 1045, p. 2400, 1988.

[35] A.Sarani, A.Y.Nikiforov, N.DeGeyter, R.Morent and C.Leys, "Surface modification of polypropylene with an atmospheric pressure plasma jet sustained in argon and an argon/water vapour mixture," *Applied Surface Science,* vol. 257, p. 8737–8741, 2011.

[36] Crow, "Polymer Properties Database," 2015. [Online]. Available: http://polymerdatabase.com/Adhesives/PO%20Adhesives.html. [Accessed 01 04 2021].

[37] M. DUNKY and A. PIZZI, "Chapter 23 - Wood adhesives," *Adhesion Science and Engineering,* vol. 2, pp. 1039-1103, 2002.

[38] M. REVELLINO, L. SAGGESE and E. GAIERO, "Compression Molding of SMCs," *Comprehensive Composite Materials,* vol. 2, pp. 763-805, 2000.

[39] Gluegun.com, "An Introduction to Methyl Methacrylate Adhesives (MMAs)," [Online]. Available: https://www.gluegun.com/blogs/adhesive-reviews/an-introduction-to-methyl-methacrylate-adhesives-mmas. [Accessed 01 07 2021].

[40] G.Belingardi, V.Brunella, B.Martorana and R.Ciardiello, "Thermoplastic Adhesive for Automotive Applications," in *Adhesives - Applications and Properties*, INTECH, 2016, pp. 341-362.

[41] R.N.Kumar and A.Pizzi, "Hot Melt Adhesives," in *Adhesives for Wood and Lignocellulosic Materials*, Scrivener Publishing LLC, 2019, p. 347–366.

[42] T.E.Rolando, Solvent-Free Adhesives, United Kingdom: Smithers Rapra Publishing, 1998.

[43] E.G.Koricho, E.Verna, G.Belingardi, B.Martorana and V.Brunella, "Parametric study of hot-melt adhesive under accelerated ageing for automotive applications," *International Journal of Adhesion and Adhesives,* vol. 68, pp. 169-181, 2016.

[44] LyondellBasell, "Hostacom CR 1171 G1A G14008," [Online]. Available: https://www.lyondellbasell.com/en/polymers/p/Hostacom-CR-1171-G1A-G14008/f45c0c3c-3fdf-4c98-98b4-0b392a4f5196. [Accessed 12 04 2021].

[45] L.Goglio, M.Peroni and M.Rossetto, "Effect of the Strain Rate on the Mechanical Behaviour of Epoxy Adhesives," *Key Engineering Materials,* vol. 347, pp. 671-676, 2007.

[46] A.Gopanna, R.N.Mandapati, S.P.Thomas, K.Rajan and M.Chavali, "Fourier transform infrared spectroscopy (FTIR), Raman spectroscopy and wide-angle X-ray scattering

(WAXS) of polypropylene (PP)/cyclic olefin copolymer (COC) blends for qualitative and quantitative analysis," *Polymer Bulletin,* vol. 76, p. 4259–4274, 2019.

[47] E.Andreassen, "Infrared and Raman spectroscopy of polypropylene," in *Polypropylene: an A-Z reference (Part of the polymer science and technology series, POLS, vol 2)*, Springer, Berlin, J. Karger-Kocsis, 1999, p. 320–328.

[48] J.P.Luongo, "Infrared study of polypropylene," *J. Appl. Polym. Sci.,* vol. 3, no. 9, pp. 302-309, 1960.

[49] P.Larkin, Infrared and Raman Spectroscopy, Amsterdam: Elsevier, 2011.

[50] A.S.Nielsen, D.N.Batchelder and R.Pyrz, "Estimation of crystallinity of isotactic polypropylene using Raman spectroscopy," *Polymer,* vol. 43, pp. 2671-2676, 2002.

[51] Y.V.Shemouratov, K.A.Prokhorov, E.A.Sagitova, G.Y.Nikolaeva, P.P.Pashinin, Y.A.Lebedev and E.M.Antipov, "Raman study of polyethylene-polypropylene blends," *Laser Physics,* vol. 19, no. 2179, 2009.

[52] T.Sundell, H.Fagerholm and H.Crozier, "Isotacticity determination of polypropylene using FT-Raman spectroscopy," *Polymer,* vol. 37, no. 15, pp. 3227-3231, 1996.

[53] G.Socrates, Infrared and Raman characteristic group frequencies: tables and charts, New York: Wiley, 2001.